UNIVERSITEIT VAN PRETORIA
UNIVERSITY OF PRETORIA
YUNIBESITHI YA PRETORIA

SIMPLIFIED FIELD ANALYSIS OF ISM-BAND, OFDM-BASED, INDUSTRIAL WIRELESS SENSOR NETWORKS

by

Pierre van Rhyn

Submitted in partial fulfilment of the requirements for the degree
Philosophiae Doctor (Electronics)

in the

Department of Electrical, Electronic and Computer Engineering
Faculty of Engineering, Built Environment and Information Technology

UNIVERSITY OF PRETORIA

June 2017

SUMMARY

SIMPLIFIED FIELD ANALYSIS OF ISM-BAND, OFDM BASED, INDUSTRIAL WIRELESS SENSOR NETWORKS

by

Pierre van Rhyn

Supervisor: Prof. G. P. Hancke

Department: Electrical, Electronic and Computer Engineering

University: University of Pretoria

Degree: Philosophiae Doctor (Electronics)

Keywords: Service level differential zone (SLDZ), committed information rate (CIR), quality of service (QoS) reference, throughput bandwidth, wireless link budget, industrial wireless.

A novel method is proposed to estimate committed information rate (CIR) variations in typical orthogonal frequency division multiplexing (OFDM) wireless local area networks (WLANs) that are applied in support of industrial wireless sensor networks (IWSNs) and operate within the industrial, scientific and medical (ISM) frequency bands. The method is based on the observation of a phenomenon of which the significance has not previously been recognized nor documented; here termed the *service level differential zone* (SLDZ). This method, which conforms to the ITU-T Y.1564 test methodology, provides the means to set a CIR reference for IEEE 802.11a/g/n OFDM systems in terms of committed throughput bandwidth between a test node and an access point (AP) at a specific range.

An analytical approach is presented to determine the relationship between the maximum operating range (in metres) of a wireless sensor network for a specific committed throughput bandwidth, and its link budget (in dB). The most significant contributions of this study are the analytical tools to determine wireless network capabilities, variations and performance in a simplified method, which does not require specialised measurement equipment. With these it becomes possible for industrial technicians and engineers (who are not necessarily information technology (IT) network experts) to field analyse OFDM WLANs and so qualify their performance in terms of Y.1564 specified service level agreement (SLA) requirements, which is a primary requirement for WSNs that are intended for use in some specialised industrial applications.

OPSOMMING

VEREENVOUDIGDE METODE OM IWM-BAND, OFDM GEBASEERDE, INDUSTRIËLE RADIOSENSORNETWERKE OPERASIONEEL TE ANALISEER

deur

Pierre van Rhyn

Studieleier: Prof G. P. Hancke

Departement: Elektriese, Elektroniese en Rekenaaringenieurswese

Universiteit: Universiteit van Pretoria

Graad: Philosophiae Doktor (Elektronika)

Sleutelwoorde: Diensvlak differensiële gebied, diensvlakverwysing, deurlaatbandwydte, radioskakelbegroting

Die studie ondersoek ‘n nuwe metode om toevertroude oordraginformasietempo (OIT) van tipiese lokale IWM (industriële, wetenskaplike en mediese) band radiodatanetwerke te bepaal, wat gebaseer op ortogonale-frekwensiedeling multipleksering (OFDM), vir spesifieke toepassing in industriële radiosensor-netwerke (IRSNe) wat breëband deurlaatwerking vereis teen `n gespesifiseerde minimum diensvlak (DV) verwysing. Dié nuwe metode is gebaseer is op die waarneming van `n onbekende verskynsel wat vervolgens na verwys word as die *diensvlak differensiële gebied* (DVDG). Hierdie metode, wat ‘n aanpassing is vanaf die Internasionale Telekommunikasie Unie (ITU) se toetsmetodologie Y.1564, bemoontlik `n simplistiese wyse om `n gespesifiseerde deurlaatbandwydteverwysing tussen toetsnodus en aansluitingpunt (AP) te bepaal in terme van `n spesifieke reikafstand (in meter).

`n Analitiese benadering word voorgestel om op `n eenvoudige wyse die verhouding te bepaal tussen die minimum deurlaat diensvlak bandwydteverwysing en die radioskakelbegroting, in desibel (dB). Die hoofbydrae van die studie is om aan die wetenskaplike gemeenskap die analitiese werktuie te voorsien wat benodig word om radionetwerkvermoëns, variasies en werkverrigting te bepaal, nie alleen volgens die aanvaarbare ruisvrye dinamiese bestek (RVDB) parameters nie, maar ook volgens die Y.1564 toetsmetodologie se voorgeskrewe diensvlakooreenkomste met betrekking tot industriële standaarde.

LIST OF ABBREVIATIONS

AES	Advanced encryption standard
AP	Access point
BSS	Basic service set
BW	Bandwidth
CIR	Committed information rate
ESS	Extended service set
ISM	Industrial, scientific and medical
IWSN	Industrial wireless sensor network
LLC	Logic link control
MAC	Media access control
Mbps	Megabits per second
MIMO	Multiple-input-multiple-output
OFDM	Orthogonal frequency division multiplexing
OFDMA	Orthogonal frequency division multiple access
OWEN	Optimised wireless Ethernet network
PCMCIA	Personal computer memory card international association
PHY	Physical layer
QoS	Quality of service
SLDZ	Service level differential zone
TKIP	Temporal key integrity protocol
USB	Universal serial bus
WEP	Wired equivalent privacy
WLAN	Wireless local area network
WPA2(PSK)	Wi-Fi protected access 2, (personal security key)

TABLE OF CONTENTS

CHAPTER 1 INTRODUCTION

1.1 PROBLEM STATEMENT

1.1.1 Context of the problem

Industrial wireless sensor networks (IWSNs) [1], [2] consist of sensor nodes that are placed in close proximity or within the phenomena they observe, according to specific measurement requirements, whilst communicating with other nodes or network access points. A true-to-type sensor node consists of a suitable sensor or transducer, a microprocessor to execute trivial logic operations or programs, a radio frequency (RF) transceiver to access the network and a suitable power supply.

Industrial wireless sensor networks have been successfully applied in environmental and temperature monitoring [3], [4], machine monitoring [5], energy monitoring [6], and more recently, in the specialised fields of computer vision [7], optical character recognition (OCR) [8], [9], and thermography [10].

Thermography measures the temperature of the entire picture that the charged-coupled device (CCD) has captured. This process consumes larger quantities of connected bandwidth, for example the Ti-300 infrared thermography imager manufactured by Fluke™ can be applied in a typical industrial solution to monitor and inspect furnaces and boilers wirelessly using its proprietary ‘SD wireless’ interface [11].

The Ti-300 provides, to Android/Linux nodes, a real-time video image and thermography analysis of the temperature distribution inside the combustion chamber or boiler. This information is crucial for process control and preventative maintenance procedures, but requires broadband capability for networked transmission.

Specified by application, many IWSNs require mission critical broadband operation. It may be due to the large data capacity requirements of a single sensor [11] or due to a multitude of sensors in simultaneous service [12].

Industrial, scientific and medical (ISM) band, OFDM WLANs is the proposed solution for IWSNs that require broadband operation with committed information rate and predetermined class of service. Two industry measurement standards for data throughput, RFC2544 [13] and ITU-T Y.1564 [14], are applicable. The terms committed information rate (CIR), excess information rate (EIR) and class of service (CoS) are defined by the ITU-T in Y.1564 [14] and by the Metro Ethernet Forum [15]. CIR and EIR are specifically defined by [14] and [15] in terms of its measurement philosophy and methodologies, as the acceptable parameters in the method to determine service performance levels that conform to modern industrial and commercial service level agreements.

Modern IEEE 802.11a/g/n systems that transport transmission control protocol/Internet protocol (TCP/IP) industrial Ethernet services should be therefore be evaluated according to the same ITU-T Y.1564 standards. It should be noted here that 802.11b is not an OFDM based system, but that 802.11a/g/n OFDM systems are backward compatible with 802.11b [16].

A major advantage of an OFDM based 802.11a/g/n gateway router, for IWSN use, is its 3G capability that facilitates a global communications connection [17], seamlessly connection dissimilar operating systems across dissimilar networks. A far-reaching application that becomes possible, is that Android/Linux based IWSNs can be deployed, operated and controlled from anywhere on the globe. Conformation to industrial requirements means that OFDM IWSNs can directly be linked to satellite or fibre services and applied in any conceivable industrial or scientific role.

Multiple-input-multiple-output orthogonal frequency division multiplex (MIMO-OFDM) wireless technology appears to fulfil the requirements of industrial WLANs [17]. MIMO-

OFDM is considered a most interesting development in the field of broadband wireless technology because it is tolerant to multi-path propagation and frequency selective fading.

OFDM is also known for its improved impulse noise rejection and spectral efficiency [17]. Based on frequency division multiplexing (FDM), OFDM is described as a technology that simultaneously transmits multiple signals in parallel, using multiple frequencies [18], [19].

Performance gains may be made in OFDM systems by the application of more than one antenna at either or both connecting points of the wireless link [20]. Multiple antennas can be used to cancel interference caused by multipath transmission distortion on single-antenna systems by coherent combining/cancelling techniques [21], and because they provide an alternative transmission path to the signal [20]. An additional fundamental channel gain is realised by the use of multiple antennas in a multiple-input-multiple-output (MIMO) configuration that improves spectral efficiency [21].

Performance gains may also be made in OFDM systems by the application of a higher gain antenna at either or both connecting points of the wireless link [22], [23]. Log periodic types are usually highly directional with a beam width of 15 to 20 degrees in sector specific direction (azimuth). Attention is drawn to vertically polarised omni-directional antennas with higher gain, such as the multiple-element collinear array [51], which will only operate satisfactorily in the horizontal plane.

Exceptional performance gains in IWSNs may be made by selecting the sufficiently developed technology of the day that is available to the industry [24]. For example, a trend observed in both the automotive and military industries is to make use of repackaged commercial off-the-shelf (COTS) technology, such as the 802.11a/b/g/n standard ISP gateway/routers, as opposed to development of turnkey systems from the ground up. These latest commercial gateway/routers operate at both ISM frequency bands of 2.4 GHz and 5 GHz in the WLAN, so providing frequency diversity. Each frequency band is utilised by two omnidirectional transceivers, thereby providing a degree of space diversity, as well as noise cancellation. The gateway employs a so called ‘hotstick’ USB modem to connect the

WLAN to the Internet service provider, typically in a licenced frequency band such as 3.8 GHz. Some progress has been made towards including the 800 MHz band (white space) into the ISM bands for unlicensed WLANs.

A related problem is to define the degree to which the sensor network has improved its service level as a result of performance optimisation attempted by the user [24]. Advantages for industrial electronics and informatics practitioners from this approach are time and cost savings that are related to the measurement platform.

Considering the research objectives, this study formulates the hypothesis that *connected bandwidth* (BW) in Mbps is directly proportional to the power density in Watts/m^2 of the radio frequency (RF) wave, or conversely to the electric field strength (E) of the RF wave in V/m, at the receiving node. Connected bandwidth refers to *digital bandwidth*, as opposed to *analogue bandwidth* which is the frequency range between the half power points of an electromagnetic energy wave. This implies that the connected BW will decrease at the same rate as the power density or the electric field strength of the RF wave, until the decline in signal to noise (SN) ratio results in termination of wireless communication.

Testing the above-mentioned hypothesis positively is a research goal that motivates the application of the well-known inverse-square law of radiated power, in conjunction with effects of a phenomenon termed here as the service level differential zone. The consideration of the service level differential zone is a novel approach that provides the methods and mathematical building blocks, which are required to solve range-, and capacity related issues of wireless systems [25].

The results of bit-rate testing by pattern transmission may be misleading if one considers a phenomenon we shall refer to as the ‘service level differential zone’ (SLDZ) of an OFDM WLAN. The SLDZ of an OFDM WLAN was observed in an industrial environment during preliminary transmission tests that were conducted by the authors during 2007, in preparation of an engine test bench for the purpose of (destructive) diesel engine testing.

This form of engine testing requires remote temperature monitoring [24] of the engine components due to the mechanical risks of engine failure which include flying shrapnel and hot oil ejection.

The first time the SLDZ of an OFDM WLAN was observed, was during preliminary transmission tests that were conducted at the Tshwane South College (in Tshwane, South Africa) during 2007 [25]. It was observed that an OFDM network will maintain broad-bandwidth transmission (video and audio soundtrack) with a node, up to a certain distance away from the access point (AP), as the separating range (r) is increased.

At a range r_{ne} (never exceeded) from the AP, the signal is suddenly compromised with little or no warning by video transmission quality. The node now has to move back a certain distance towards the AP to r_{max} in order to regain transmission. This distance moving back was observed to be a considerable percentage of the total apparent transmission range r_{ne}. It is this considerable range between r_{max} and r_{ne} that we shall refer to as the SLDZ. The quality of service (QoS) level of a network cannot be accurately determined when nodes are deployed within (or outside) the SLDZ of the network. The SLDZ appears to conform to the magnetic hysteresis phenomenon and the underlying physical laws that describe it, e. g. the Jiles and Atherton (JA) model of hysteresis [26].

This thesis proposes a method to determine the excess information rate (EIR) and the committed information rate (CIR) by detection, using the SLDZ dynamic hysteresis phenomenon. This technique is combined with scaled video streaming to represent the user defined throughput bandwidth. Previous methods used the file transfer protocol (ftp) method which was not accurate because not all the key performance indicators (KPIs) are considered namely latency and jitter. The d-CIR (detected CIR) provides a quality of service reference, which conforms mostly to the ITU.Y-1564 test philosophy.

This study intends to contribute the scientific equations and methods that are required to determine wireless network capabilities, variations and performance, during industrial deployment or field tests. With these it becomes possible to qualify OFDM WLANs in

terms of their service performance according to acceptable standards such as Y.1564, which is a key requirement for industrial applications.

1.1.2 Research gap

A research gap in the field of wireless Ethernet that now exists is caused by financial considerations. Advances in WLAN technology were significant over the past ten to fifteen years, making available ISM access point router/adapters capable of up to a few hundred Megabits per second for only a few hundred rand. However, the test and measurement equipment to determine network performance in terms of a predetermined CIR may cost well in excess of a few thousand rand. For example, a trend observed in both the automotive and military industries is to make use of commercial off-the-shelf (COTS) technology, repackaged to IP65 standards, as opposed to development of turnkey systems from the ground up. These devices incorporate 802.11a/g/n compatible WLAN capabilities, as well as multiple connectivity options. Their capabilities to connect dissimilar operating systems across dissimilar networks place them functionally on par with OSI model, level 7 gateways.

This approach holds many advantages for industrial electronics and informatics practitioners because of time and cost savings related to the measurement platform. For the same reasons, the application of Android/Linux based platforms has become prolific according to National Instruments' article published in 2016. ('What is a wireless sensor network?' *NI White Paper 7142/EN*. www.ni.com/white-paper/7142/en/. Last accessed 10 May 2016.) However new test methods need to be developed that can perform non-invasive measurement of electrical parameters because no other access can be easily gained to the internal circuit boards due to the very large scale integration of design and construction of these devices.

1.2 RESEARCH GOALS

This research project is intended to benefit scientists and technicians from various disciplines and fields of study, that are not necessarily information technology specialists.

1.2.1 Determine performance capabilities

The first intention is to provide these user groups with a simplified method to determine the capabilities of a deployed IWSN, that does require expensive and complicated measuring tools.

1.2.2 Predict increased performance

Secondly, when attempting to improve the network capability, the user group is provided with a set of equations to predict increased performance when external high gain antennas are considered which are readily available from commercial suppliers.

1.2.3 Physical layer testing according to SFDR parameters

An extended research goal of this study is therefor to propose a method to compare different OFDM WLAN physical layers in terms of their dynamic performance. A dynamic range performance parameter is required when considering improvement to the link quality, because it will determine the maximum extent to which the link budget can be increased.

The study proposes the spur-free dynamic range parameters namely SFDR*min* and SFDR*fs* to express OFDM WLAN dynamic range performance. These are mostly used in the specialised field of high speed digital to analogue conversion (DAC) and analogue to digital conversion (ADC) [29]. The SFDR parameters can be derived from the d-CIR and d-EIR using the SLDZ detection method previously described in this paper.

1.3 HYPOTHESIS AND APPROACH

This thesis formulates the hypothesis that *connected bandwidth* (BW) in Mbps is directly proportional to the power density in Watts/m^2 of the radio frequency (RF) wave, or alternatively the electric field strength (E) of the RF wave in V/m, at the receiving node. Connected bandwidth refers to *digital bandwidth*, as opposed to *analogue bandwidth* which is the frequency range between the half power points of an electromagnetic energy wave. This implies that the connected BW will decrease at the same rate as the power

density (or electric field strength) of the RF wave, until the decline in signal to noise (SN) ratio results in termination of wireless communication.

Testing the hypothesis positively is a research goal that motivates the application of the inverse-square law of radiated power to estimate wireless network performance. This novel approach provides the mathematical building blocks that are required to solve range-, and capacity related issues of wireless systems.

1.4 RESEARCH OBJECTIVE AND QUESTIONS

Testing the hypothesis positively is a research goal that motivates the application of the inverse-square law of radiated power to estimate wireless network performance. This novel approach provides the mathematical building blocks that are required to solve range-, and capacity related issues of wireless systems.

Due to the importance of energy saving [6], [24] another research goal is to provide users with a simple method to reduce transmitted power, whilst maintaining their agreed bandwidth throughput rates, with a method that does not require expensive test sets.

Research questions include the following:

Is it possible to evaluate throughput bandwidth rate of a network by observing the quality of a streaming video file at the receiving node?

Is there a mathematical relationship between the transmitted RF power level and the maximum range for a specific QoS bandwidth throughput?

Is there a mathematical relationship between the transmitted radio frequency (RF) power level and the maximum bandwidth throughput for a specific range?

The research objective is to develop a simplified, cost effective method to determine the QoS level reference, or variations thereof, of a wireless Ethernet network applied in IWSNs.

The first task to achieve the research objective is to find an alternative method to determine the committed throughput bandwidth reference in terms of network range.

The second task is to find an alternative method to determine range improvement, as a function of link budget, whilst maintaining the committed QoS bandwidth throughput.

The third task is to find an alternative method to predict bandwidth throughput improvements as a function of link budget (in dB).

Devising a simplified evaluation method to estimate QoS levels depends critically on answering these research questions.

1.5 RESEARCH CONTRIBUTION

This paper proposes a method to determine the excess information rate (EIR) [14], [49] and the committed information rate (CIR) [14], [49] by detection, using the dynamic hysteresis phenomenon. This technique is combined with scaled video streaming to represent the user-defined throughput bandwidth. The d-CIR (detected committed information rate) provides a quality of service reference which conforms mostly to the ITU.Y-1564 test philosophy.

This paper intends to contribute the scientific equations and methods that are required to determine wireless network capabilities, variations and performance. With these it becomes possible to qualify OFDM WLANs in terms of their service performance according to acceptable standards such as Y.1564, which is a key requirement for industrial applications.

1.6 OVERVIEW OF STUDY

1.6.1 The research methodology

The study is based on data obtained from test results that were obtained by physical experimentation, as well as from test results obtained by industry leading chipset manufacturers and wireless modem manufacturers.

Typical test networks were deployed and the transmission characteristics were recorded reflecting connected BW as a function of transmission range whilst observing transmission quality until full signal deterioration. Characteristics were then observed while reducing transmission range until transmission recovery.

1.6.2 The data

The data used was historical in nature at the time it was used. The data reflected the following:

- International transmission standards and specifications of Ethernet networks.
- Radio transmission theory applicable to modern information technologies.
- Typical ISM band wireless Ethernet transmission characteristics obtained from test results obtained by leading industry manufacturers.
- Typical ISM band wireless Ethernet transmission characteristics obtained from experimentation

1.6.3 The samples

The samples were drawn in the quantitative denominations as determined by underlying algorithms contained in the firmware of the wireless AP and node adapters, between predetermined boundaries of interest. The characteristic curves obtained by the drawn samples require mathematical logarithmic averaging, due to the stepped nature of some transmission results obtained.

1.6.4 Data processing methodology

The following steps were taken in the execution of the study:

- A literature study of radio transmission theory and international transmission standards, recommendations and specifications of wireless Ethernet compatible networks was conducted, to consider all options before test and measurement guidelines could be specified.
- Based on the hypothesis formulated in section 1.3, two equations were derived from fundamental principles to express link budget power level in dB as a function of committed throughput bandwidth (BW) in Mbps, or as a function of transmission range (r) in metres.
- Samples were drawn from comparative transmission characteristic curves obtained by physical experimentation within the range and BW delimitations of interest, and are compared with theoretical calculations using the equations as referred to above.
- Discussion and conclusions were then made.

1.6.5 The delimitations

The study considered the development of repeatable experiments with the electronics of typical ISM band OFDM wireless Ethernet networks, including the related test and measurement methodology and components. The study only considered the following factors:

- Performance specifications obtained from experimental analysis of the typical electronic device under test.
- Measurable specifications set after completion of the literature study. Informal testing of the electronics in a locally distributed IWSN.

The study did not consider the following factors:

- Multiple nodes deployed within the wireless network and their respective transmission characteristics.
- The effects on the transmission characteristics of the AP, which is caused by the additional encryption of the information transmitted.

1.6.6 Assumptions

The first assumption is that software based test solutions are sufficiently accurate to obtain meaningful data, and the second assumption is that a multi-media video stream can be converted to video formats of different bitrate speeds. These assumptions are important to note because either may have an effect on the accuracy of test results obtained during experimentation.

1.6.7 Definition of terms

Electronics. All components, products, equipment and systems manufactured for the purpose of processing, storing of transferring data or images by means of electro-magnetic phenomena, but excluding the raw materials from which such items are made.

Compression. Any method to encode or decode transmitted or distributed signals to reduce the required bit-stream rate.

Encryption. Any method to encode or decode transmitted or distributed signals to prevent unauthorised monitoring.

1.7 STRUCTURE OF DOCUMENT

Chapter 1 is the opening introduction, from the problem statement to the overview.
Chapter 2 contains the literature study.
Chapter 3 describes the test environment.
Chapter 4 reveals the results obtained.
Chapter 5 considers data analysis.
Chapter 6 estimates dynamic performance.
Chapter 7 presents discussion.
Chapter 8 concludes the thesis.
References are attached.

CHAPTER 2 LITERATURE STUDY

2.1 CHAPTER OBJECTIVES

This chapter summarises the related work done in the field of IWSNs. Also, the emerging standard ITU-Y.1564 is reviewed in a summary that provides an overall understanding of the parameters that quantify the observed transmission characteristics. A brief review of wireless IP Ethernet provides an understanding of the advantages of this protocol. The chapter is concluded with the analytical approach that considers the related radio theory in terms of the hypothesis formulated and the consequently derived equations.

2.2 RELATED WORK

The related work conducted in this field may be considered in two sub-sections, namely work conducted by industry leading manufacturers of wireless Ethernet routers and works published by academic researchers. Both sources are considered for completeness, and also because both focus mostly on range related QoS issues.

2.2.1 Industry leading manufacturers

The first experiment of significance related to the inverse squared law of radiated power, that is referred to, was conducted by Wavion Technology [30]. The radio transmission coverage of the company's WBS-2400 base station with multiple antenna and transceiver technology was compared to conventional Wi-Fi technology.

The WBS-2400 base station makes use of six radio transceivers each fitted with a +7.5dBi antenna, employing space division multiple access (SDMA) technology and advanced spatially adaptive digital beam-forming to focus radio energy in an optimal manner to network clients on a per-packet basis.

The conventional Wi-Fi made use of a single transceiver and a single +1.3dB antenna. Both sets were tested at +18dBm RF transmitted power. The actual link budget gain in dB may otherwise be calculated as the gain factor of the Wavion antennas (7.5dB), minus the conventional antenna gain (1.3dB), equals 6.2 dB.

In spite of the fact that six transceivers are used, each with its own antenna, the calculated results suggest that the RF power required to double the maximum end of the range, must be increased by approximately 6 dB, which is four times the original value. This is descriptive of the *inverse square law of irradiance,* a typical logarithmic relationship [16].

2.2.2 Published work by academic researchers

Considering the dynamic performance of ISM-band OFDM WLANs, for example the experimental test networks, two analogies emerge that conform to its functional characteristics, namely (i) a radio receiver and (ii) a digital to analogue converter (DAC).

As a radio receiver, the mobile node has to accept a modulated RF signal and demodulate the analogue video signal and corresponding audio sound track(s). As a DAC, the mobile node accepts a complexly digitally coded signal and converts it to an analogue output signal comprising a video signal and audio sound track(s).

In the field of electronics, dynamic range is the ratio of a specified maximum level of a parameter, such as power, current, voltage or frequency, to the minimum detectable value of that parameter. In a transmission system, dynamic range is the ratio of the overload level (which means the maximum signal power that the system can tolerate without signal distortion) to the noise level of the system. In digital systems or devices, dynamic range is the ratio of maximum to minimum signal levels required to maintain a specified bit error ratio for a specific data throughput.

Before the dynamic performance of the test network is estimated, the parameters that are referred to by both the analogies are briefly reviewed, as well as the parameters that are specifically related to each analogy separately [27] – [29].

The prolific use of DACs in the fields of telecommunications and frequency analysing systems necessitate that high speed DACs and their performance be described and specified in the *DAC dynamic performance terms* of frequency, rather than time. Included in the minimum specifications are SNR, THD (total harmonic distortion), total harmonic distortion plus noise (THD+N) and spurious free dynamic range (SFDR). Testing DAC conformance to these parameters requires a high-end synthesized multi-tone signal generator to excite the DAC under test.

In the early 1970s, a popular black box approach to testing DACs and ADCs was prolific [27]. The source ADC under test and its paired DAC were connected in a back-to-back configuration and the ADC was presented with an appropriate analogue signal. The DAC's output, noise and distortion was then measured with an analogue spectrum analyser and the specifications were recorded for the pair as a unit.

The black box approach appeared logical because many signal processing systems required an ADC with a companion DAC and a digital signal processor situated in the centre between. It was obviously not possible to attribute the checksum of errors accurately per cause between these system components. Because modern ADC and DAC components are not necessarily used in pairs any more, they are independently tested and specified [27], [28]. However the black box method remains a useful approach to evaluate a complex system when the internal algorithms and processes cannot be clearly identified.

This study proposes a method to determine the excess information rate (EIR) and the committed information rate (CIR) by detection, using the dynamic hysteresis phenomenon, and to equate these to the SFDR characteristics of the physical layers under test. This technique is combined with scaled video streaming to represent the user defined

throughput bandwidth. The d-CIR (detected CIR) provides a quality of service reference, which conforms mostly to the ITU.Y-1564 test philosophy.

This study intends to also contribute the scientific equations and methods that are required to estimate wireless network capabilities, variations and performance during industrial deployment or field tests, according to the well-known SFDR parameters. With these it becomes possible to compare OFDM WLAN physical layers in terms of their service performance, not only according to acceptable standards such as Y.1564 which is a key requirement for industrial applications, but also the well accepted SFDR parameters [27], [28], [29].

Previous work in the field of QoS estimation [31, 32] suggests the use of predetermined bitrate streams of MPEG (motion pictures experts group) video in order to determine the main contributing key performance indicators of video degradation, in both cases frame loss. The focus of some other published work was to estimate the perceptual QoS (pQoS) in order to adjust the transmission content by scaling the video code and the application of multi-dimensional bitrate techniques in order to improve the end-user's video quality [31].

Lee et al. observed the hysteresis phenomenon [33] that manifests itself as the *ping-pong effect*, where a node that ambulates within the SLDZ disconnects. Due to near-node far-node effect [34], the cell size increases and the node reconnects. Once connected, the cell size shrinks and the node disconnects, and so on. The paper [33] focuses on reducing the *ping-pong effect* and describes the typical green, yellow and red zones for node deployment but does not indicate how to determine these zones.

Some researchers focused on optimal node placement [34]–[37], while others investigated the relationship between QoS and SNR [38] and QoS and the protocol used [39].
Several papers indicate that predicting wireless link variations remain a challenging task [40]–[45], along with security and the effects of security protocol on the wireless link capability [46], [47], and [48].

2.3 ITU-Y.1564 ETHERSAM TEST STANDARD

With Ethernet's continuous evolvement as the preferred technology for data transport and service, telecommunication networks, Internet service providers (ISPs) as well as device manufacturers are directing their business activity towards broadband networks and multimedia products such as *apps* that may be traded as a result. The mere provision of electronic data communications appears to have become extremely competitive. For example, legacy monopolies such as Telkom now has to compete with liberalised entities like Neotel for the fixed-line market and with experienced GSM/mobile operators for the smartphone/tablet market share.

A variety of applications based on voice, video or data (sounds, pictures or messages) are now supported by OFDM Ethernet for mobile 3G, LTE, mobile Wi-Fi and ISM band technology. ISM is particularly interesting to WSNs. The new applications require increased network performance and so necessitate that more stringent methodologies be applied by operators to make sure their broadband products are up to the expected standard and meet their clientele's service demands.

The following section briefly reviews a summary of the *Ethernet Service Activation test Methodology* (EtherSAM), as standardised by the International Telecommunications Union in ITU-T Y.1564 [14]. Y.1564 is a modern measurement philosophy and technical standard that advises on installation, commencing service, technical configuring and performance estimation of broadband Ethernet service.

Accepted as a modern cutting edge standard, EtherSAM proposes a suitable procedure for service-level agreement (SLA) validation with a single test at a sufficiently high level of accuracy.

2.3.1 Modern network requirements

Modern broadband networks based on Ethernet are required to service *in-time* as well as *mission-critical* applications and solutions. The term *service* refers to the provision of

electronic communication that the network must establish in order to meet its intentional requirements. Data traffic on a broadband network can be grouped into three distinct types as indicated in Table 2.1; normal error-corrected data, in-time data and mission critical data (high priority).

Table 2.1. Grouping of network traffic types

Traffic Type	Applications	Service examples
Normal data	Error-corrected data transport (no in-time data)	Normal data, Internet, FTP service, storage/server applications
In-time data	In-time transmitted data that is not possible to be reconstructed if erroneously received	VoIP, streaming video, IPTV, IP radio, video conferencing, on-line gaming
Mission critical (high priority)	System data that maintains stability in the network	Network synchronization, OAM frames, routing control, frame switching

The different types of traffic are each affected in another manner by the network's characteristic features and must be prepared and processed to achieve specified performance expectations.

To be able to guarantee QoS, networks have to be correctly configured otherwise traffic prioritization cannot be implemented in the network. Traffic prioritisation is possible after firstly the assignment of priority levels of different weights to each type of service and secondly to accordingly configure the appropriate (algorithmically based) prioritization process.

The method which is used to grade the traffic of different services into prioritized groups with the use of specific inherent fields within the frame information is what the QoS assurance refers to, and it provides better service to some frames, compared to others. A network element is thus allowed to distinguish between traffic types and so in this manner sort network traffic by priority.

2.3.2 Importance of the service level agreement (SLA)

In commercial terms, the SLA is a legal document in which the service provider guarantees the performance of the service it offers to its clientele. This becomes a legal agreement when the client accepts the service at a specified price. The SLA specifies the minimum performance and the critical forwarding characteristics that are guaranteed for each characteristic in Table 2.2:

Table 2.2. Critical forwarding characteristics

Type of traffic or data	In-time	Mission critical	Best-effort
CIR (green) in Mbps	5	10	2.5
EIR (yellow) in Mbps	0	5	5
Frame delay (ms)	<5	5-15	<30
Frame delay variation (ms)	<1	not applicable	not applicable
Frame loss (%)	<0.001	<0.05	<0.05
VLAN	100	200	30

Traffic types are grouped into three separate conditional classes, and each is tagged with an identifying colour where green is for CIR traffic, yellow for EIR traffic and red indicates the conditions at which traffic is dropped, as indicated in Table 2.3.

Table 2.3. Customer traffic classes

Traffic class	Range indicated	Traffic type	Conditions
Green (G)	0–CIR	Certified	KPIs certified in spec
Yellow (Y)	CIR–EIR	Best effort	KPIs not certified in spec
Red (R)	>EIR	Discarded	n/a

CIR (Green): Refers to the data rate that is certified to be available for a specific service level; for CIR traffic the KPIs are certified to conform to specifications.

EIR (Yellow): Refers to the data rates higher than CIR that may be obtained but for which the KPIs are not certified to conform to specifications.

Discarded (Red): Refers to the data rates that are higher than EIR rate. No attempt is made to forward this data because it will affect other services, and therefore it is dropped or discarded.

2.3.3 Key Performance Indicators (KPIs)

A number of the inherent characteristics features of the network's data profile will have a direct and immediate effect on network performance and so also the QoS. These are known as KPIs and must be guaranteed for all transmission under the green traffic condition. The four main KPIs are:

1. Bandwidth

This is the term for the *quantity of data bits transmitted during one second*. Bandwidth is therefore also a term for the highest rate of data that can be sent across the network. Bandwidth can be classified as *committed* or *excess* with correspondingly different performance guarantees. When multiple services share a link, bandwidth must be controlled. Each service must be limited evenly so that the other services are not affected. Exceeding the bandwidth limitations results in frame loss and slows down the network due to the process of buffering frames for data integrity purposes, eventually termination service communication.

2. Latency

Also known as frame delay, latency is the parameter that indicates the time it takes to transmit a data packet to a receiving node. This measurement is typically based on time domain reflectometry (TDR) because it similarly determines the time taken for the transmission from the source to the destination as well as the time taken from the destination back to the source. This parameter is specifically crucial for audio and video transmission because a too high latency figure will have adverse conditions on reception quality resulting in echoes, incoherent conversations, distorted video or dropped links.

3. Errors

Frame loss occurs as a result of data errors that may be related to transmission distortion or noise sources as well as too much traffic or the network. Some transmission errors occur during frame transmission due to a physical phenomenon noted in the area of field comparison which is a term for checking of the frames' proper sequencing. It results in the network elements like routers and switches dropping frames. Network congestion also

causes frame loss errors, because networking elements must drop frames to prevent link saturation in congested network traffic conditions.

4. Jitter

Also known as packet jitter or frame jitter, this parameter indicates the variance in packet transfer time or frame delivery. Because packets are transmitted from node to node to their end destinations they are often queued in a network. Thus packets are transferred during short time frames at high speeds in a burst-like fashion. Prioritised randomly, packets are then being transmitted at randomly variable data rates. Frame jitter then occurs when packets arrive at variable time intervals. In-time broadband applications like video and audio are specifically affected by frame jitter. The design requirement of modern buffers therefore compels the temporarily storage of a specific number of audio or video packets, which are then re-sequenced to promote a smoother reception at the receiving node. Table 2.4 shows the effects of KPIs on different traffic types. The effects are classified in three typical groups: *Extreme* effect renders the traffic unusable. *Noticeable* effect means throughput is possible but affected by the deteriorating KPI and thus cannot be guaranteed. *No* effect means KPI does not affect the traffic throughput at all.

Table 2.4. Effects of KPIs on different traffic types

KPIs	**Normal data**	**In-time data**	**Mission-critical data**
Bandwidth	Extreme effect	Noticeable effect	Noticeable effect
Errors	Extreme effect	Extreme effect	Extreme effect
Latency	Noticeable effect	Noticeable effect	Noticeable effect
Jitter	No effect	Extreme effect	No effect

2.3.4 Previous testing methodology: RFC 2544

For some time, RFC 2544 was the preferred methodology for Ethernet acceptance tests [13]. Originally developed as standard method for benchmarking interconnecting devices in laboratories, it was also used for field-testing Ethernet. RFC 2544 enabled measurement of throughput, frame loss, latency and burst ability. However RFC2544 can no longer fully certify Ethernet because it does not consider packet jitter or QoS measurements.

2.3.5 Improved testing method: EtherSAM (ITU-T Y.1564)

To solve the problems experienced with previous methodology, the International Telecommunications Union has approved a measurement standard known as the ITU-T Y.1564 [14]. EXFO was the test equipment manufacturer to initially incorporate ITU-T Y.1564 into its Ethernet testing products [49], termed *EtherSAM,* which is the industry used acronym for *Ethernet Service Acceptance (testing) Methodology*. EtherSAM's approach that service performance evaluation considerations are separated in two different groups: *First*, the technical configuration of the network elements and *second*, the network service performance when subject to excessive traffic loading.

1. Service reference and technical configuration

Network elements comprise the basic topology of any network that interconnects different segments. The network elements must therefore be suitably set up to accommodate the CIR reference otherwise results obtained during performance evaluation will not be valid.

2. Service Performance

The capability of a network to carry more than one CIR service is called service performance. It refers to service without any compromise to KPIs below acceptable levels. As network elements are loaded with increased traffic, they prioritise traffic flow performance failures may then become be the result.

EtherSAM focus on three aspects of service testing:

- First, as a confirmation tool the methodology ensures that the network functions correctly and is suitably configured to conform to the CIR in terms of the SLA for a specific service within the committed range at specific rates.
- Second, as a certification tool the methodology confirms that KPI performance objectives are met certifying the network to conform to specifications under maximum load.
- Thirdly, as a soak test tool, service testing can be conducted over extended test periods, to check that network elements function while operating under stress.

2.3.6 Tests/subtests

Referencing and performance evaluation comprises two distinct groups of tests: the service reference tests and the service performance tests [49].

1. Service reference testing

The service reference test determines the CIR reference bandwidth and EIR reference bandwidth for a specific service. It is a per-service test that defined by the end user. Three key phases are followed in the process which observes all KPIs simultaneously.

1st Phase: *Bandwidth range between minimum and CIR*

During the first phase, the data throughput or service rate is gradually increased in steps from the minimum speed to the CIR. This confirms the network capability to deliver a service at a specific predetermined throughput speed. It provides a safe manner in which to speed up performance while monitoring the network for unacceptably early KPI compromise in the event that the network or its elements are not properly set up.

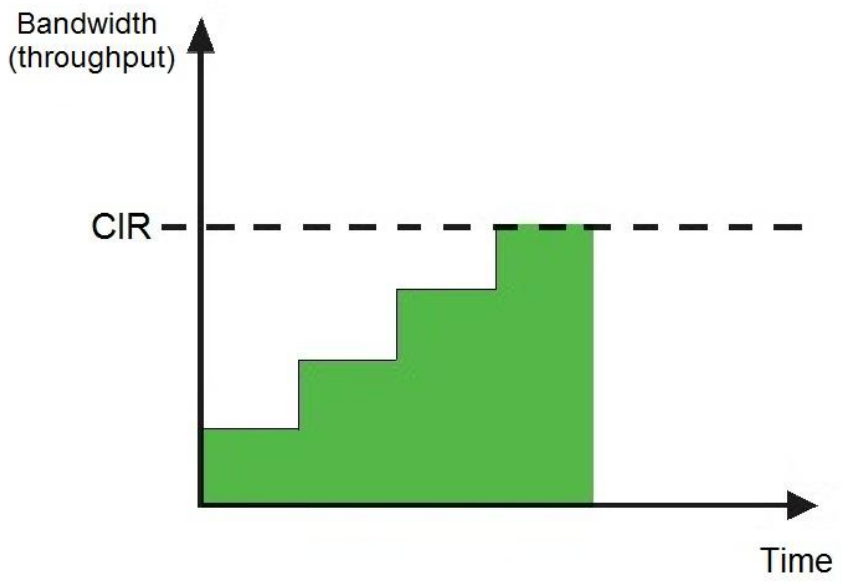

Figure 2.1. Phase 1 testing. Adapted from [14], with permission.

The system monitors the KPIs automatically during steps, as the speed is gradually increased in steps up to the CIR, so to make sure that the minimum service reference performance objectives are met. The test phase fails if any performance objective fails. All performance objectives during the gradual speed-up must be met (in terms of the CIR) for this phase to pass.

2nd Phase: *Between CIR and EIR*

During this sub-test, the speed is gradually increased in steps from the CIR to the EIR. It measures the speed at which EIR is reached and confirms further that network is suitably set up for optimal transmission performance. KPIs are not evaluated as per accepted principles, and therefore EIR performance cannot be guaranteed.

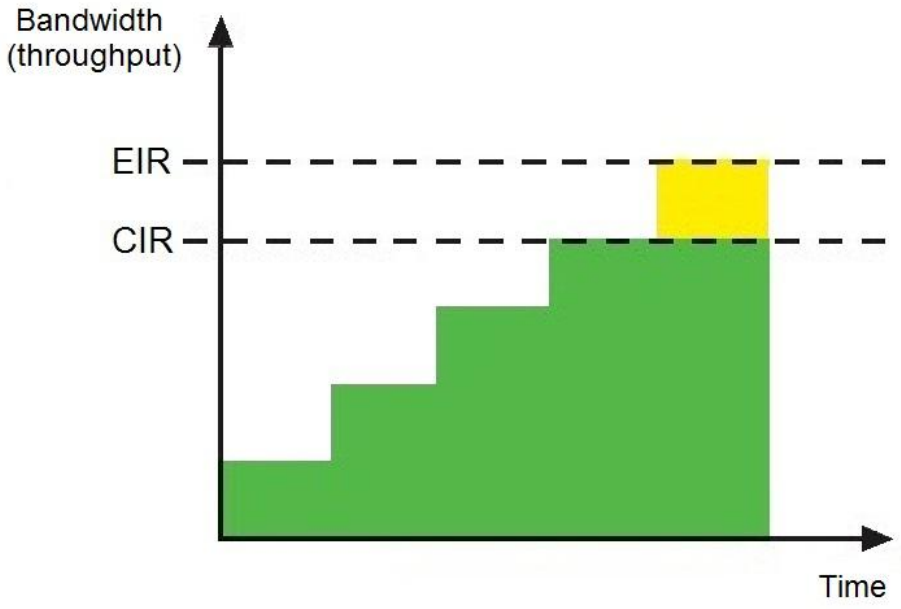

Figure 2.2. Phase 2 testing. Adapted from [14], with permission.

Figure 2.2 indicates EIR relative to the CIR and thereby also the *yellow* region. Not all data speeds higher than CIR will be possible in the yellow region. A positive test evaluation condition validates the CIR reference and reveals the EIR as the maximum data speed obtained during the test. Any speed lower the CIR is considered as unsuccessful and thus a failed test.

3rd Phase: *Overload testing*

Packet transmission is characterised by its ability to communicate data in bursts. During transmission bursts, conditions may occur when data speed exceeds the EIR, which result in dropped packets.

During this phase, traffic is transmitted at a rate higher than the EIR while monitoring the received rate, as indicated in Figure 2.3. Firstly, the CIR reference must be obtained. The EIR would also be achieved depending on network congestion/resources.

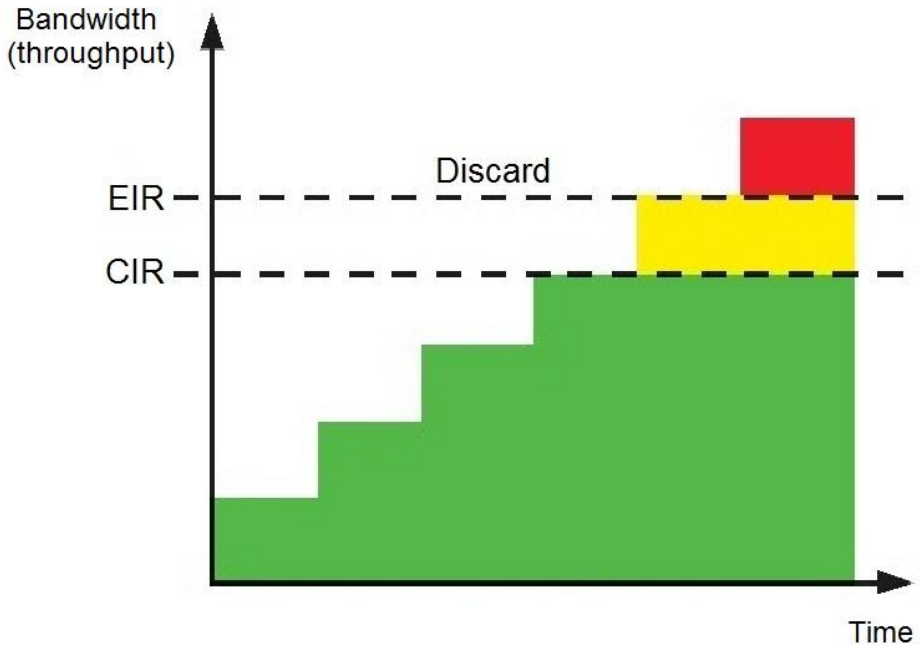

Figure 2.3. Phase 3 testing. Adapted from [14], with permission.

Figure 2.3 indicates the red zone where traffic should be dropped. To prevent overloading, any data rate higher EIR should be discarded. When data rates are received that are higher than the EIR it indicates a network element that is not suitably configured, and declares a failed test.

In summary of reference testing: The three test phases are executed per service; for multiple services each service should be tested sequentially. This determines the CIR reference bandwidth and maximum service performance of that specific service.

The Ethernet service reference test provides a clear evaluation of the network elements and the serviceability of their technical configuration to communicate applications whilst maintaining acceptable QoS.

2. Service performance evaluation

The service performance evaluation specifically focus on the QoS parameters like KPIs by simulating all committed in-time services, whereas the service reference test focus only on determining the CIR reference for a single service and the suitable technical configuration of the network elements.

All configured services are committed simultaneously at equal CIR in this test for a soak test duration which may take minutes or days according to test requirement. Services are individually monitored during this period and a ‘fail’ condition is declared if KPI parameters fail for any individual service.

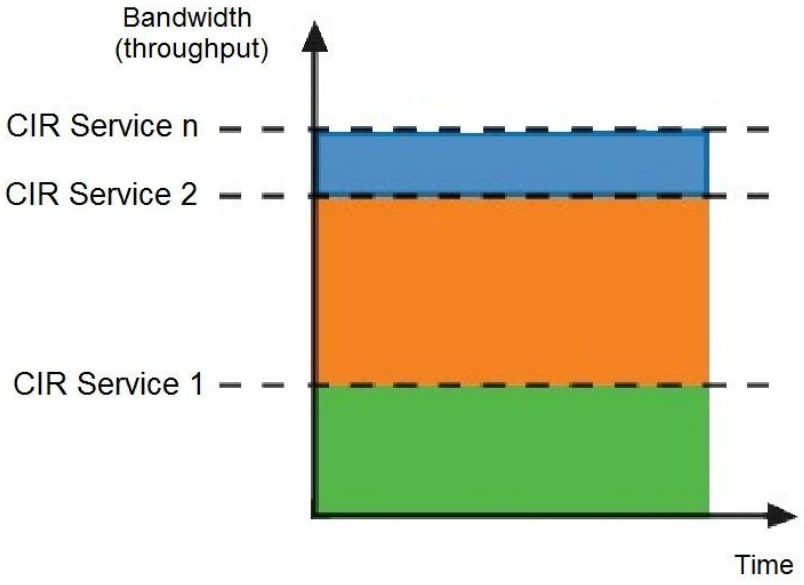

Figure 2.4. Service performance test. Adapted from [14], with permission.

The two tests reviewed above provide a complete test methodology and collect all the crucial results in a single simplified procedure. Configuration faults are quickly identified for services as well as the network elements along the network links. The final test then concentrates on the network's simultaneous all-services capacity. The circuit is ready to be commissioned once both phases are evaluated and passed.

2.3.7 Summary EtherSAM

To be applied in the modern industrial arena, Ethernet services must be reliably evaluated. Assessing performance with the previous RFC 2544 method is insufficient to commission or activate modern services with confidence. EtherSAM provides a simplified philosophy and approach to bridging the gap between service validation and performance assessment, and is therefore favourably considered as a model to measure wireless Ethernet transmission in the ISM bands.

2.4 WIRELESS ETHERNET

Wireless Ethernet is one of many ways to establish a network in order to connect computers and share information. This section will briefly discuss wireless networking in terms of technology that enables it.

2.4.1 Wireless networking

With wireless networking, radio signals is the medium across which the nodes (or computers) communicate their information. It renders computers completely mobile and interconnected, for example, a tablet, notebook, laptop or smartphone can communicate with each other using radio signals even while displacing their physical positions but within the range limits.

Modern networking opportunities of the day are compelling service providers to establish dispersed Wi-Fi hotspots for connectivity, as opposed to previous 3G base stations, in order to extend customer mobility demands which have become prolific with smartphones and bandwidth appetite.

In wireless terms, most networks are configured to function as a client/server. Nodes connect and communicate across a common access point, which regulates data flow to and from the wireless adapters installed in each computer.

Before considering Wi-Fi, it is necessary to review the IEEE's wireless-Ethernet standards known as IEEE 802.11. This series specifies data speeds and frequency plans and originally envisaged two methods of communication between nodes. Both methods, namely FHSS (frequency-hopping spread spectrum) and DSSS (direct-sequence spread spectrum), use frequency-shifted-keying (FSK) modulation, which is also used in power-line communications. Both methods are operating in the 2.4 GHz range and are based on spread-spectrum radio waves.

Devices using direct-sequence spread spectrum send data at any time in packets across a predetermined number of separate frequencies in the specified ranges that are available for use. Devices with DSSS communicate through multiplexing data into several streams and sending them at the same time on separate frequencies. DSSS consumes a relatively large span of bandwidth, typically around 22 MHz.

FHSS means that data is sent a short burst, the frequency is adjusted (frequency shift or hop) and the next short burst of data is sent. The FHSS communicating devices use predetermined frequencies to shift to and pause at each for a relatively short period (less than 400 milliseconds) before shifting on.

More than one independent FHSS network can operate within the same radio access limits and not interfere with one another. FHSS radios transmit data just two to four frequencies at the same time and therefor consume only 1 MHz or less of bandwidth.

2.4.2 Wireless adapters

The actual wireless transceiver, also known as the wireless adapter, is constructed in ISA, PCI, PCMCIA or USB card together with a small integrated antenna. Modern computers and smartphones contain wireless adapters either within the processor chipset or integrated within motherboards. Adapters operate according to acceptable standards for example IEEE 802.11, which enables nodes to connect at the highest designated speed under suitable conditions and manages connected bandwidth against transmission conditions.

2.4.3 WECA and Wi-Fi

Wireless Ethernet was standardized by WECA (wireless Ethernet compatibility alliance). The popular *Wi-Fi* (wireless fidelity) mark on products is a confirmation that the electronics comply with the IEEE specification known as IEEE 802.11b. [50]. This standard employs DSSS because of its higher data speed capability over FHSS.

Nodes connect at 11 Mbps with IEEE 802.11b whenever possible. If data is disrupted by any reason like reduced signal, distortion or noise, connection speed will be reduced by

approximately one half to 5.5 Mbps, or 2 Mbps and eventually to 1 Mbps. This stepped reduction in bandwidth in order to maintain connectivity is managed by on-chip firmware algorithms within the wireless adapter. This keeps the network stable and extremely reliable although it may occasionally slow down. IEEE 802.11b makes use of the 2.4 GHz band and is an extended specification of IEEE 802.11.

2.4.4 OFDM WLAN

IEEE 802.11a specification employs OFDM and makes use of the 5 GHz frequency plan. The possible data rates for IEEE 802.11a are 6, 9, 12, 36, 48 and 54 Mbps.

IEEE 802.11g specification also uses OFDM for speeds of up to 54 Mbps in the 2.4 GHz frequency plan. This standard meets the IEEE 802.11 *x/EAP* security standard and remains reversely compatible with existing IEEE 802.11b devices. The connecting speeds for IEEE 802.11g are 1, 2, 3, 4, 6, 9, 12, 18, 24, 36, 48 and 54 Mbps. With MIMO incorporated, connecting speed of 108 Mbps is possible.

Wi-Fi's advantages are that it is reliable and fast with a reasonable operating range. It can be connected with existing wired-Ethernet networks. The disadvantages are fluctuating speed and range, and some products can be difficult to configure.

Wi-Fi offers Ethernet speeds wirelessly. Wi-Fi depends on access points, which can cost from a few hundred rand upwards. Many access points operate at router level (OSI level 3) and some at gateway level (OSI level 7) which means they can interconnect dissimilar networks.

Most Wi-Fi access points incorporate an omni-directional antenna to communicate in all directions with other the wireless transceivers [51]. Notably, Apple's Airport access point which was designed specifically for Apple computers, will also accept signals from any 802.11b/g/n adapter.

Discrete Wi-Fi transceivers are mostly available in USB configuration, although, the PCMCIA card type may still be available. In the future Wi-Fi will be integrated on all communicating devices [50].

LTE (long term evolution) is a new mobile standard that will replace legacy GSM/3G systems, now aggressively adopted by all smartphone and tablet manufacturers. The extremely low cost availability of access points and built-in wireless adapters in virtually every device available has resulted in the explosive use of wireless Ethernet.

2.5 RADIO DYNAMIC PERFORMANCE

For any radio receiver, the noise performance and therefore the signal to noise ratio (SNR) is a crucial parameter. The SNR is an indication of the sensitivity performance of a receiver. For all applications of radio and electronic communications, this is of prime importance [52].

Receiver sensitivity of a can be determined by comparing the signal level to the noise levels for a known signal, which is expressed as the SNR. The higher the value of the SNR, the better is the radio receiver sensitivity performance.

The front end RF amplifier should be a low noise amplifier because it is regarded as the most crucial in terms of the overall receiver sensitivity. The reason for this is the fact that the noise added to the first RF amplifier will be amplified and added by all cascading amplifier stages as well.

2.5.1 Concept of SNR

The SNR is the simplest method to indicate the sensitivity of a radio receiver, and therefore widely accepted as a measure of receiver sensitivity.

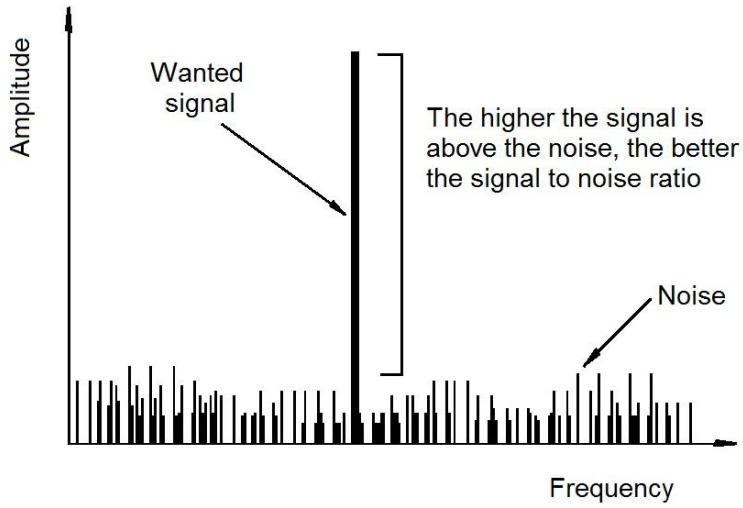

Figure 2.5. Concept of SNR

Figure 2.5 depicts the signal elevation above the noise. S/N is preferably shown as a ratio, in dB. The input signal level is usually expressed in microvolts and must be provided to determine SNR because the signal input is part of the equation.

Receiver sensitivity may typically be expressed as a certain minimum input signal level in microvolt that results in a predetermined SNR, for example, 10 dB for AM radio.

SNR may be expressed as:

$$SNR = \frac{P_{signal}}{P_{noise}}$$

It can also be expressed from a logarithmic basis using decibels:

$$SNR_{dB} = 10\ Log\ \frac{P_{signal}}{P_{noise}}$$

The expression may be simplified, if all levels are expressed in decibels:

$$SNR_{dB} = P_{signal_{dB}} - P_{noise_{dB}}$$

These power levels may be expressed in any form by which the levels can be compared in dB terms, such as dBm (decibels relative to a milliwatt).

Bandwidth effect on SNR

The bandwidth of the receiver is one of a number of factors that affects the SNR specification. It is noted that, as the receiver bandwidth increases, so increases the noise level, because noise spreads out over all frequencies. The receiver bandwidth therefore needs to be specified according to its SNR.

It is also noted that the AM level of modulation has an effect on SNR. The reason for this is found in the method to measure the noise performance by measuring the receiver output and so also the AM effects that modulation has on SNR. For AM SNR the measurement is specified for 30% modulation level.

SNR specifications

For HF communications receivers, the SNR method of measuring sensitivity is preferred. Typically, for SSB or Morse, a sensitivity 0.4 μV for a 10 dB S/N may be expected for a 3 kHz bandwidth. Typical sensitivity for AM is 1.4 μV for a 10 dB S/N, with a 5 kHz bandwidth and 30% modulation.

2.5.2 SINAD and SINAD measurements for radio receivers

The SINAD is another parameter used to evaluate receiver sensitivity performance. For any radio communication device, the SINAD also indicates the extent to which the signal is degraded at a specific range by unwanted distortion or noise signals. However the SINAD is the preferred measurement that is widely used for specification of modern receiver sensitivity.

The SINAD equation can be derived from the ratio of the useful signal power level to the unwanted signal power level, which equals (Psignal + Pnoise + Pdistortion)/ (Pnoise +

Pdistortion). Therefore, as the SINAD improves, so improves the quality of the demodulated receiver output signal.

SINAD (dB) can be expressed by a simple equation:

$$SINAD = 10\ Log\ \frac{SND}{ND}$$

where:

SND = algebraic sum total of signal, noise and distortion power levels

ND = algebraic sum total of noise and distortion power levels

Note that SINAD is only expressed in terms of power with this equation, and not in terms of voltage ratio.

1. Conducting SINAD related measurements

The figures for the signal/noise/distortion and noise/distortion levels are acquired by measurement using suitable test equipment that usually comprise a standard signal generator with attenuator setting as well as receiver output analysis equipment such as band-pass filter and frequency analyser.

The parameters obtained by receiver input/output measurements are used in a simple calculation to determine the value of SINAD for a receiver or any specific device under test.

2. SINAD applications

The (audio or video) output signal quality of a receiver can be assessed using the SINAD, when the receiver is used under various different signal conditions. It can therefore also be used to assess different categories of receiver performance.

Receiver sensitivity: To evaluate the sensitivity radio receiver is the most common use of the SINAD parameter. The sensitivity can be determined by observation of the RF input

signal level for a SINAD of 12 dB. This value is used because it implies noise+distortion level of 25% for a 1 kHz modulating tone. Other conditions also need to be specified, such as the modulation depth and tone for AM as well as the level of frequency deviation for FM. For analogue FM systems, a 12.5% deviation level of channel frequency is specified by ETSI. For a typical VHF receiver, sensitivity may be stated as 0.24 μV for 12 dB SINAD. The smaller the RF input signal voltage for a 12dB SINAD, the better the receiver performance level.

Adjacent channel rejection: The receiver capability to reject adjacent RF channel frequencies is called adjacent channel rejection. It was noted that the SINAD value degrades as the level of an adjacent channel frequency increases. This degrading in SINAD performance in the presence of adjacent signals can be used as a measure to express adjacent channel rejection.

SINAD is a useful measure to estimate receiver performance in a variety of situations. Mainly used for VHF systems, it is also applied HF (AM and SSB) and in various radio communications links. Typical SINAD value for VHF systems is 12 dB, although higher frequency systems will require corresponding higher values, typically between 13 and 15 dB.

The overall figure for SINAD depends mainly on the noise rejection of the first RF amplifier in any radio receiver. A low noise amplifier at the front end always provides a good overall SINAD performance.

SINAD can also be used to evaluate digital radio systems, although a method known as bit error rate (BER) testing is popularly used by IT engineers. However BER measurements do not allow for data packet sequencing challenges such as frame loss or frame jitter as experienced in modern video streaming applications.

2.6 DAC DYNAMIC PERFORMANCE

The prolific use of DACs in the fields of telecommunications and frequency analysing systems necessitate that high speed DACs and their performance be described and specified in terms of frequency, rather than time. Included in the minimum specifications are SNR, THD (total harmonic distortion), THD+N (total harmonic distortion plus noise) and SFDR spurious free dynamic range. Testing DAC conformance to these parameters requires a high-end synthesised multi-tone signal generator to excite the DAC under test.

In the early 1970s, a popular black box approach to testing DACs and ADCs was prolific [27]. The source ADC under test and its paired DAC were connected in a back-to-back configuration and the ADC was presented with an appropriate analog signal. The DAC's output, noise and distortion was then measured with an analogue spectrum analyzer and the specifications were recorded for the pair as a unit.

The black box approach appeared logical because many signal processing systems required an ADC with a companion DAC and a digital signal processor situated in the centre between. It was obviously not possible to attribute the checksum of errors accurately per cause between these system components. Because modern ADC and DAC components are not necessarily used in pairs any more, are independently tested and specified [27], [28].

2.6.1 Measuring distortion and noise of a high speed DAC

Figure 2.6 depicts the typical test configuration to measure a DAC's distortion and noise. The generation of the digital signal to drive the DAC is the primary consideration. This can be obtained by programmable arbitrary waveform generators such as the Tektronix AWG2021 or digital word generators such as the Tektronix DG2020. High grade instruments such as these are minimum specifications for accurate testing of DACs in terms of the frequency domain [27].

These generators have standard simple waveforms pre-programmed in most cases, such as multi-tone sine and triangular waves for example, as well as the capability to generate complicated test-specific digital waveforms which are required for communications applications such as GSM, QAM and CDMA test signals[28], [29]. These can drastically improve the duration of evaluation process.

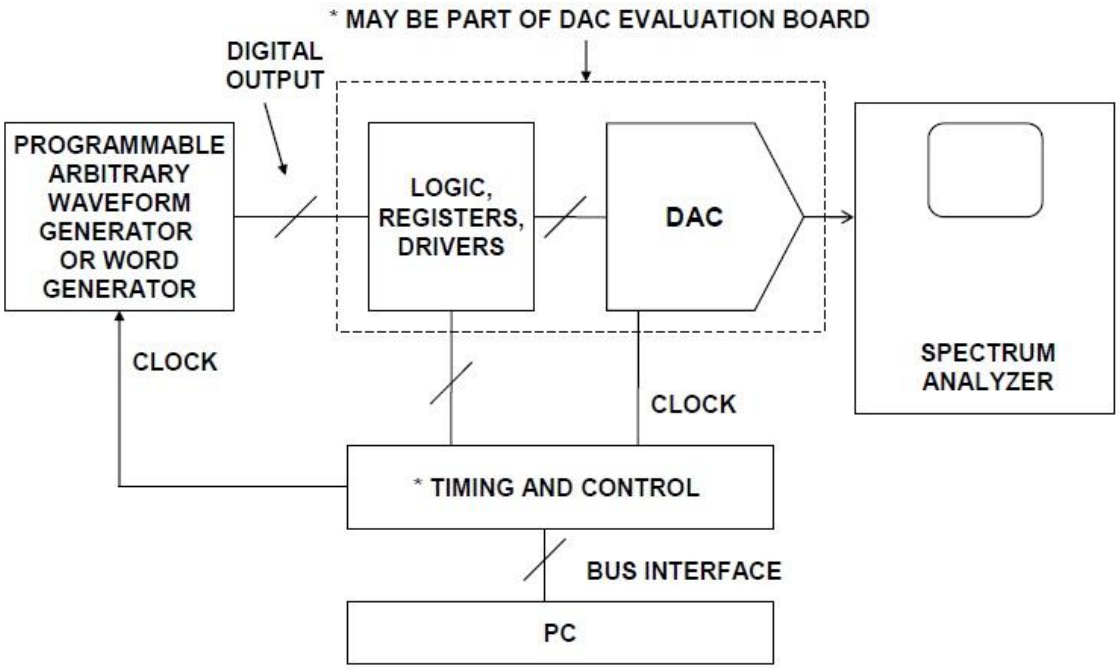

Figure 2.6: Test configuration to measure DAC noise and distortion. Taken from [29] with permission.

Manufacturers of high performance DACs like *Analog Devices* and others, provide evaluation boards to simplify interfacing which the test equipment. These boards conveniently interface with PCs across USB, parallel, or serial ports.

Adjusting the various DAC modes and options requires Windows®-based software for many of the telecommunications DACs like the TxDAC® that have extensive on-chip control logic.

It is somewhat easier to test a DAC which is part of a direct, digitally synthesized system because no digital signal generator is required. To test these DACs only requires a spectrum analyzer, evaluation board, PC and a stable time reference.

The task of measuring the noise and distortion parameters such as SFDR, THD, SNR and SINAD is much simplified if a suitable spectrum analyser is used. The resolution bandwidth setting on the analyser must be sufficiently reduced to be able to resolve the harmonic products higher than the noise floor. A typical high speed DAC output within the frequency domain is depicted in Figure 2.7 [29].

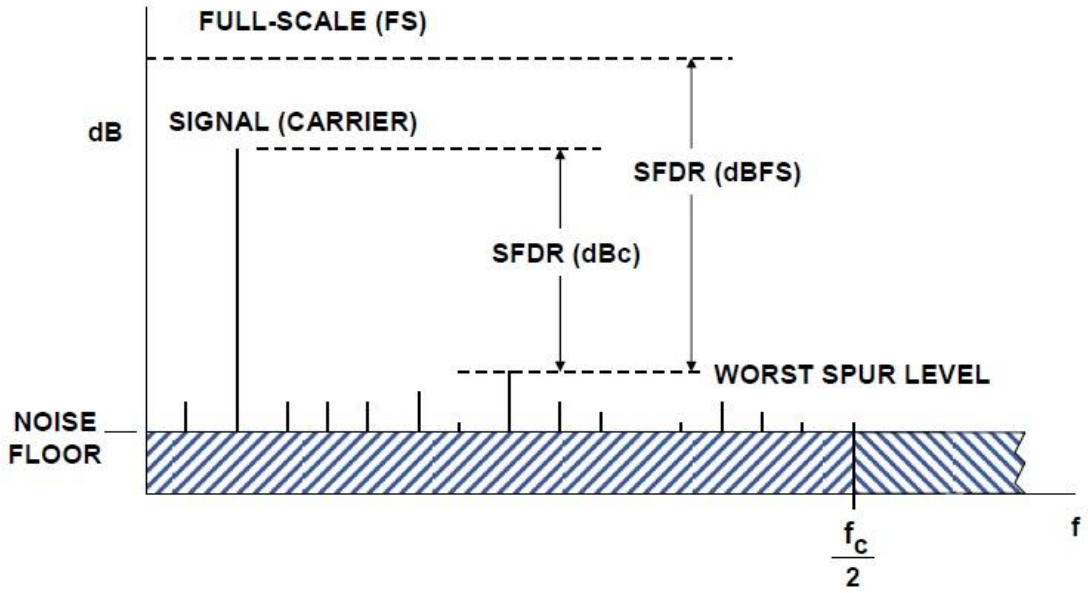

Figure 2.7: Typical high speed DAC output within frequency domain. Taken from [29] with permission.

Figure 2.7 indicates the key parameters that are required to estimate the dynamic performance of a high speed DAC. Note that when the signal carrier level is set to the minimum value for acceptable throughput of the specified input range of frequencies, SFDR (dBc) may be equated to *BW SINAD* (dBcir) previously described.

2.7 ANALYTICAL APPROACH TO BASIC UNDERLYING THEORY

In order to test the hypothesis, samples were drawn from the results obtained by measurement as described in Chapter 3. These samples were then processed with an equation $dB = 20Log\frac{r_2}{r_1}$ (3), which is based on the inverse square law of irradiance (or radiated power) and derived from first principles later in this section. Each of the processed results is compared with the expected value.

The hypothesis formulated is that connected bandwidth (BW) in Mbps is directly proportional to the power density (P_D) in Watts/m^2, or to the electric field strength (E) in V/m, of the RF wave at the receiving node. The hypothesis motivates the application of *the inverse square law of irradiance* [52] to estimate wireless network performance.

The point source radiator or isotropic antenna has to be considered in the study of the radiated field from the antenna. Practical antennas and their performance are often referenced in terms of this basic radiator [52].

2.7.1 Derivation of the range equations

As illustrated in Figure 2.8, energy radiates equally in all directions from the isotropic antenna; therefore the spherical radiation pattern in any plane is circular, for example in the ground plane.

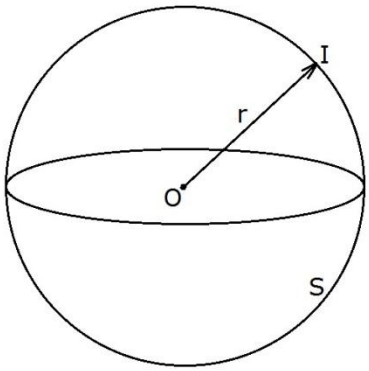

Figure 2.8. Isotropic radiator

The isotropic radiator depicted in Figure 2.8 is supplied with a power of *P* watts at the origin *O*. The power flows outward from this point and through the spherical surface *S*, which has a radius *r*.

The intensity of radiation i.e. the power density P_D at point I can be defined as [52]:

$$P_D = \frac{P}{4\pi r^2} \qquad Watts/m^2$$

This equation illustrates the effects of the *inverse square law of irradiance*: At twice the range (2 x *r*), with *P* at a constant, the power density P_D decreases by a factor of four or by -6 dB. Also, to obtain the same P_D at double the range (2 x r), the power P would have to increase fourfold or by +6 dB.

Maxwell's theorem defines the relationship between the power density P_D and the E-field and H-field vectors as follows [53]:

$$P_D = E \times H \quad Watts/m^2$$

The absolute magnitude of the power density or intensity of irradiation is thus

$$|P_D| = EH = \frac{E^2}{120\pi}$$

where impedance of free space is 120π, which is approximately 377Ω.

According to the inverse square law, the ratio of two power densities at their respected ranges from the source of radiation can be expressed in terms of the link budget, in decibel:

$$Link\ budget\ (dB) = 10\ Log \frac{\frac{P_{D_1}}{r_1}}{\frac{P_{D_2}}{r_2}} \quad \ldots\ldots\ldots\ldots\ldots\ldots\ldots\ldots\ldots\ldots (1)$$

Manipulation yields:

$$Link\ budget\ (dB) = 10\ Log \frac{P_{D_1}}{P_{D_2}} \times \frac{r_2}{r_1}$$

Since $P_D = E^2/120\pi$ [52]:

$$\therefore Link\ budget\ (dB) = 10\ Log \frac{\frac{{E_1}^2}{120\pi}}{\frac{{E_2}^2}{120\pi}} \times \frac{r_2}{r_1}$$

$$\therefore Link\ budget\ (dB) = 10\ Log \frac{{E_1}^2}{120\pi} \times \frac{120\pi}{{E_2}^2} \times \frac{r_2}{r_1}$$

$$\therefore Link\ budget\ (dB) = 10\ Log \left(\frac{E_1}{E_2}\right)^2 \times \frac{r_2}{r_1}$$

But according to the hypothesis, the electric field strength *E* is directly proportional to the connected bandwidth *BW*:

$$\therefore Link\ budget\ (dB) = 10\ Log \left(\frac{BW_1}{BW_2}\right)^2 \times \frac{r_2}{r_1}$$

$$\therefore Link\ budget\ (dB) = 20\ Log \frac{BW_1}{BW_2} \times \frac{r_2}{r_1} \quad \ldots\ldots\ldots\ldots\ldots\ldots\ldots\ldots\ldots\ldots (2)$$

Assuming bandwidth $BW_1 = BW_2$, then the ratio of the two respective ranges may be expressed as:

$$Link\ budget\ (dB) = 20\ Log \frac{r_2}{r_1} \quad \ldots\ldots\ldots\ldots\ldots\ldots\ldots\ldots\ldots\ldots\ldots\ldots\ldots\ldots\ldots (3)$$

Also, assuming range $r_1 = r_2$, then the ratio of two bandwidths may be expressed as:

$$Link\ budget\ (dB) = 20\ Log \frac{BW_1}{BW_2} \quad \ldots\ldots\ldots\ldots\ldots\ldots\ldots\ldots\ldots\ldots\ldots\ldots\ldots\ldots\ldots (4)$$

2.8 CONCLUSION TO LITERATURE STUDY

The chapter has considered all necessary deciding factors to motive the formulation of the hypothesis from a fundamental scientific law and a theoretical base.

The related theoretical factors, standards and previous work that were considered, serves to explain the phenomena that are observed and the conclusions that are consequently drawn.

CHAPTER 3 TEST ENVIRONMENT

3.1 CHAPTER OBJECTIVES

This chapter describes the experimental methods and the conditions under which the test results were obtained, so that the experiments may easily be replicated for continuous review and investigation. Then, the analytical approaches are briefly reviewed before the data analysis method is described.

3.2 PHYSICAL ENVIRONMENT

Radiation measurements have to be conducted in an anechoic chamber or open-space antenna measurement range. Results otherwise obtained will be regarded as *conduction measurements* rather than radiation measurements, the results of which do not interest this research. Since the methods described here is intended for actual field use and refers to the SINAD parameter (ratio of signal to noise and distortion), the results were required to include the effects introduced by external noise and distortion. Also, measurements made in anechoic chambers do not indicate the effects of noise and distortion on the transmitted signal.

Since the typical range at which ISM equipment can operate can be up to a hundred metres, anechoic chambers were firmly ruled out and the transmission tests were therefore conducted on an old cricket pitch with the kind permission of the Tshwane South College in Centurion. This provided a relatively large open space with an evenly flat ground plane.

The test area was surrounded by pine and cedar trees at a range of approximately one hundred and fifty metres from the centre of the field, and densely populated on the eastern side between the sports field and the N1 motorway. These are not believed to have caused reflections of significance within either the azimuth of transmission, or the transmission range of interest, because the characteristic bunching effects associated with reflections were not observed on the transmission characteristic curves.

3.3 TEST TOPOLOGY

The test topology is shown in Figure 3.1. The typical OFDM test network comprises of two mobile computers and an ISM 802.11.g access point (AP) router. The 802.11g system was used as an example because this system version (g) was already well developed in terms of industrial packaging and antennas and accessories available. We also used 802.11g because of interest in the results obtained from single transceiver systems, as opposed to multiple transceivers as in MIMO operation. The fact of the matter is that similar results will (predictably) be obtained when repeating these tests with any of the IEEE ratified systems 802.11a/g/n.

The server node is directly connected to the AP via Cat 5 cable, and also controls the AP adapter settings with a browser based GUI (guided user interface). For the mobile node's adapter, *Intel PROSet Wireless* adapter software is used with the mobile node because it is freely available and easy to use. The installation of this additional software enhances the functionality and user perception of the measurement experience. A brief review of the measurement software is presented in section 3.6 of this chapter.

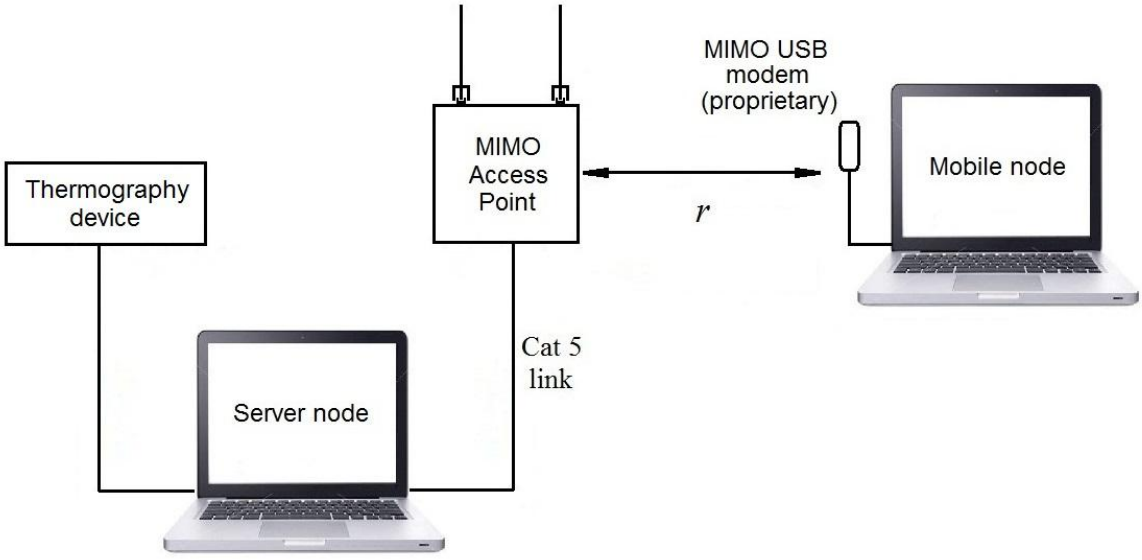

Figure 3.1. Experimental test network topology.

Figure 3.1 depicts the typical test network topology for experimentation. Typical ISM band OFDM networks were deployed for streaming video transmission. Performance results were measured and are presented for connected bandwidth (BW) in Mbps, as a function of transmission range (r) in metres. The server node is directly connected to the AP via Cat 5 cable, and also controls the AP adapter settings with a browser based guided user interface (GUI). For the mobile node's adapter, Intel PROSet Wireless adapter software is used with the mobile node because it is freely available and easy to use. The installation of this additional software enhances the functionality and user perception of the measurement experience.

Testing is in accordance with the neural black-box method combined with the mathematical approach of functional approximation. The digital inputs to the entire system are compared with the analogue video and audio output obtained in terms of observed quality. The inner hardware of the node or the physical layer cannot be manipulated by the user so it remains irrelevant to this study.

As depicted in Figure 3.1, the typical test network server node accepts streamed video data from the thermography device. The data stream varies around 480 kbps to 525 kbps, depending on the complexity of the picture it transmits. For our experimental test network, an overhead was incorporated to round off our CIR at 600 kbps, which means the minimum guaranteed data throughput which is required to guarantee our service level agreements. For the drawn out test procedures, the thermography device was not actively used. A bit stream was generated in the server node that best represents the thermography device's streamed output. The video bit-stream rate was predetermined to represent the committed information rate (CIR) or agreed QoS throughput, set at nominally 600 kbps maximum for the experimental requirement. This was achieved by selecting a suitable length video clip and scaling it down in H.264 with Apple's video editing software until the desired bitstream was obtained. The resulting audio/video interleave (AVI) file was then saved on the server node in a shared folder. Several video clips were created in this way for 64 kbps, 128 kbps, 256 kbps, 600 kbps, 1.024 Mbps and 2.048 Mbps.

Video transmission commences when the mobile node runs the file in the server node's share folder with Window media player. The use of a predetermined video bit-stream is applied in a test *detection technique*: If the video stream at a specific pre-scaled rate has no perceptual impairment in terms of sound or picture, it conforms completely to the agreed CIR. If any noise or video distortion is perceived, it means any one or more of the key performance indicators (KPIs) are compromised and the video stream does not conform to the agreed CIR.

3.4 PASSIVE TESTING

The first set of experiments focussed on *passive testing*. This means the determination of the transmission characteristics for a throughput of 600 kbps for example, with any transmission variations imposed in a passive (viz inactive) manner, as compared with the standard low-complexity (+1dBi) antenna characteristics as in Experiment 1.

These characteristics are compared to transmission characteristics when using an antenna with a higher gain characteristic, for example a vertical (+6dBi) collinear design for 2.4 GHz [51] in Experiment 2. The test was repeated using inline resistive attenuators (–6dB each) in conjunction with the +1dBi antennas in Experiment 3.

3.4.1 Experiment 1: Determination of service reference

This experiment determined the service reference for the electronics that was utilised. The electronics used for this test employed OFDM MIMO technology, manufactured by Belkin, AP model 802.11g+ MIMO with fixed transmit power at +17dBm. With the mobile node equipped with the matching Belkin USB g+ MIMO modem, the two transceiver system enabled a near range data connection rate of 108 Mbps. The set-up for Experiment 1 is depicted in Figure 3.1. The transmission test range is shown in Figure 3.2.

Figure 3.2 shows the plan area of the transmission test range. The approximate latitude and longitude of the test station is indicated, as well as the imaginary range line and markers. The d-CIR and d-EIR ranges for the three transmission series in Experiments 1, 2 and 3 are also indicated.

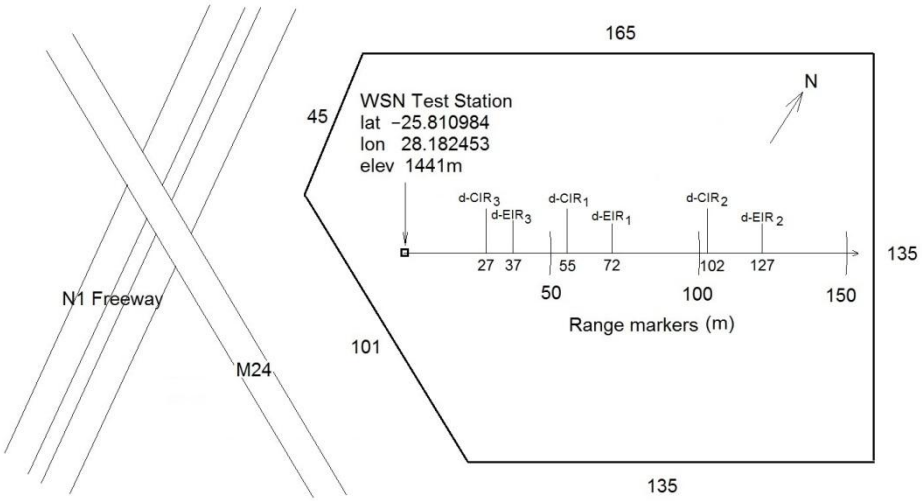

Figure 3.2. Transmission test range.

After starting the video transmission, the BW was recorded at suitable distance intervals whilst increasing the transmission range to the point of total signal deterioration, as indicated in Figure 3.3. This point was marked as the *detected excess information rate* (d-EIR) range. The transmission range was then reduced until video transmission restarted. This point was marked as the *detected committed information rate* (d-CIR) range. The service level differential zone (SLDZ) is defined as the range between d-CIR and d-EIR.

A more complete transmission test may be conducted in terms of max range determination, for a throughput of a 64 kbps bit-stream file as indicated in broken line.

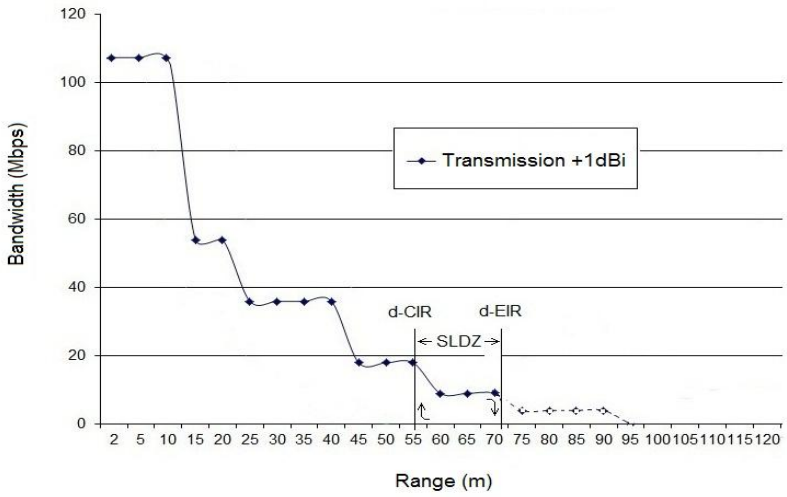

Figure 3.3. Transmission characteristics for Experiment 1 test network with +1 dBi antennas.

The data collected is shown in Table 3.1 and Figure 3.3.

Table 3.1. Transmission data for test network Exp. 1 (+1dBI antennas).

Range (m)	Bandwidth (Mbps)
2	108
5	108
10	108
15	54
20	54
25	36
30	36
35	36
40	36
45	18
50	18
55	d-CIR
60	9
65	9
70	9
72	d-EIR

Table 3.1 contains the data collected during Experiment 1. Note the range at which transmission fails (72 m) corresponds to approximately 6 Mbps. Reducing the transmission range, the transmission restarts at 55 m, approximately 18 Mbps. The maximum range across which reliable transmission may be effected (55 m) comprises approximately only two thirds of the apparent maximum range at 72 m.

Figure 3.3 contains the data collected during Experiment 1 in a graph generated with the aid of MS Excel. The indicated d-CIR and d-EIR are for a bitrate of 600 kbps (video file) that is continuously monitored in terms of all the key performance indicators namely

bandwidth, latency, jitter and *errors*. Note the continuation of the transmission curve beyond d-EIR, indicated in broken line, which was determined using the same method but with a lower bitrate audio file of 64 kbps. Note also the range at which transmission fails (72 m) corresponds to approximately 6 Mbps. When reducing the transmission range, the transmission restarts at 55 m at approximately 18 Mbps. Note the stepped curve which is due to the manufacturer's (Intel) internal algorithms that are contained in the firmware of the OFDM WLAN physical layers, which can be smoothed with the use of external software packages like Excel.

The SLDZ manifests itself in the same manner as a typical hysteresis curve [26]; transmission failing suddenly at EIR and restarting back at CIR. This pattern will repeat itself as the mobile node approaches or recedes from the access point AP across the SLDZ.

3.4.2 Experiment 2: Determination of the improvement in service performance

This experiment determined the *improvement* in the service reference for the electronics that was utilised. The electronics used for this test also employed OFDM MIMO technology, manufactured by Belkin, AP model 802.11g+ MIMO with fixed transmit power at +17dBm. The test network for Experiment 2 is shown in Figure 3.4.

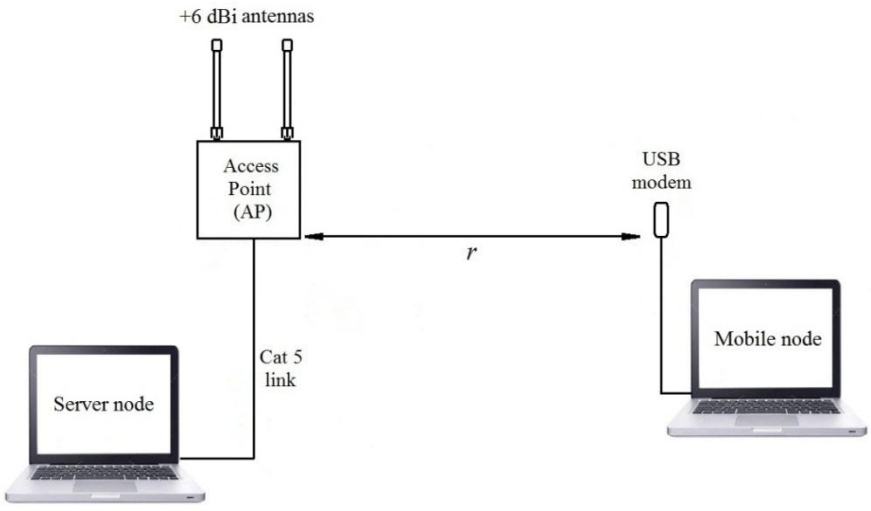

Figure 3.4. Test network set-up for Experiment 2.

The test network shown in Figure 3.4 is fundamentally the same as for Experiment 1. However, instead of the standard +1 dBi antennas, the AP was equipped with two +6 dBi antennas. The mobile node was equipped with the matching Belkin USB g+ MIMO modem. The two transceiver system enabled an improved range data connection rate of 108 Mbps.

The data collected during Experiment 2 is shown in Figure 3.5 and Table 3.2.

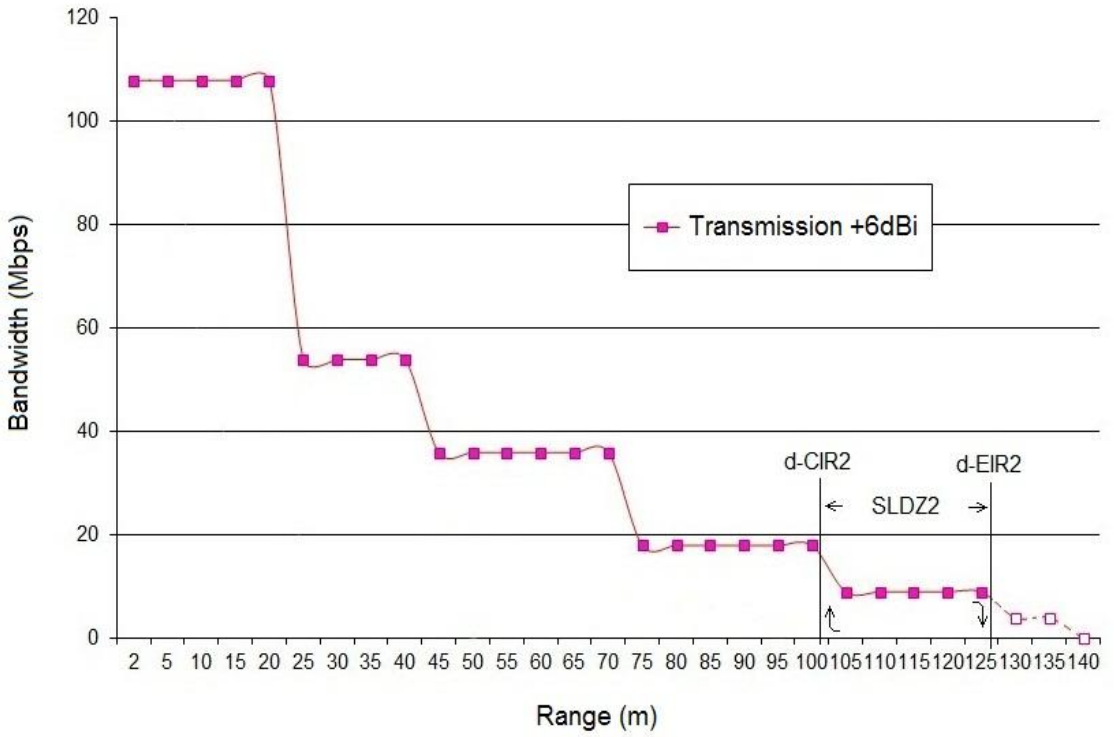

Figure 3.5. Transmission characteristics for Experiment 2 test network with +6 dBi antennas.

Figure 3 indicates the test results obtained with +6dBi antennas instead of +1dBi, which means the link budget was improved by 5dB.

A more complete transmission test was conducted in terms of max range determination, with the use of a 64 kbps bit-stream file, the results of which are indicated in broken line.

Table 3.2. Transmission data for test network Exp. 2 (+6 dBi antennas).

Range (m)	Bandwidth (Mbps)
2	108
5	108
10	108
15	108
20	108
25	54
30	54
35	54
40	54
45	36
50	36
55	36
60	36
65	36
70	36
75	18
80	18
85	18
90	18
95	18
100	18
102	d-CIR2
105	9
110	9
115	9
120	9
125	9
127	d-EIR2

3.4.3 Experiment 3

This experiment determined the *reduction* in the service reference for the electronics that was utilised, as a control experiment. The electronics used for this test also employed OFDM MIMO technology, manufactured by Belkin, AP model 802.11g+ MIMO with fixed transmit power at +17dBm.

However, instead of the standard +1 dBi antennas, the AP was also equipped with two 6 dB attenuators fitted in-line with each antenna as shown in Figure 3.6.

Since the mobile node was equipped with the matching Belkin USB g+ MIMO modem, the two transceiver system resulted in a reduced range data connection rate of 108 Mbps.

The set-up for Experiment 3 is shown in Figure 3.6.

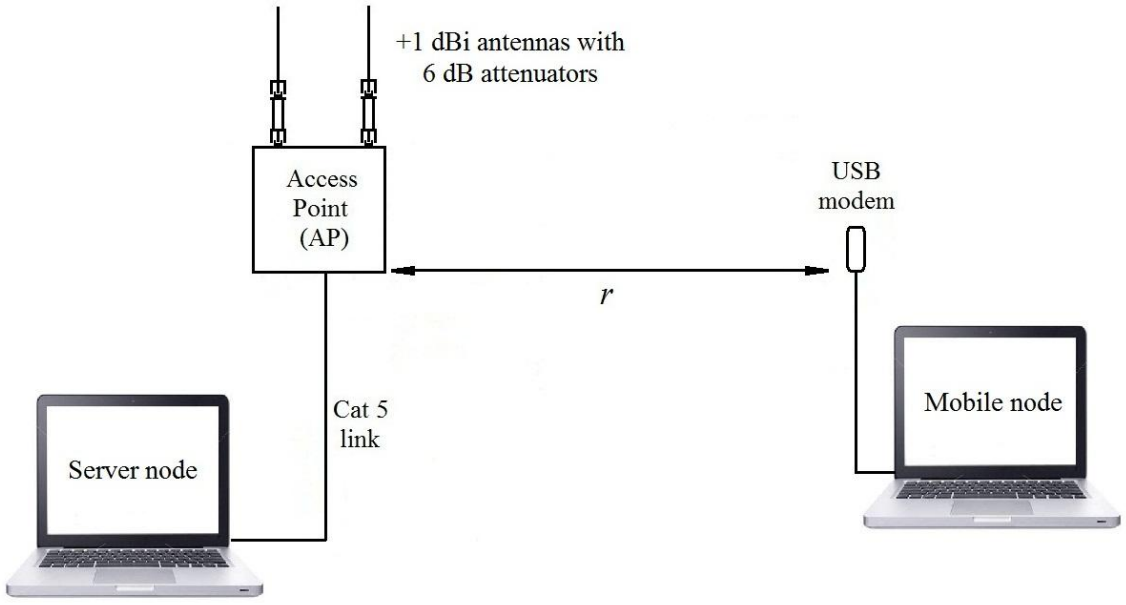

Figure 3.6. Test network set-up for Experiment 3.

The data collected during Experiment 3 is depicted in Figure 3.7 and shown in Table 3.3.

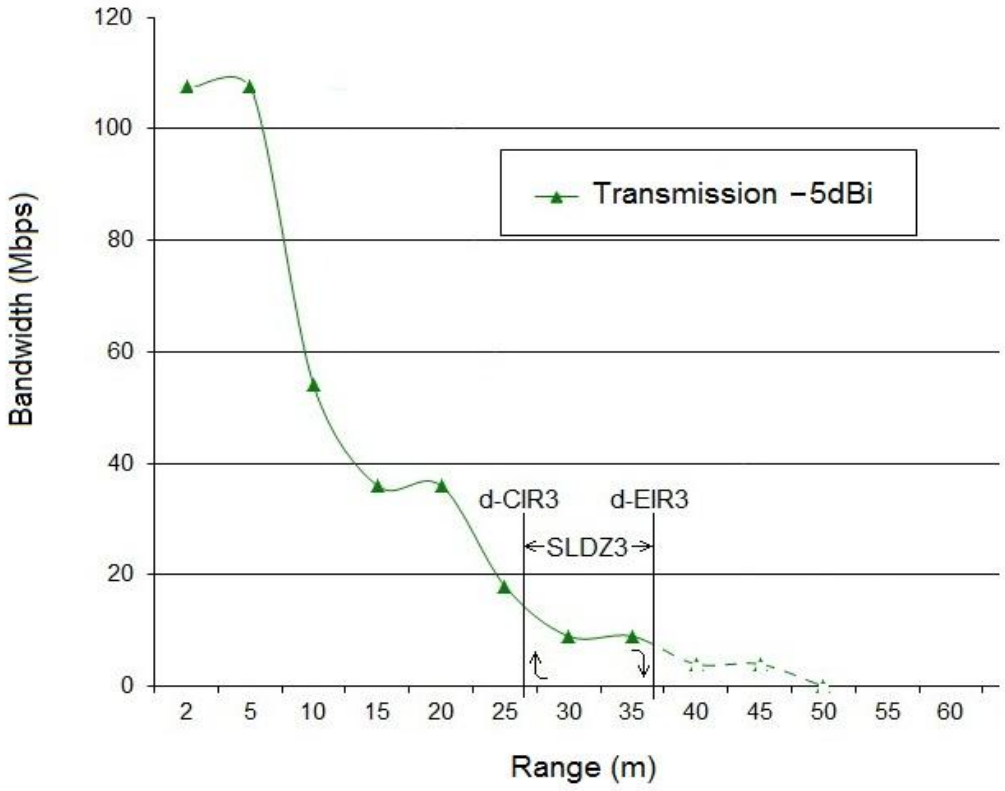

Figure 3.7. Transmission characteristics for Experiment 3 test network with 6 dB attenuators.

Figure 3 indicates the test results obtained with 6 dB attenuators fitted in-line with the +1dBi antenna, which means the link budget was reduced by 6 dB.

A more complete transmission test was conducted in terms of max range determination, with the use of a 64 kbps bit-stream file, the results of which are indicated in broken line.

Table 3.3. Transmission data for test network Experiment 3 (6 dB attenuators).

Range (m)	Bandwidth (Mbps)
2	108
5	108
10	54
15	36
20	36
25	18
27	d-CIR
30	9
35	9
37	d-EIR

3.4.4 Antennas and attenuators

Antennas may be commercially obtained from the manufacturers or various electronics retailers. For Experiment 2 a pair of 6 dBi antennas manufactured by Poynting Antennas (Pty) Ltd was used. For experiments 1, 3, 4 and 5, the AP manufacturers' standard +1dBi antennas were used.

Two types of antenna that I have constructed are briefly detailed here to enable interested readers of this thesis to construct their own test antennas for a much lower cost than commercial antennas. The antennas had to be characterised specifically in terms of isotropic gain (dBi) by a SANAS accredited test centre, university or industry institution with suitable test facilities.

1. Coaxial eight-element collinear array coaxial line antenna

Many of the commercial designs for 2.4 GHz omnidirectional antenna are based on coaxial transmission line principles [50], [51]. Some interesting design use brass tubing and the inner core plus dielectric sleeve of LMR-400 cable, neither of which are available any more. Two designs were obtained from my mentor Professor Duncan Baker's collection of

radio amateur literature, based on commercial coaxial cable using the same idea: A coaxial cable type of suitable quality that is commercially available is RG-213. By using RG-213 cable and its characteristic features, a design for 444 MHz lower UHF band was recalculated for 2.4 GHz for an antenna design that would theoretically produce between 6 – 8 dBi gain.

To obtain 6 dBi gain or more from the transmission line antenna, 8 sectors would theoretically be required (four times the gain of a dipole antenna), plus a 1/4 wave radiating section at the top which is the load impedance, terminating the end of the transmission line. The antenna is connected to a radio device with a suitable type cable and connectors such as N-connector via cable to SMB or whatever else the AP requires.

Many of the designs encountered in industry literature incorporated a toroidal decoupler at the feedpoint of the antenna. Various designs quoted a decoupler length of 1/4 wavelength, while others specified 1/4 wavelength times the velocity factor of its decoupler tube (in the case of brass tubing the figure is quoted as 0.95). Anyways the location of the decoupler seems different in each design. By omitting the decoupler, the design may be simplified because no matching transition needs to be made if the design is constructed for 6 dBi gain.

To accommodate line velocity, each sector of the antenna must be 1/2 wavelength in length multiplied by the cable's velocity factor, which is 0.66 for RG-213. When using higher grade cable for instance LMR-400, the velocity factor of that specific cable must be incorporated when calculating the physical sector lengths. The schematic design is shown in Figure 3.8.

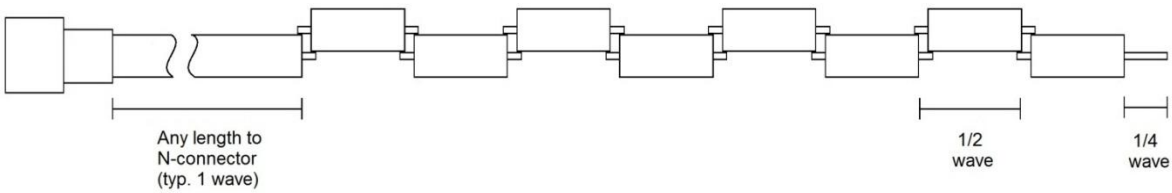

Figure 3.8. Schematic design for collinear array transmission line antenna

The ½ wavelength sector length is calculated as follows:

$$\left(\frac{\lambda}{2}\right) = \frac{v \times c}{2 \times f}$$

$$= \frac{0.66 \times 299.792458 \times 10^6}{2 \times 2441 \times 10^6}$$

$$= 0.0404\ m$$

$$= 40.5\ mm$$

where:

v = 0.66 (velocity factor of RG213)

c = 299792458 m/s absolute velocity,

f = 2441000000 Hz (centre of ISM 2.4GHz band)

The length of the 1/4 wave element section is not adjusted by the velocity factor, because it radiates into free space and therefor calculates to 31 mm. For RG213 the total antenna length is 355 mm.

Considering antenna construction, the overall length of each sector of RG-213 (40.5 mm) is more important than mere sector barrel length. It was noted that 37 mm barrel length with 6 mm protruding centre core on each end would provide sufficient overlap to assemble the segments by soldering as shown in Figure 3.9.

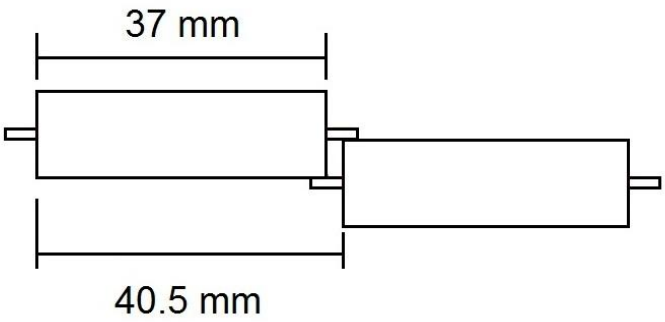

Figure 3.9. Sector length for correct spacing

To hold the sectors together as they are soldered may require a holding jig constructed from wood, as shown in Figure 3.10. Note the right side clamps need not be longer than 30 mm. The entire length of the completed antenna needs to be supported by the base plate of the jig, during the soldering, because the antenna is not sufficiently rigid to support itself in the horizontal plane from one fixed end.

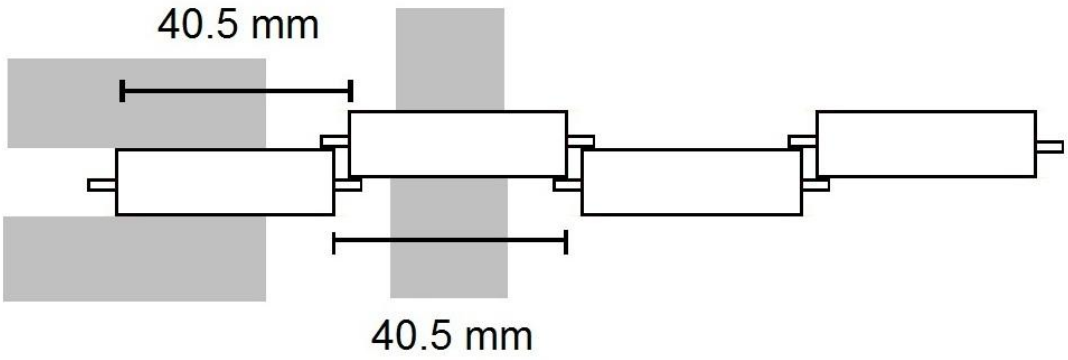

Figure 3.10. Soldering jig schematic for assembly

Clamps should not be constructed too tightly, as the cable needs to be lifted out after it has been soldered.

Care should be taken to ensure correct spacing of each sector. Measuring from one end of the shielding of any sector to the same end on the next sector, the overall length of each sector needs to be 40.5 mm. The accuracy of this dimension critically affects the direction of transmission and hence the performance. A small gap of 3 mm should be left between the sheaths of each sector.

2. Open feed-line collinear 6 dB antenna

This section considers the design of another collinear antenna for 802.11g wireless networking, which has an approximate gain of 6 dBi. With an additional ¼ wavelength stub, the antenna may be properly matched to the feed-line and close to 6 dBi gain may then be obtained.

The expected 6 dBi gain may be improved by increasing the number of elements. Each doubling of the number of elements will result in an increase of approximately 3 dBi or double the gain.

The design of an open feeder type collinear array is shown in Figure 3.11 consisting of a suitable length of copper wire incorporating ½-wave length loop traps at specific locations. The dimensions are shown in the diagram below may be regarded as sensitive to construction accuracy. The connector is a panel-mount feedthrough N-type connector.

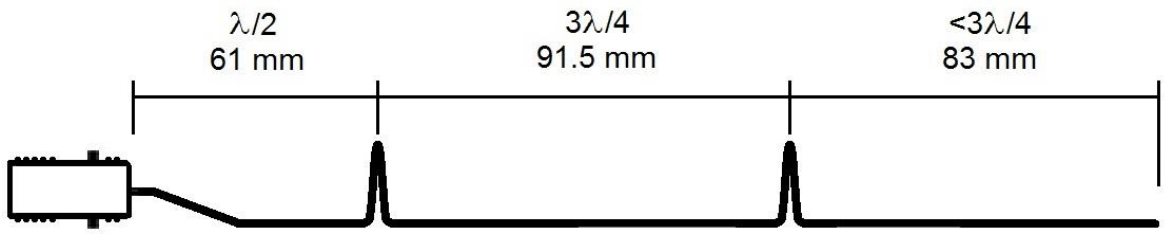

Figure 3.11. Schematic dimensions of open feeder collinear antenna

The bottom section length from the connector side is 1/2 wavelength, with the middle section at 3/4 wavelength and the whip section on the right at slightly less than 3/4 wavelength, to reduce the capacitance effect.

For the centre of the 802.11g frequency range, which spans from 2.412 GHz to 2.484 GHz a 1/2 wavelength calculates at 61mm, and 3/4 wavelength at 91.5 mm. The dimensions indicated here correlate with similar antennas commercially available.

For outdoor use a radome constructed from conduit tubing provides suitable enclosure. The preferred method of mounting the antenna is shown in Figure 3.12 with a suitable length of right-angle galvanised steel or aluminium. This provides a ground plane which is required by the open feeder type antenna for optimum transmission.

The antenna can be attached to the galvanised steel through a suitable hole drilled in one side, and by feeding it through the hole in the galvanised steel before attaching the connector. The antenna will be firmly held between the end cap and the N-connector.

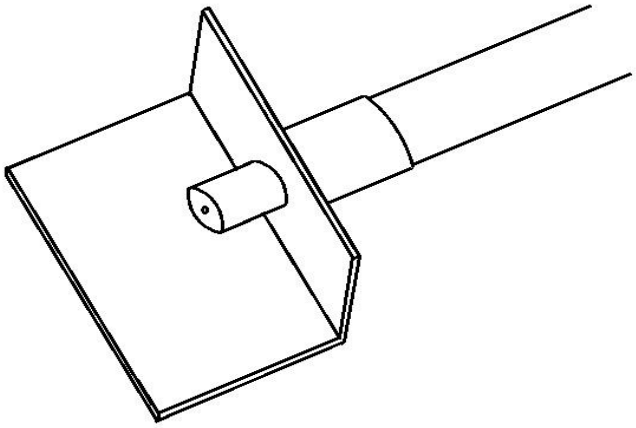

Figure 3.12. Enclosed collinear with mounting using a metal bracket

3. Matched resistive attenuator

Precision attenuators may be purchased for a specified attenuation and specific characteristic impedance. An in-line design would be fitted with male and female connectors of the same type as used by the AP antenna, nominally SMA or SMB type.

An attenuator or set of attenuators may also be designed and constructed. The preferred design approach is from the symmetrical T-type network model of a transmission line, as depicted in Figure 3.13.

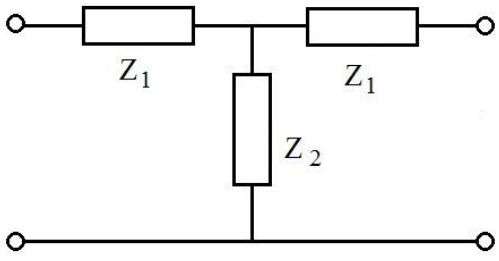

Figure 3.13. Symmetrical T-network modelling of transmission line.

For a specific characteristic impedance and attenuation Z_1 (R_1) and Z_2 (R_2) may be calculated as follows:

$$R_1 = Zo \times Tanh\ \frac{\alpha}{2}$$

$$R_2 = \frac{Zo}{Sinh\ \alpha}$$

where Zo = characteristic impedance and α = attenuation in nepers (1 neper = 8.686 dB).

With Zo = 50 Ω and α = 6/8.686 = 0.69:

$$R_1 = 50 \times Tanh\ \frac{0.69}{2} = 16.6\ \Omega$$

and

$$R_2 = \frac{50}{Sinh\ 0.69} = 67\ \Omega$$

Standard values for 5% tolerance chip resistors are 16 Ω and 68 Ω respectively. With 1% tolerance components the possible values are 16.5 Ω and 66.5 Ω.

With the actual values known for R_1 and R_2, the characteristic impedance Zo and attenuation factor α may be calculated using the following equations:

$$Zo = \sqrt{{R_1}^2 + 2R_1R_2}$$

$$\therefore Zo = \sqrt{16.5^2 + 2 \times 16.5 \times 66.5}$$

$$\therefore Zo = 49.66\ \Omega$$

$$now\ \alpha = ln\frac{R_1 + R_2 + Z_o}{R_2}$$

$$\therefore \alpha = ln\ \frac{16.5 + 66.5 + 49.66}{66.5} = ln\ 1.9939$$

$$\therefore \alpha = 0.69\ nepers = 5.9941\ dB$$

3.5 ACTIVE TESTING

The second set of experiments focussed on *active testing*. This means that the transmission characteristics for a throughput of 600 kbps for example, were determined for different settings of transmitted power levels, which were electronically controlled by browser-based GUI and *Intel's PROSet Wireless* software.

The transmission characteristics of a typical 802.11g single transceiver network operating at 20% of maximum power were determined in Experiment 4. The test was repeated for a power setting of 80% of maximum power in Experiment 5.

3.5.1 Experiment 4: Service reference for low RF power, active setting

Experiment 4 determined the service reference for the electronics that was utilised when operating a node at 20% of maximum power. The electronics used for this test was an 802.11g AP router with single transceiver manufactured by D-Link operating at +18 dBm. The set-up for Experiment 4 is shown in Figure 3.14.

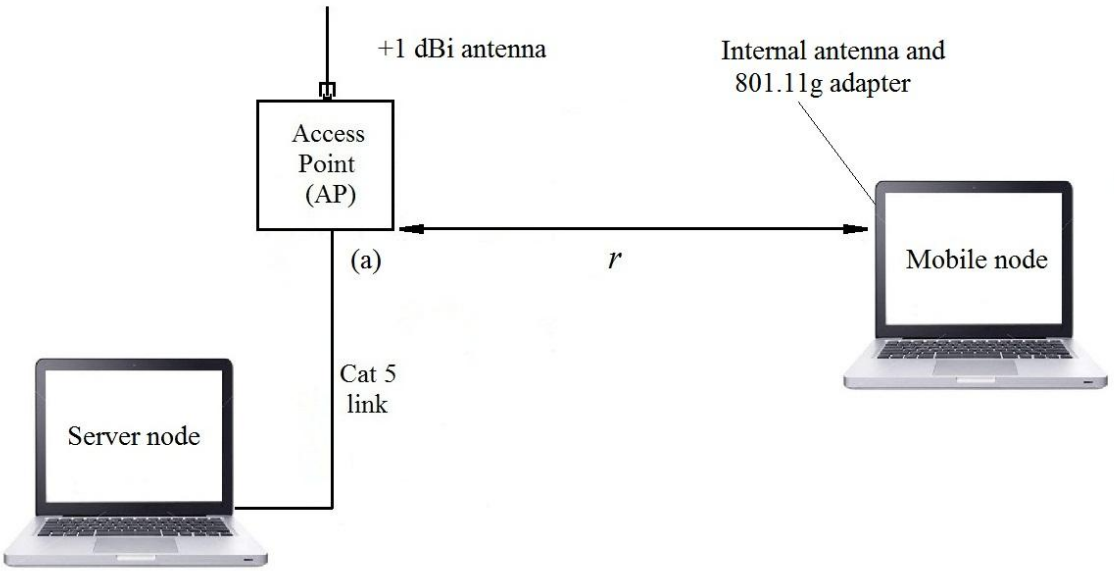

Figure 3.14. Test network set-up for Experiment 4.

The GUI adapter control software made it possible to set RF power in 20% decrements from maximum (+18 dBm/63 mW) to zero. For this test the AP's RF power was set to 12.6 mW or +11 dBm.

The single transceiver system enabled a near range data connection rate of 54 Mbps.

The data collected during Experiment 4 is shown in Figure 3.15 and Table 3.4.

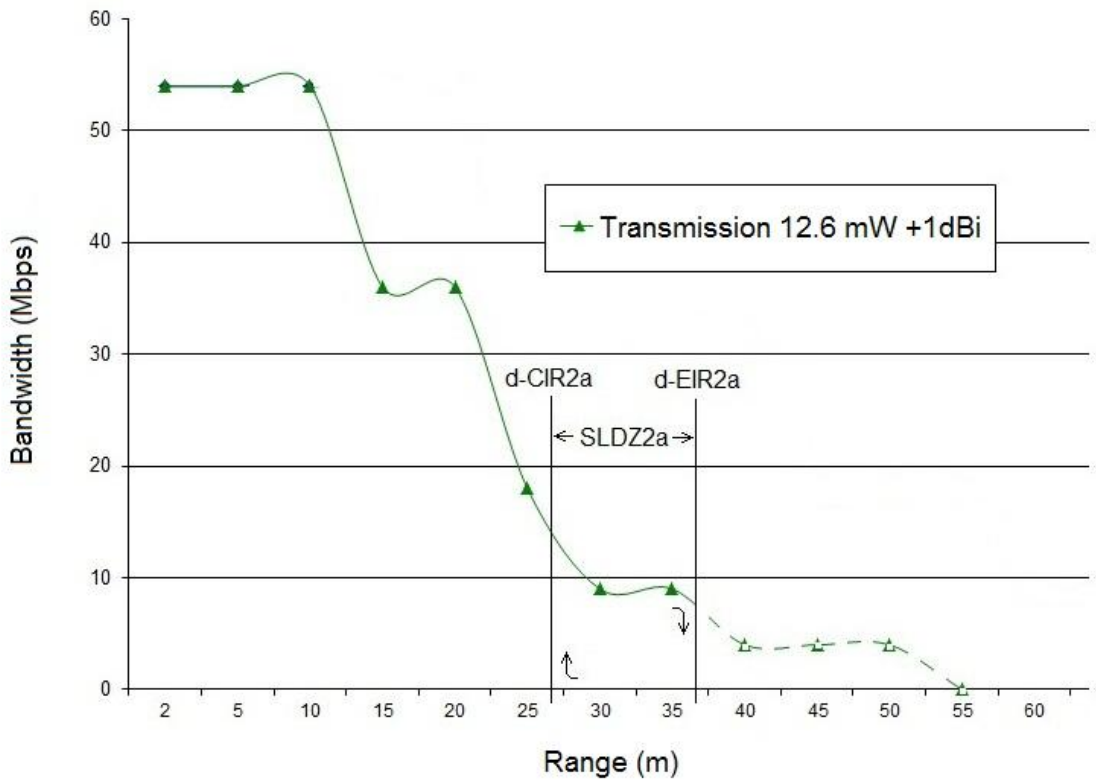

Figure 3.15. Transmission characteristics for Experiment.4 test network with 20% transmit power

Figure 3.15 presents the transmission results with RF power set to +11 dBm or 12.6 mW.

Table 3.4. Transmission data for test network Experiment 4 (20% Tx power).

Range (m)	Bandwidth (Mbps)
2	54
5	54
10	54
15	36
20	36
25	18
27	d-CIR
30	9
35	9
37	d-EIR

3.5.2 Experiment 5: Service reference for 80% RF transmit power active setting

This experiment determined the service reference for the electronics that was utilised when operating a node at 80% of maximum power.

For this test the mobile node RF power was set to 50 mW or +17dBm. The single transceiver system enabled a near range data connection rate of 54 Mbps.

The set-up for Experiment 5 is shown Figure 3.16.

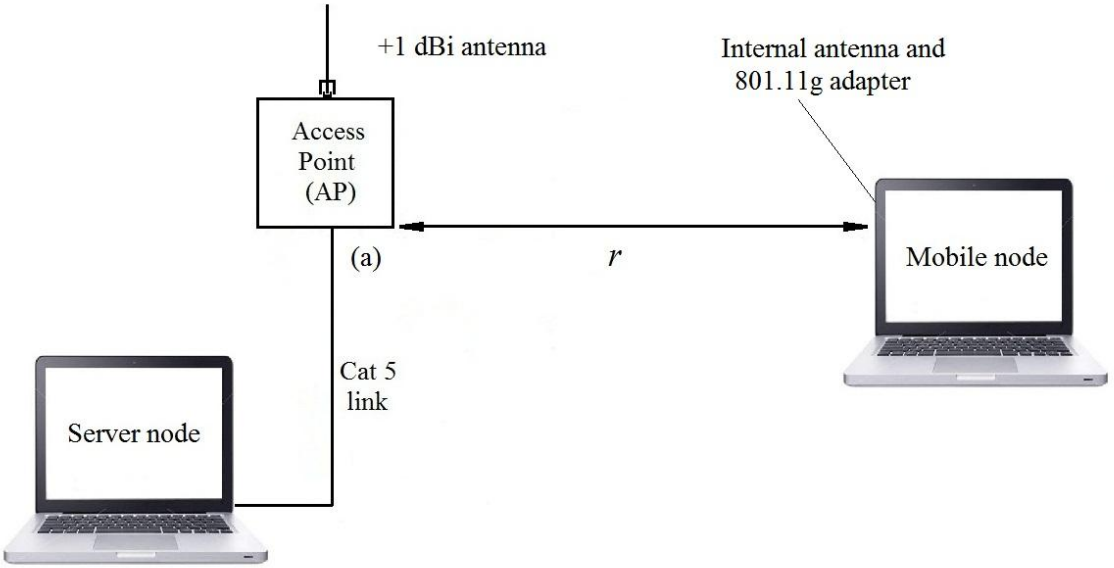

Figure 3.16. Test network set-up for Experiment 5.

The data collected during Experiment 5 is shown in Figure 3.17 and Table 3.5.

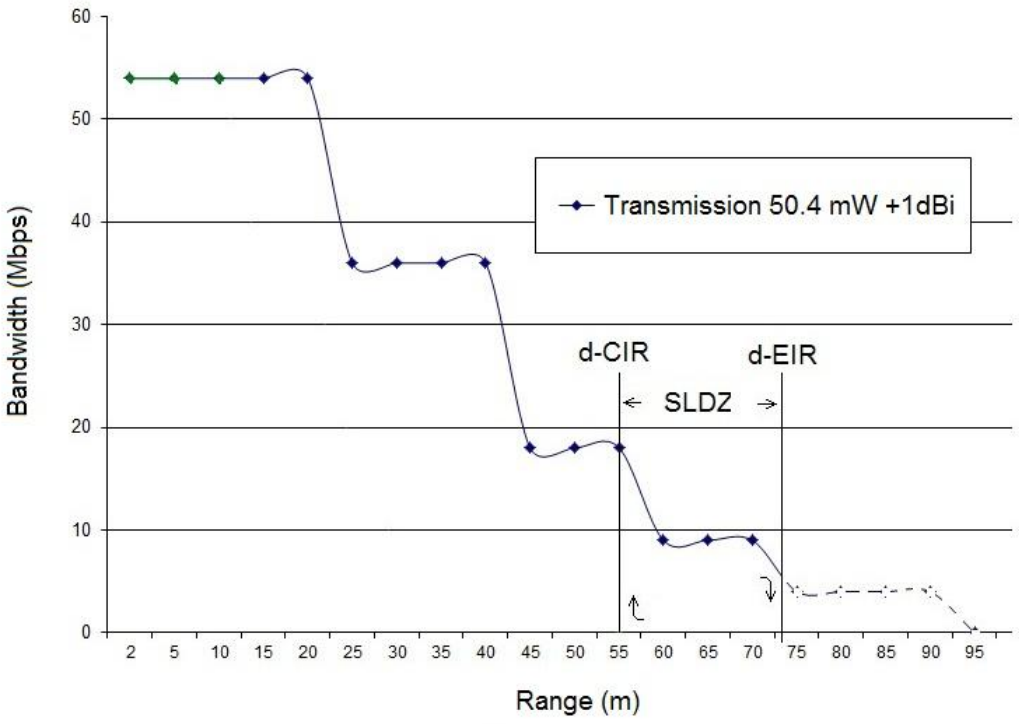

Figure 3.17. Transmission characteristics for Exp.4 test network with 80% transmit power.

Figure 3.17 depicts the data in Table 3.5 with the use of Excel. By noting the d-CIR and d-EIR as in previous experiments, the SLDZ is observed at approximately 55 m to 73 m.

Table 3.5. Transmission data for test network Experiment 5 (80% Tx power).

Range (m)	Bandwidth (Mbps)
2	54
5	54
10	54
15	54
20	54
25	36
30	36
35	36
40	36
45	18
50	18
55	d-CIR
60	9
65	9
70	9
73	d-EIR

Table 3.5 contains the transmission data that was collected during Experiment 4, for a mobile node at 80% RF power.

Figure 3.15 presents the transmission results with RF power set to +11 dBm, and Figure 3.16 the results for the RF power set to +17dBm. Figure 3.16 thus indicates the transmission range improvement when the RF output power setting is adjusted by +6 dB, which is four times greater than the original setting.

3.6 MEASUREMENT SOFTWARE AND VIDEO MONITORING

3.6.1 Measurement suite and network utilities

The measurement suite comprised Intel's *PROSet/Wireless* software. The reason for this is fourfold; firstly, as with the processors in computers and smart mobile devices, the majority of chip-sets used in on-board computer adapters and access point wireless adapters, are manufactured by Intel. Secondly, the use of the full software installation enhances measurement accuracy and the measurement experience for the user. Thirdly, with the full measurement suite there are added functionality and features to measure additional parameters, if so required. Finally, the software is free to download and easy to use. Figure 3.18 shows the configuration and connection utility.

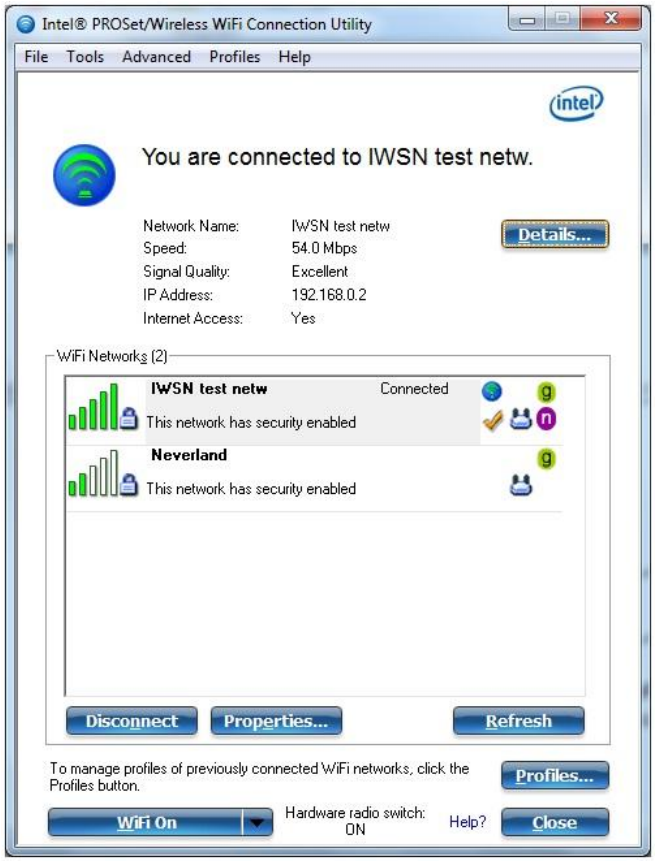

Figure 3.18. Test network configuration and connection utility.

Screengrab from Intel's *ProSet/Wireless* free software.

The connection utility window shown in Figure 3.18 indicates basic information like network name, connecting speed and IP address. Pressing the "Details…" button opens the *Connection Details* utility as shown in Figure 3.19.

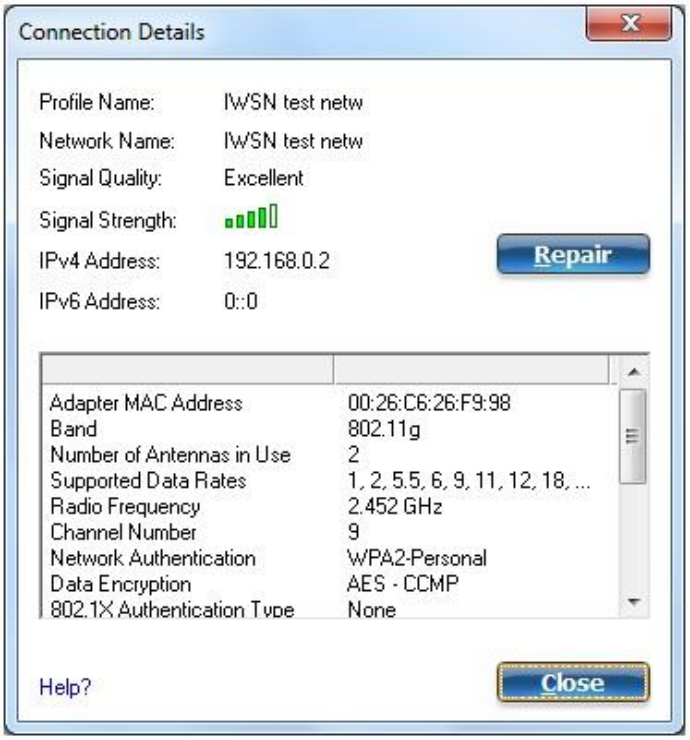

Figure 3.19. Test network connection details utility.
Screengrab from Intel's *ProSet/Wireless* free software.

The connection details utility indicated in Figure 3.19 contains extensive wireless network information such as band information, radio frequency and channel number.

Also indicated are the MAC address, number of antennas used and data encryption information.

Extended connection details are indicated in Figure 3.20. This is obtained by manipulation of the window slider on the right hand side of the information window.

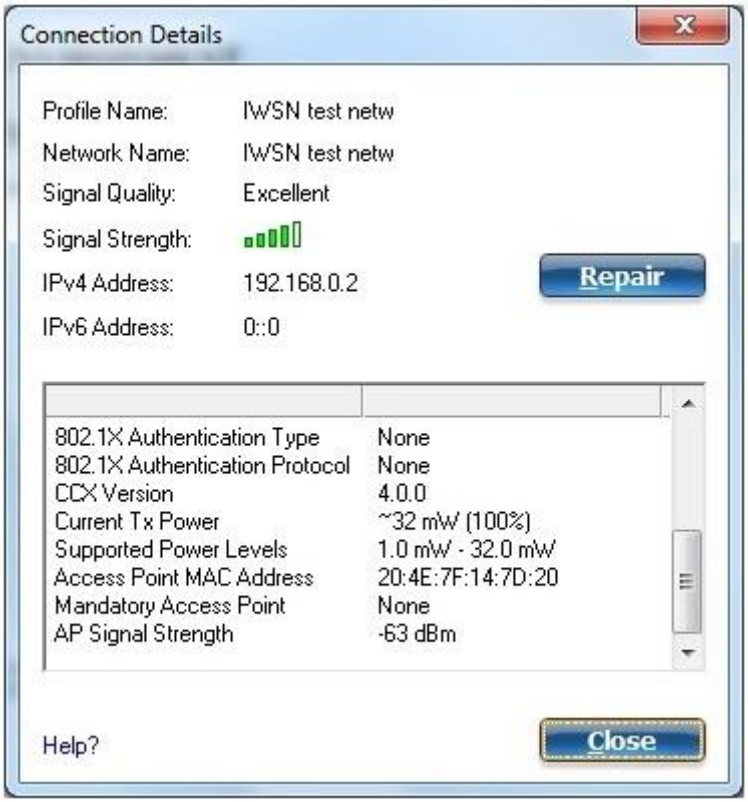

Figure 3.20. Test network extended connection details.
Screengrab from Intel's *ProSet/Wireless* free software.

Figure 3.20 indicates additional connection details. The current transmit power setting is indicated as well as the supported power levels for energy saving. An extremely useful feature is indicated here for Cisco (or compatible) access points, namely the AP signal strength in dBm. This was added in a software update as recently as February 2013.

3.6.2 Monitoring instrumentation

The video transmission may be monitored by Windows Media Player because it has several useful features over and above from accurately displaying the video and reproducing the audio track. Figure 3.21 shows a video track with several monitoring windows deployed, so that critical parameters may be observed while the video track is monitored for video and audio quality.

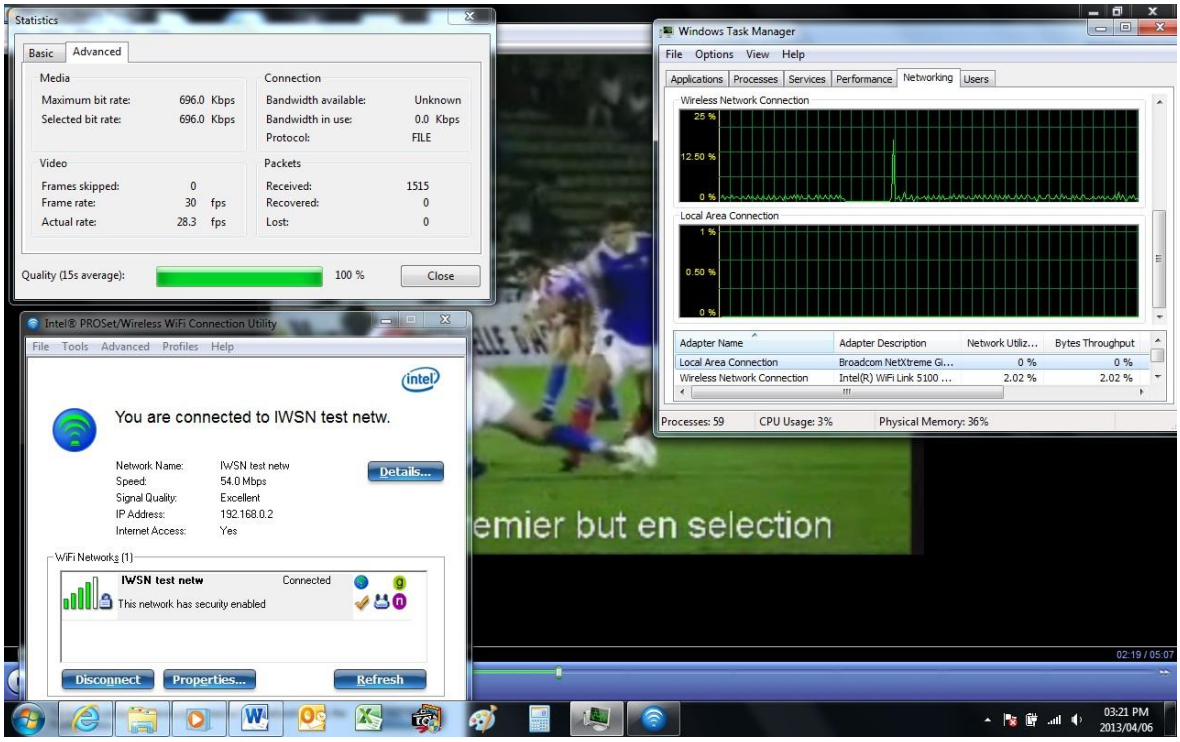

Figure 3.21. Streaming media player with monitoring utility panes.
Screengrab from Intel's ProSet/Wireless free software.

Figure 3.21 indicates a video test clip played by Windows Media Player, while important parameters regarding the transmission link can be observed.

The *Statistics-Advanced* window is obtained by selecting 'View' on the media player and clicking 'Statistics'. The actual data throughput is indicated in this case 696 kbps at an actual frame rate of 28.3 frames per second.

The Windows Task Manager is obtained by right-clicking on the Windows 7 taskbar and clicking *Task Manager*. This is a facility supported by the Windows 7 operating system but inevitably linked to the wireless adapter by virtue of system driver software as well as the PROSet/Wireless drivers. Throughput is indicated as a percentage of connecting speed. The Intel PROSet/Wireless Connection utility indicated actual connection speed to the IWSN test network. This facility was used to measure the results obtained.

3.7 CONCLUSION TO TEST ENVIRONMENT

This chapter has reviewed the test conditions which are relevant when considering the reconstruction of the test experiments.

The experiments are described within the test topologies that the data were obtained. The methodology is simplistic and does not require any special skill or equipment to conduct the tests.

Although the chapter reveals the data collected, the next chapter (4) presents the data in a suitable form for visual review and processing.

The tests distinguish between passive tests and active tests. The passive testing is the focus of the study because this will be the method mostly applied by users to improve the network performance.

The passive attenuation test serves as a control for the passive amplification. For results to be valid the increase or decrease of performance should be validated to conform to the same mathematical expression.

The active tests serves as a control set for the passive tests conducted. During the active tests, two sets of data demonstrates the same effects in an active manner as when performance is increased or decreased in a passive manner.

The test and measurement software is reviewed in the concluding part of the chapter, because this was used to measure the results that were obtained during experimentation.

CHAPTER 4 RESULTS

4.1 CHAPTER OBJECTIVE

This chapter presents the combined measurement results, which contain the data that is required for processing and testing of the hypothesis. The data are not immediately discussed, but requires analysis as in Chapter 5 before discussion is presented in Chapter 6.

4.2 PASSIVE TEST RESULTS

Results for the passive testing are shown in Figure 4.1.

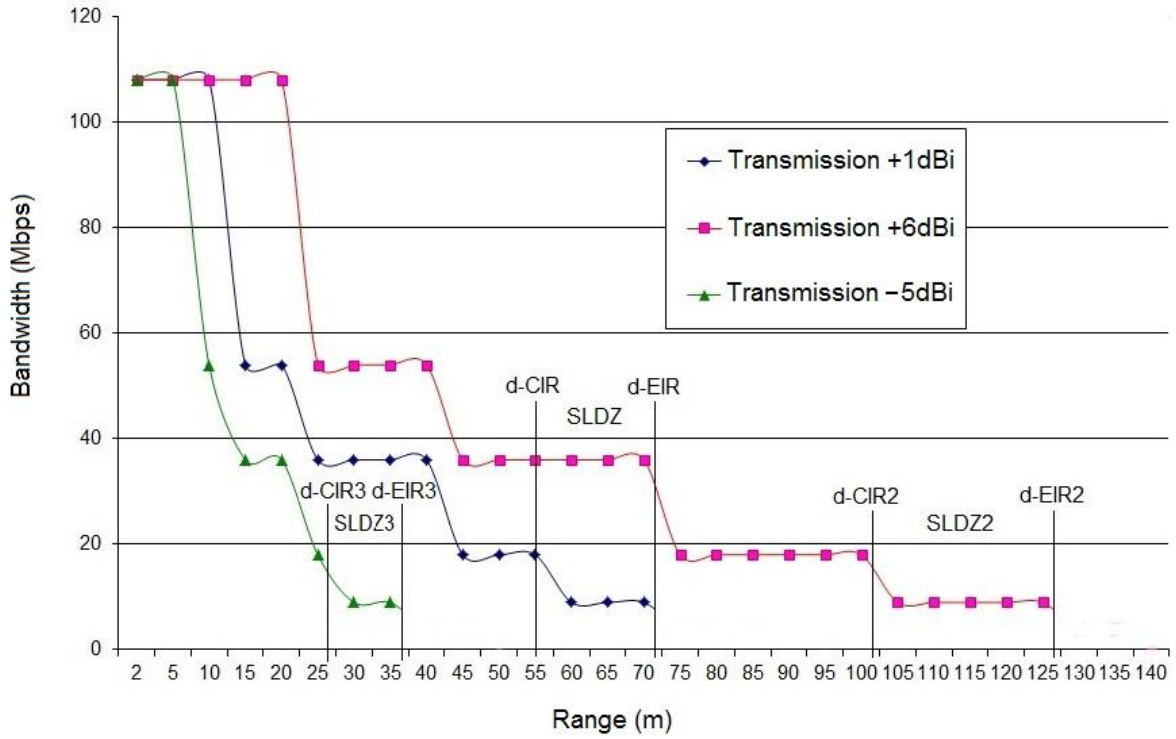

Figure 4.1. Transmission results with passively controlled variable transmit power.

Figure 4.1 illustrates the effects of passive signal attenuation and amplification. 'Transmission +1 dBi' depicts the transmission performance with two standard omnidirectional +1dBi antennas.

'Transmission –5 dBi' shows the reduction in range performance when two in-line attenuators (6 dB each) are inserted between the standard antennas and the AP. 'Transmission +6dBi' shows the improvement in transmission range when the standard antennas are replaced with two +6dBi omnidirectional antennas.

4.3 ACTIVE TEST RESULTS

In Figure 4.2, the first series presents the transmission results with the wireless adapter's RF power set to 12.6 mW or 11dBm. The second series of results are for RF power set to 50.4mW or 17dBm. This represents a 6 dB difference is power level, or a 1 to 4 power ratio.

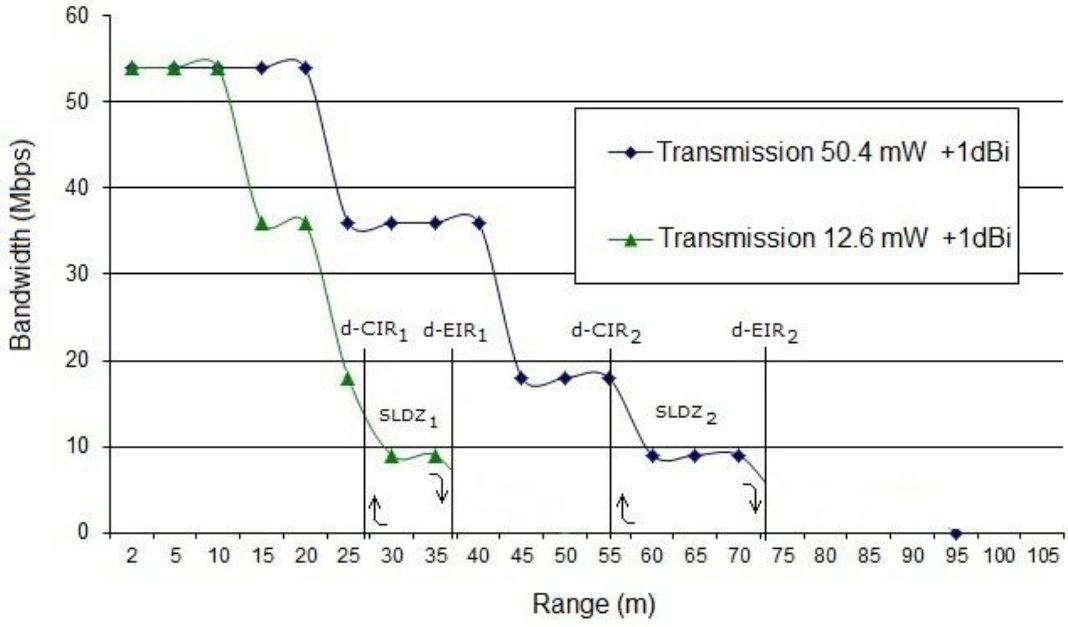

Figure 4.2. Transmission results with actively controlled variable transmit power.

Figure 4.2 indicates the transmission range extension when the RF output power setting is increased by 6 dB, which is four times the magnitude of the original setting.

4.4 INDUSTRIAL MIMO TEST RESULTS

For the sake of completeness, the results obtained by Wavion Technology are considered here [27]. The radio transmission coverage of the company's WBS-2400 base station with multiple antenna and transceiver technology was compared to conventional single-transceiver Wi-Fi technology.

The Wavion WBS-2400 base station employs six +7.5 dBi antennas with six radio transceivers. By the application of space division multiple access (SDMA) technology and advanced spatially adaptive digital beam-forming, radio energy may be optimally focused to and from network node on a per-packet basis. The SDMA technology Wavion has developed can communicate two concurrent data streams to two different users from the base station. The downlink capacity of each base station is doubled when compared to single transceiver technology. The conventional Wi-Fi used a single transceiver and a single antenna with an estimated gain of +1.3 dBi. Both systems were tested at +18 dBm RF transmitted power.

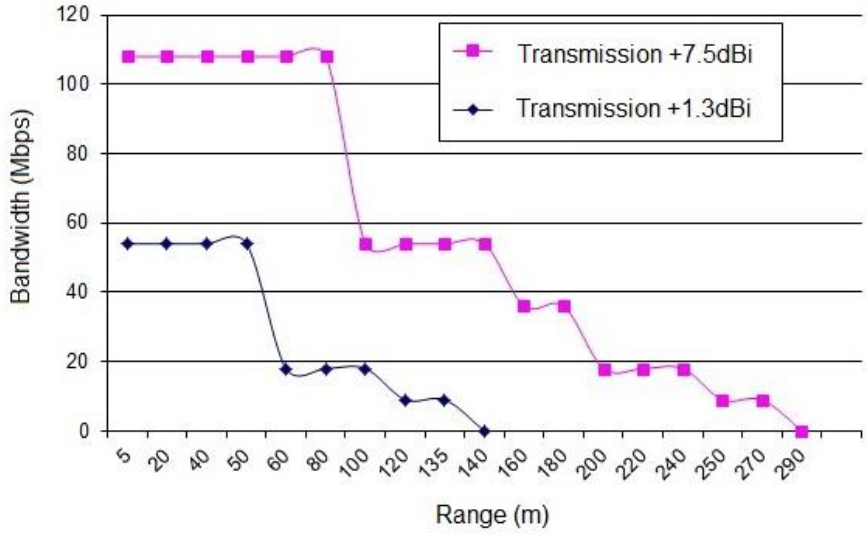

Figure 4.3. Wavion SDMA (+7.5dBi) vs. conventional Wi-Fi (+1.3dBi).

Figure 4.3 indicates, in graphical form, the performance gains that Wavion Technology obtained over conventional Wi-Fi by application of higher gain antennas and MIMO operation.

4.5 CONCLUSION TO TEST RESULTS

Chapter 4 presents the test results and conversely the data required to test the hypothesis.

Results for passive tests are combined and graphically depicted with the aid of MS Excel. The active test results are separately presented. The combination of results allows for visual comparison and presents all results per test category in a single depiction for each.

For the sake of completeness results obtained by a leading industry manufacturer was included for processing. These results are interesting to this study because it compares MIMO with single transceiver technology. Analysis of these results will reveal the different effects on the improved transmission characteristics imposed by MIMO techniques compared with improved characteristics as a result of increased transmission power.

CHAPTER 5 DATA ANALYSIS

5.1 CHAPTER OBJECTIVES

Chapter 5 explains the data analysis method and tests the hypothesis. The analytical approach is mathematically simplified. In the method followed to test the hypothesis, samples are drawn from the results presented in the previous chapter. These samples are then processed with an equation (3) derived in Chapter 2 which is based on the inverse square law of irradiance (or radiated power):

$$Link\ budget\ variation\ (dB) = 20\ Log\ \frac{r_2}{r_1} \ldots\ldots\ldots (3)$$

The equation reveals the relationship between range variation (r1/r2) and signal strength (dB) when the bandwidth (BW) is constant (at 600 kbps). Each of the processed results is then compared with the expected value.

5.2 PASSIVE TEST ANALYSIS

Considering Section 3.3 (Passive testing) and the results presented in Figure 4.1, samples were drawn at 36-,18-, 9-, and 4 Mbps. Table 5.1 compares the results obtained with the standard +1dBi antennas (r1) to the results obtained with a 6 dB attenuator set fitted in-line (r2), thus a known and expected link budget variation of –6 dB.

Table 5.1. Transmission results +1dBI Antenna vs. –6dB Attenuator.

Measured result			**Calculated result**	**Expected result**
Data rate (Mbps)	**r_1**	**r_2**	**dB = ($20Log r_2/r_1$)**	**dB = (+17 – 11 dB)**
36	17	37	6.7	6
36	20	40	6	6
18	25	50	6	6
CIR	27	54	6	6
9	32	65	6.1	6
9	35	70	6	6
EIR	37	73	5.9	6
Standard deviation			16.6%	-

Table 5.2 compares the results obtained with the standard +1 dBi antennas to the results obtained with +6dBi antennas, thus a total link budget variation of +5dB.

Table 5.2. Transmission results +1dBi Antenna VS +6dBi Antenna.

Measured result			**Calculated result**	**Expected result**
Data rate	**r_1**	**r_2**	**dB = ($20Log r_2/r_1$)**	**dB = (+6 – 1 dB)**
36	25	45	5.11	5
36	32	57	5.01	5
36	40	70	4.86	5
18	45	75	4.43	5
18	50	90	4.81	5
18	55	100	5.19	5
CIR	57	102	5.05	5
9	65	115	4.95	5
9	70	125	5.03	5
EIR	72	127	4.93	5
Standard deviation			13%	-

5.3 ACTIVE TEST ANALYSIS

Considering Section 3.4 (Active testing) and Figure 4.2, samples were drawn at 36-, 18-, 9-, and 4 Mbps. Table 5.3 compares the results obtained with the RF transmit power set to 50.4 mW (+17 dBm) , to the results obtained with the RF transmit power set to 12.6 mW (+11 dBm). This represents a 6 dB difference in power level, or a 4 to 1 power ratio.

Table 5.3. Transmission results +17dBm RF-OUT vs. +11dBm RF-OUT

Measured result			**Calculated result**	**Expected result**
Data rate	**r_1**	**r_2**	**dB = ($20Log r_2/r_1$)**	**dB = (–6 dB)**
36	40	20	–6	–6
18	50	25	–6	–6
CIR	55	27	–6.1	–6
9	60	30	–6	–6
9	70	35	–6	–6
EIR	72	37	–5.7	–6
Standard deviation			5.5%	-

5.4 STANDARD DEVIATION

The standard deviation for each of these three series in Table 5.1 to Table 5.3, are respectively estimated at 16.6%, 13%, and 5.5%. This is regarded as excessive in the first and second cases and can be attributed to the stepped transmission curves.

5.4.1 Processing data

A second method of data analysis considers processed data in order to reduce the standard deviation i.e. accuracy of the measurements. The following Figure 5.1 indicates a logarithmic trend-line for the series +6 dBi shown in Figure 4.1. Note how the d-CIR and d-EIR are translated into the Y.1564 "Green Zone, Yellow Zone and Red Zone". According to the Y.1564 definitions, when mobile nodes are deployed within the "Green Zone", the specified CIR can be guaranteed. Within the "Yellow Zone" the specified CIR is possible but cannot be guaranteed. Mobile nodes deployed within the "Yellow Zone" may not be able to reconnect after a reset or brown-out. Data throughput is not possible for a mobile node deployed in the "Red Zone".

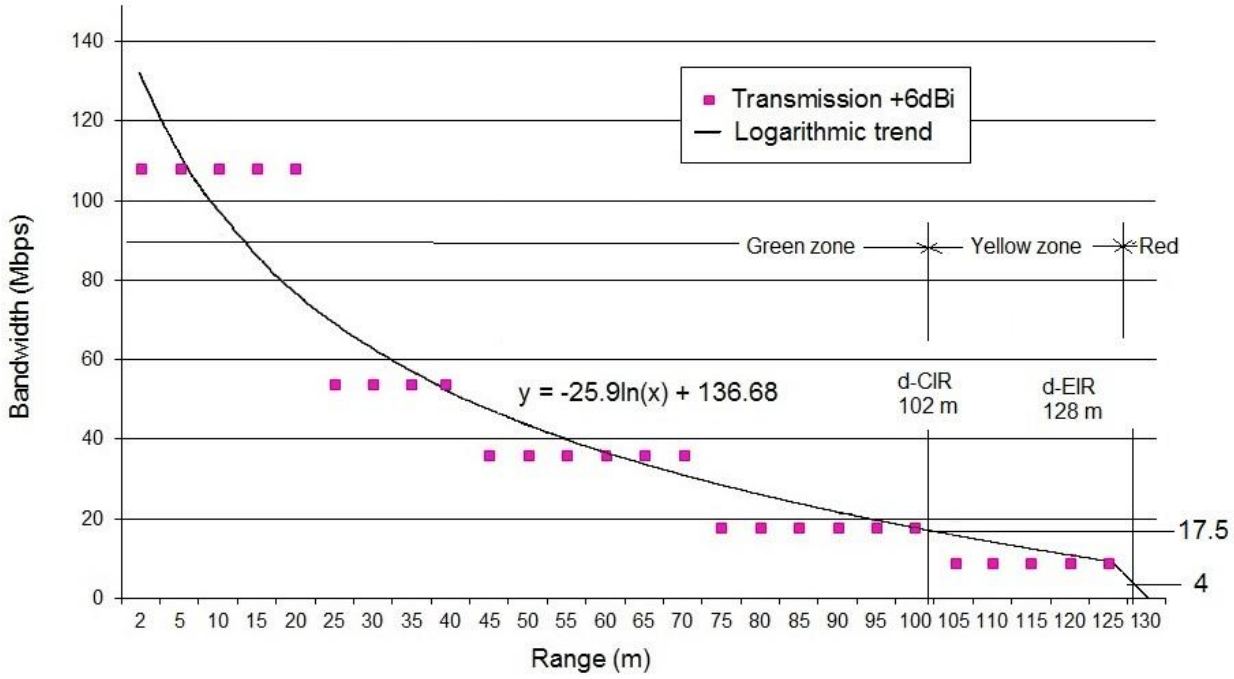

Figure 5.1. Transmission characteristics for +6 dBi with logarithmic trend-line.

Using the logarithmic trend-line, specific values can be extracted for the respective data rates 36 Mbps, 18 Mbps, 9 Mbps, d-CIR and d-EIR. Similarly, specific values were extracted from the series in Figure 2, and the two sets of processed values can again be compared in terms of the expected results, as shown in Table 5.4:

Table 5.4. Transmission results +1dBi antenna vs +6dBi antenna

Measured result			**Calculated result**	**Expected result**
Data rate (Mbps)	**r_1**	**r_2**	**dB = 20Logr_2/r_1)**	**dB = (+6 –1 dB)**
36	36	62	4.72	+5
18	56	100	5.03	+5
CIR	57	102	5.05	+5
9	70	125	5.03	+5
EIR	72	127	4.99	+5
Standard deviation			2.6%	-

5.5 INDUSTRIAL MIMO TEST ANALYSIS

Considering Section 4.3 (Industrial MIMO testing) and Figure 4.3, samples were drawn at 18-, 9 and 1 Mbps from Wavion's results [27] and presented with their processed correlating range values in Table 5.4.

Table 5.4. Transmission range results: Wavion WBS-2400 vs. conventional Wi-Fi.

Measured result			**Calculated result**	**Expected result**
Bandwidth	**r_1**	**r_2**	**dB = (20 Log r_2/r_1)**	**dB = (7.5dBi –1.3dBi)**
18	80	220	8.7	6.2
18	100	240	7.6	6.2
9	120	250	6.3	6.2
9	135	270	6	6.2
1	145	295	6.1	6.2

The actual link budget gain (in dB) may be calculated as the gain factor of the Wavion antennas (7.5dB), minus the conventional antenna gain (1.3dB), equals 6.2 dB.

In spite of the fact that six transceivers are used, each with its own antenna, the calculated results suggest that the RF power required to double the maximum end of the range, must be increased by approximately 6 dB, which is four times the original value. This is descriptive of a typical logarithmic relationship [17], as well as the inverse square law of irradiance [49], [50].

Note the stepped curves which are due to the manufacturer's (Intel) internal algorithms that are contained in the firmware of the OFDM WLAN physical layers. The stepped curves can be smoothed with the use of external software packages like Excel. Our method to use a trend-line is applied so that more accurate information may be extracted from the stepped transmission curves, or by using the characteristic equation $y = -m(x) + \boldsymbol{c}$, also generated with the use of Excel**.** The data presented here may appear erratic, because several range values are indicated for a single value of bandwidth. By using logarithmic trend-lines, a function of MS Excel, a larger number of samples may be drawn and more meaningfully interpreted. The trend-lines are indicated in Figure 5.2:

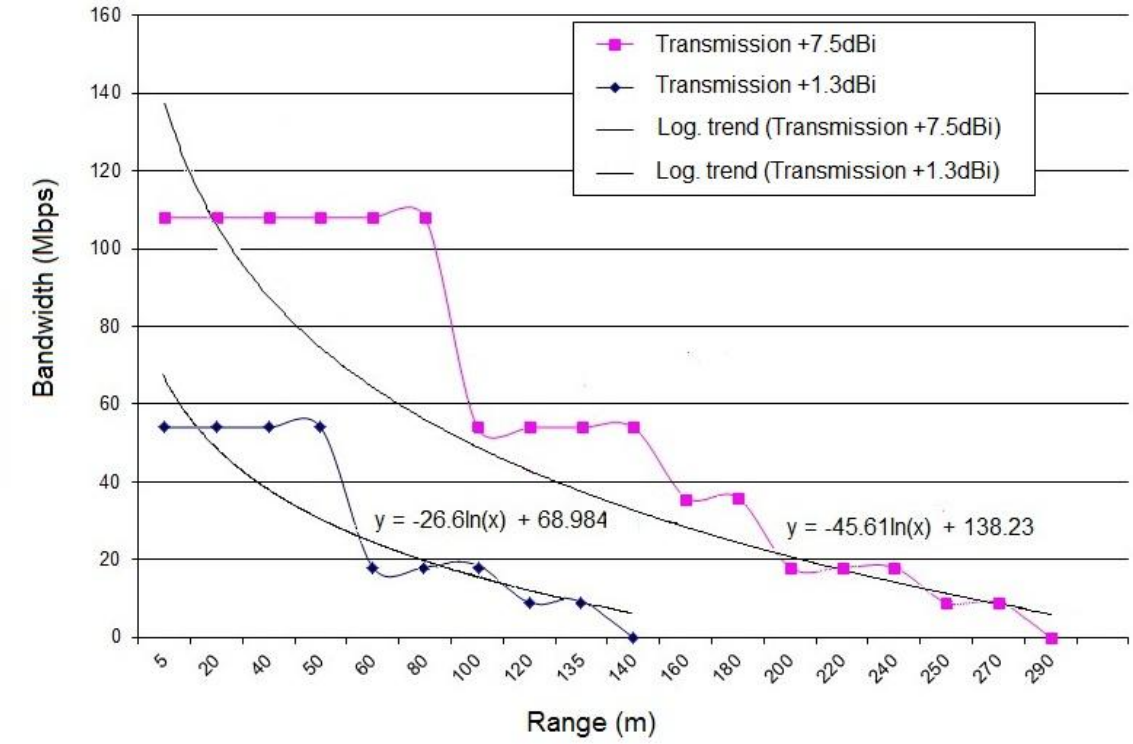

Figure 5.2. Mathematical analysis using logarithmic trend lines.

Figure 5.2 indicates, with the aid of corrected Excel trend-lines, the performance gains that Wavion Technology obtained over conventional Wi-Fi by application of higher gain antennas and MIMO operation. The trend-lines were corrected by adjusting the y-axis intersection until the trend-line intersects with the last known minimum, while maintaining the gradient as estimated by Excel.

The curves differ drastically in terms of gradient and y-axis cut-off. It initially appears a complicated task to compare the two curves in any other terms but maximum range.

5.6 CONCLUSION TO DATA ANALYSIS

For each test conducted, the data analysis presents the expected values next to processed values in tabulated form. In this manner values can individually be compared with the known values. The expected values compare sufficiently favourable with the processed values to confirm that the described mathematical relationship exists. Discussion is presented in the following chapter 7.

It was noted that MIMO technology appears to improve the BW in close range to the AP more than the BW at maximum range specification. This conclusion was also drawn by Wavion engineers that transmission power ultimately extends the usable range limit of a wireless network for a specific data throughput rate.

MIMO technology solves many of the close range problems associated with multiple access networks. These include the shrinking cell phenomenon which ultimately causes the ping-pong effect, and the reduced bandwidth phenomenon. These problems present important research questions that are not addressed by this study.

Specific attention is however drawn to equation (4) derived in Chapter 2. This equation estimates performance increase in terms of BW capability at a stationary node when the network performance is improved by RF wave intensification or signal amplification.

CHAPTER 6 DYNAMIC PERFORMANCE

6.1 CHAPTER OBJECTIVES

In the field of electronics, *dynamic range* is the ratio of a specified maximum level of a parameter, such as power, current, voltage or frequency, to the minimum detectable value of that parameter.

In a transmission system, *dynamic range* is the ratio of the overload level (which means the maximum signal power that the system can tolerate without signal distortion) to the noise level of the system. In digital systems or devices, *dynamic range* is the ratio of maximum to minimum signal levels required to maintain a specified bit error ratio for a specific data throughput.

This chapter considers the dynamic performance of the test network described in chapter 3 according to two analogies that conform to its functional characteristics, namely (i) a radio receiver and (ii) a digital to analogue converter (DAC).

- As a radio receiver, the mobile node has to accept a modulated RF signal and demodulate the analogue video signal and corresponding audio sound track(s).
- As a DAC, the mobile node accepts a complexly digitally coded signal and converts it to an analogue output signal comprising a video signal and audio sound track(s).

Before the dynamic performance of the test network is estimated, this chapter draws specific reference to chapter 2.5 – 2.6, which briefly reviews the parameters that are referred to by both the analogies, as well as the parameters that are specifically related to each analogy separately [27] – [29].

6.2 ESTIMATION OF TEST NETWORK SINAD PARAMETERS

Considering the results obtained from the test network described in chapter 3, an interesting phenomenon observed is that the CIR (in the example's case 600 kbps max) requires in all cases between a minimum of approximately ten times the connected bandwidth-, to a maximum of approximately thirty times the connected bandwidth, to reconnect or reset [25].

This means the 600 kbps CIR fails at a connected bandwidth value below 6 Mbps, and reconnects or recovers from reset at approximately 18 Mbps connected bandwidth.

With specific reference to the observation above, attention is drawn now to the SINAD, which is a parameter for the quality of the output signal produced by a communications device, often defined as [49], [50]:

$$SINAD = \frac{P_{signal} + P_{noise} + P_{distortion}}{P_{noise} + P_{distortion}}$$

This suggests by comparison that the d-EIR is the transmission range at which the signal level of the CIR has deteriorated to the point that it is overcome by the noise and distortion level.

Conversely, the d-CIR is the transmission range at which the CIR signal level is at a sufficiently higher ratio elevated above the noise and distortion level for acceptable video transmission.

This situation relatively represents what will henceforth be referred to as the *digital BW SINAD* ratio for wireless OFDM Ethernet ISWNs [53], which can be calculated from the proposed equation:

$$BW\ SINAD\ (dBcir) = 10\ Log\ \frac{Effective\ bandwidth}{CIR} \quad \ldots\ldots\ldots\ldots (5)$$

With reference to the results of the passive tests in Figure 3.3, we calculate the *BW SINAD* for the reference transmission characteristics after applying the Excel logarithmic trend-line to determine the approximated graph, and by adjusting the y-intersection until the curve intersects with the distant minimum, as indicated in Figure 6.1:

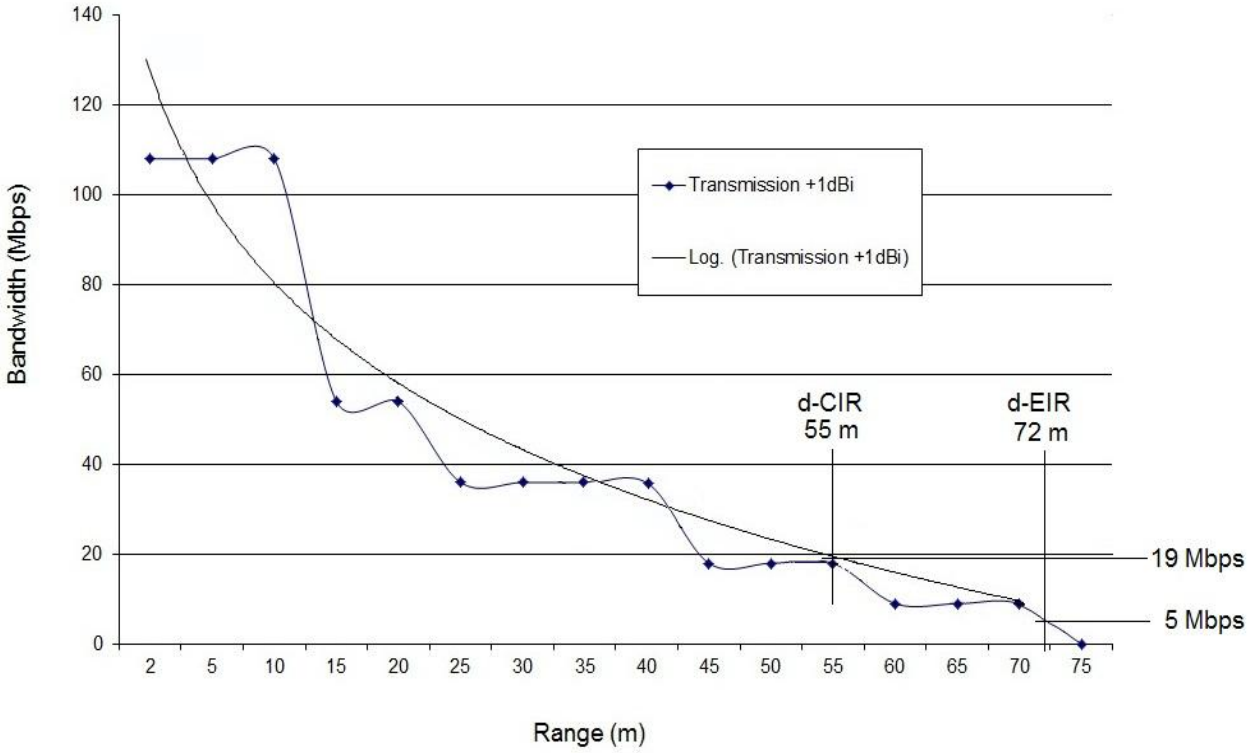

Figure 6.1: Test network transmission characteristic with correcting logarithmic trend graph

With the aid of the trend graph indicated in Figure 6.1, the *BW* values corresponding to the d-CIR and d-EIR can be more accurately extracted from the data collected. As indicated, the transmission characteristics were measured in decreasing steps as determined by the wireless adapter's on-board firmware and algorithms. The result is a rather erratic stepped curve with more than one range value for each *BW* value below 54 Mbps.

According to the trend graph (which can also be described by $y = -26.6 \ln(x) + 125.6$ for the section of interest) the *BW* value at a range of 55 m (d-CIR) is 19 Mbps. The trend graph extends in range up to the last measured *BW* value before transmission was terminated.

For the section of graph beyond 70 m, the way to estimate the *BW* at 72 m (d-EIR) is by assuming a straight line graph section between 70 m (9 Mbps) and 75 m (0 Mbps). If 72.5 m corresponds to 4.5 Mbps, then the bandwidth at 72 m is approximately 5 Mbps.

For example, for the curve *Tx +1dB* the *BW SINAD* can then be calculated from the proposed equation:

$$BW\ SINAD\ (dBcir) = 10\ Log \frac{BW_{dCIR} - BW_{dEIR}}{CIR} \ldots\ldots\ldots\ldots (6)$$

$$\therefore BW\ SINAD\ = 10\ Log\ \frac{19 \times 10^6 - 5 \times 10^6}{600 \times 10^3}$$

$$\therefore BW\ SINAD\ = 13.35\ dBcir$$

The *sensitivity* specification of the mobile node as a radio receiver can also now be estimated as 19 Mbps for a 13.35 dB *SINAD* at throughput CIR of 600 kbps. (18 Mbps may be used being the closest standard *BW* value that the network can connect, for an approximated value of 13 dB *SINAD*).

6.3 ESTIMATION OF TEST NETWORK SFDR PARAMETERS

Following the hypothesis that BW is directly proportional to signal strength, Figure 6.2 shows the typical digital spectral output in Mbps where the SFDR of the test network is estimated.

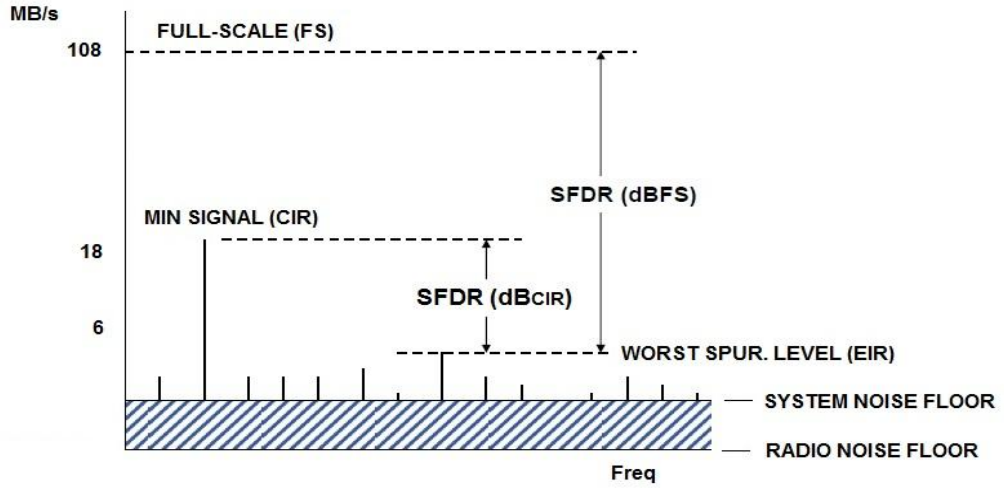

Figure 6.2: Estimating test network Spurious Free Dynamic Range (SFDR). Adapted from [29] with permission.

Figure 6.2 depicts the test network's output in Mbps, indicating CIR and EIR in the frequency domain. The test network minimum (MIN) dynamic range performance can now be estimated:

$$SFDR_{MIN}\ (dBcir) = 10\ Log\frac{BW_{dCIR} - BW_{dEIR}}{CIR} \quad \ldots\ldots\ldots\ldots\ldots (7)$$

$$\therefore\ SFDR_{MIN}\ = 10\ Log\ \frac{19 \times 10^6 - \ 5 \times 10^6}{600 \times 10^3}$$

$$\therefore SFDR_{MIN}\ = 13.35\ dBcir$$

Before the test network's full-scale (FS) dynamic range can be estimated, the ratio of connected bitrate versus real overall throughput bitrate for OFDM WLANs must be considered in order to define a correction factor that must be used in Eq. (7). Some industry publications suggest that the digital communications system will consume approximately one third (0.33) of the available bandwidth to establish and maintain the stability of the link, leaving two thirds (0.66) for throughput.

From recent results published by Microchip Technology, when testing their wireless microprocessors with Ethernet communications, a real throughput rate of between 31Mbps is suggested for a 802.11g connected link speed of 54 Mbps with more than one access node [54]. This 31 Mbps represents a factor of 0.57 of the total 54 Mbps. For a single connecting node a throughput of 34 Mbps is estimated, at a fraction of 0.629 of the connected 54 Mbps. To de-rate this factor slightly further, it was decided to use the golden number equivalent (GNE) as a correction factor which is approximately 0.618.

The MIMO test network full-scale (FS) dynamic range performance can now be estimated for the MIMO test network (where GNE=0.618):

$$SFDR_{FS}\ (dBfs) = 10\ Log\frac{(GNE)(BW_{FS} - BW_{dEIR})}{CIR} \quad \ldots\ldots\ldots (8)$$

$$\therefore\ SFDR_{FS}\ = 10\ Log\ \frac{(0.618)(108 \times 10^6 - \ 5 \times 10^6)}{600 \times 10^3}$$

$$SFDR_{FS}\ = 22.34\ dBfs$$

6.4 COMPARATIVE ANALYSIS OF MOBILE NODES OR PHYSICAL LAYERS ACCORDING TO THE SFDR PARAMETERS

A suitable performance parameter is required in conjunction with a simplified measurement procedure before the dynamic range can be estimated. With these, the performance characteristics of different physical layers can easily be compared in broad performance terms.

The main research goal of this section of the study was therefore to propose a method to compare different OFDM WLAN physical layers in terms of their dynamic performance. A dynamic range performance parameter is required when considering improvement to the link quality, because it will determine the maximum extent to which the link budget can be increased.

This section of the study proposes the spur-free dynamic range parameters namely *SFDRmin* (minimum) and *SFDRfs* (full scale) to express OFDM WLAN dynamic range performance. These are mostly used in the specialised field of high speed digital to analogue conversion (DAC) and analogue to digital conversion (ADC). The SFDR parameters can be derived from the d-CIR and d-EIR using the SLDZ detection method [25]. The SFDRfs is proposed as the definitive test parameter to describe OFDM WLAN physical layer dynamic performance.

The dynamic performance of the experimental test networks is considered according to two analogies which conform to its functional characteristics, namely (i) a radio receiver and (ii) a digital to analogue converter (DAC): As a radio receiver, the mobile node has to accept a modulated RF signal and demodulate the analogue video signal and corresponding audio sound track(s). As a DAC, the mobile node accepts a complexly digitally coded signal and converts it to an analogue output signal comprising a video signal and audio sound track(s).

In the field of electronics, *dynamic range* is the ratio of a specified maximum level of a parameter, such as power, current, voltage or frequency, to the minimum detectable value of that parameter. In a transmission system, *dynamic range* is the ratio of the overload level (which means the maximum signal power that the system can tolerate without signal distortion) to the noise level of the system.

In digital systems or devices, *dynamic range* is the ratio of maximum to minimum signal levels required to maintain a specified bit error ratio for a specific data throughput [25].

6.4.1 Test Methods

The test topology is shown in Figure 2 (a) and (b). The typical OFDM test network consists of two mobile computers and an ISM 802.11.g access point (AP) router.

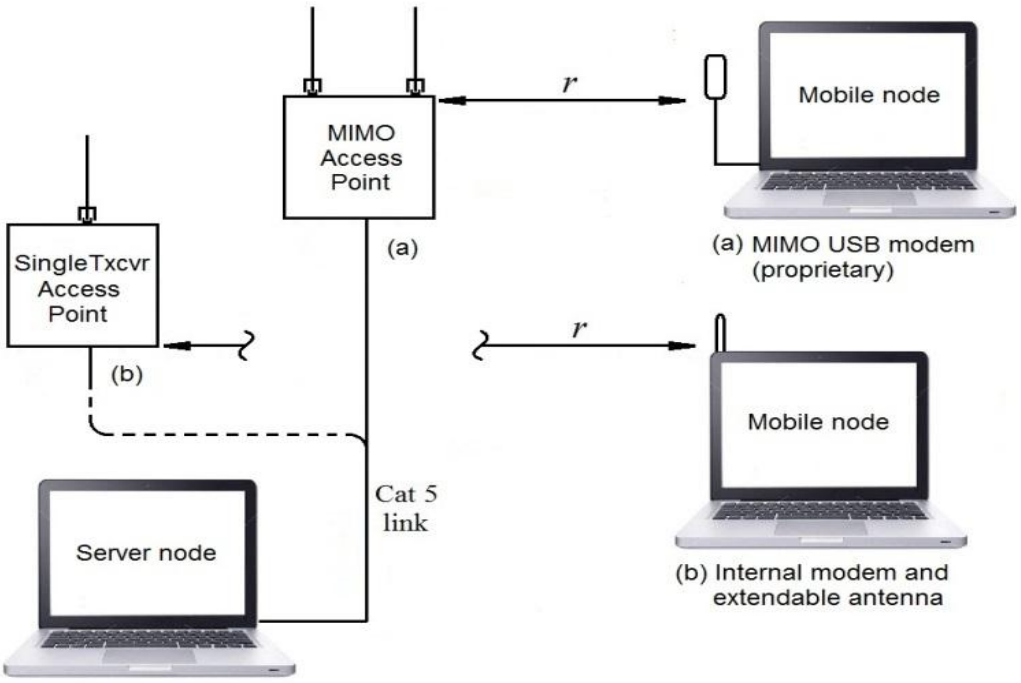

Figure 6.3: Physical layer experimental test network. (a) MIMO AP. (b) Single transceiver AP.

Figure 6.3 depicts the network options for testing. The server node is directly connected to the AP via Cat 5 cable, and also controls the AP adapter settings with a browser based GUI (guided user interface). For the mobile node's adapter, *Intel PROSet Wireless* adapter software is used with the mobile node because it is freely available and easy to use.

Figure 6.4 contains the data collected during *Experiment 1*, described earlier in this document, in a graph generated with the aid of Excel. The indicated d-CIR and d-EIR are for a test bitrate of 600 kbps that is continuously monitored at the receiver node in terms of all the key performance indicators.

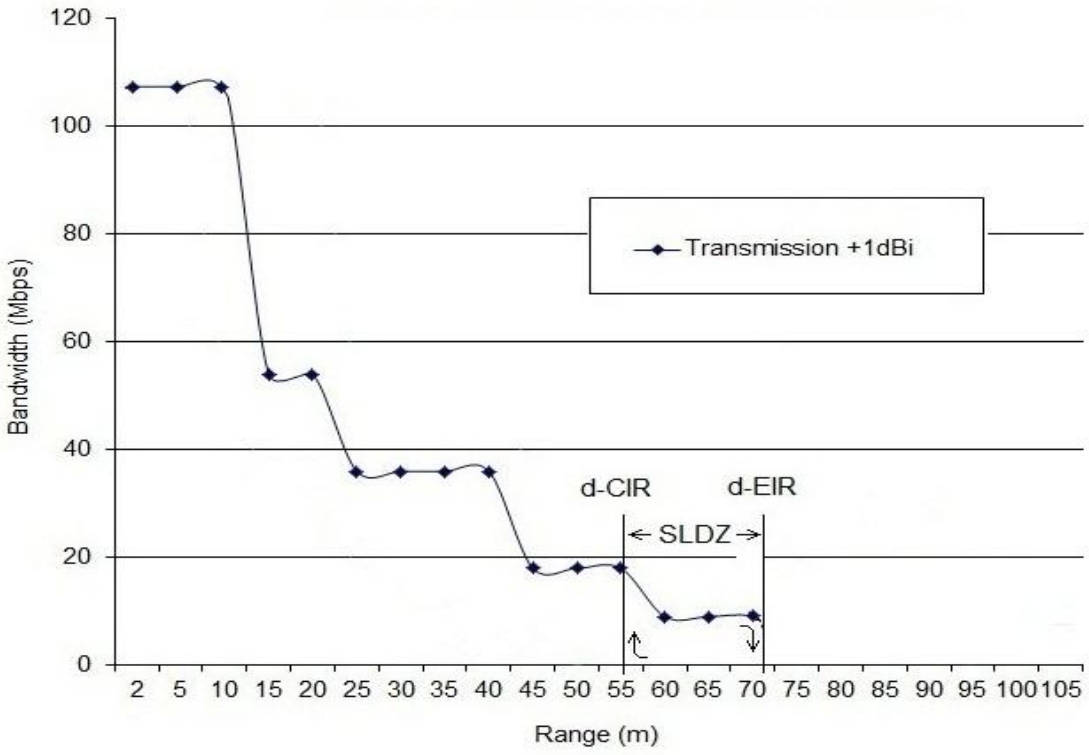

Figure 6.4: Transmission characteristic data for MIMO test network.

Note in Fig. 6.4 the range at which transmission fails (72 m) corresponds to approximately 6 Mbps. When reducing the transmission range, the transmission restarts at 55 m at approximately 18 Mbps.

The SLDZ manifests itself in the same manner as a typical hysteresis curve; transmission failing suddenly at d-EIR and restarting back at d-CIR. This pattern will repeat itself as the mobile node approaches or recedes from the access point AP across the SLDZ.

Experiment 5 determined the service reference for the electronics that was utilised when operating a link with a different receiving node. The electronics used for this test was an 802.11g AP router with single transceiver manufactured by D-Link operating at +18 dBm.

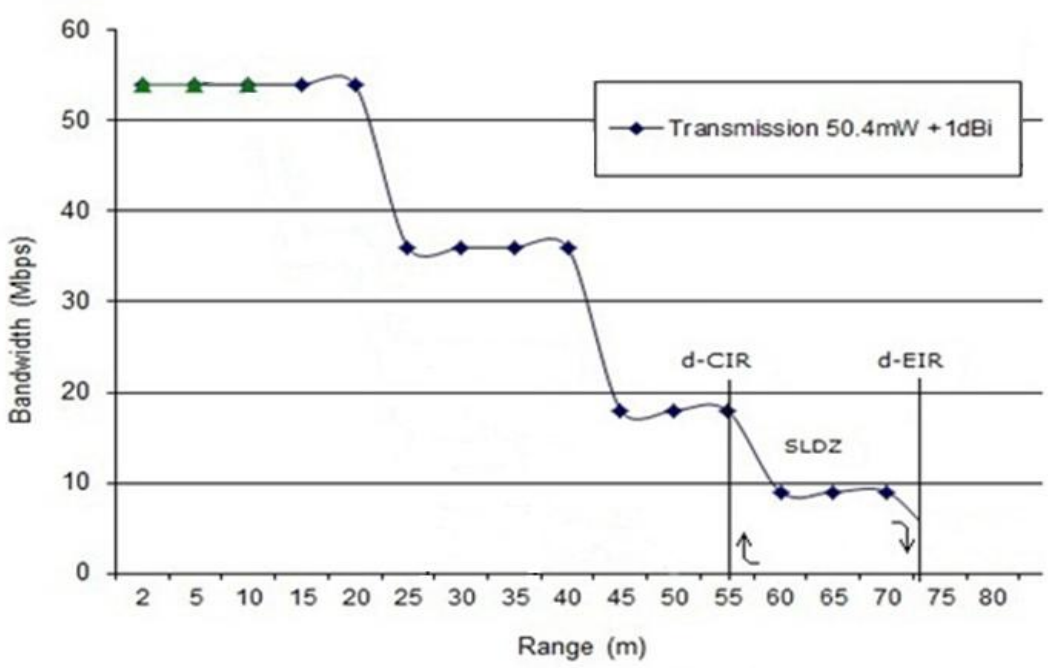

Figure 6.5: Transmission characteristic data for single transceiver test network.

In Figure 6.5, transmission results are depicted with the RF power set to +17dBm. The AP's guide user interface (GUI) made it possible to set RF power in 20% decrements from maximum (+18dBm/63mW) to zero. For this test the RF power was set to 50 mW or +17 dBm. The single transceiver system enabled a near range data connection rate of 54 Mbps.

6.4.2 Analytical approach

All data was first captured into MS Excel, and then processed to produce logarithmic trend-line equivalent curves with corresponding mathematical expressions.

The resulting trend-line's y-intersect was then adjusted until the curve intersected with the last minimum recorded (70 m) at the distance boundary, as shown in Figure 6.6 for the MIMO test network and Figure 6.7 for the single transceiver.

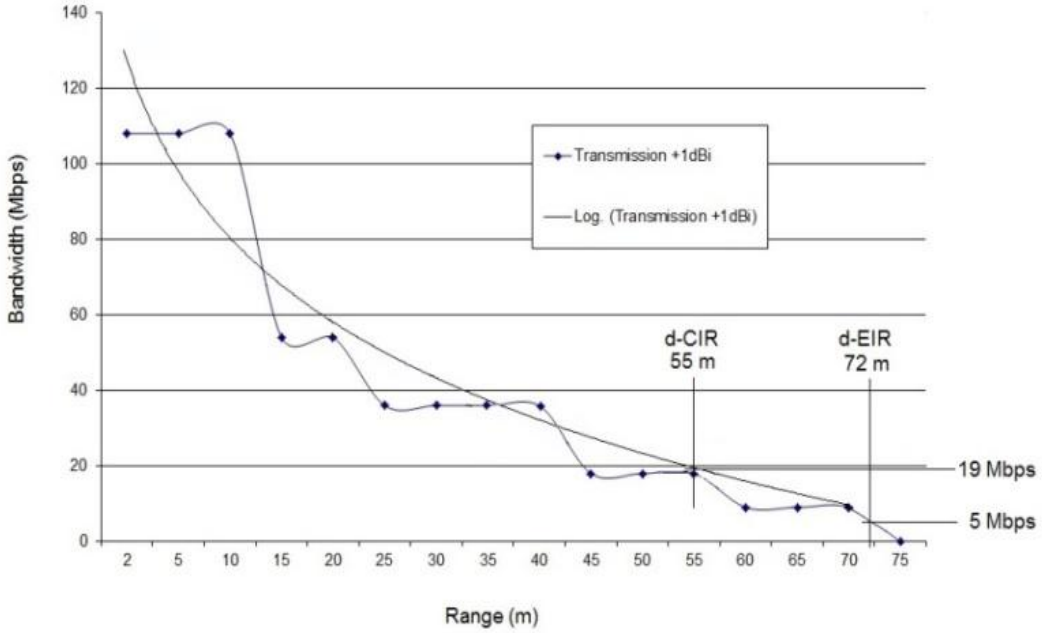

Figure 6.6. MIMO test network transmission characteristic with correcting logarithmic trend graph

With the aid of the logarithmic trend graph indicated in Figure 6.6, the *BW* values corresponding to the d-CIR and d-EIR can be more accurately extracted from the data collected. As indicated, the transmission characteristics were measured in decreasing steps as determined by the wireless adapter's on-board firmware and algorithms. The result is a rather erratic stepped curve with more than one range value for each *BW* value below 54 Mbps.

According to the trend graph indicated in Figure 6.6 (which can also be described by the expression $y = -26.6\ ln(x) + 125.6$ for the section of interest), the *BW* value at a range of 55 m (d-CIR) is 19 Mbps. The trend graph extends in range up to the last measured *BW* value before transmission was terminated.

For the section of graph beyond 70 m, the method used here to estimate the *BW* at 72 m (d-EIR) is by assuming a straight line graph section between 70 m (9 Mbps) and 75 m (0 Mbps). If 72.5 m corresponds to 4.5 Mbps, then the bandwidth at 72 m is approximately 5 Mbps.

Considering the single transceiver's characteristics and resulting logarithmic trend graph $y = -14.17ln(x) + 71.356$ as depicted in Figure 6.7, the d-CIR range corresponds to a connected bandwidth value of 14.5 Mbps and the d-EIR range a value of 2.5 Mbps.

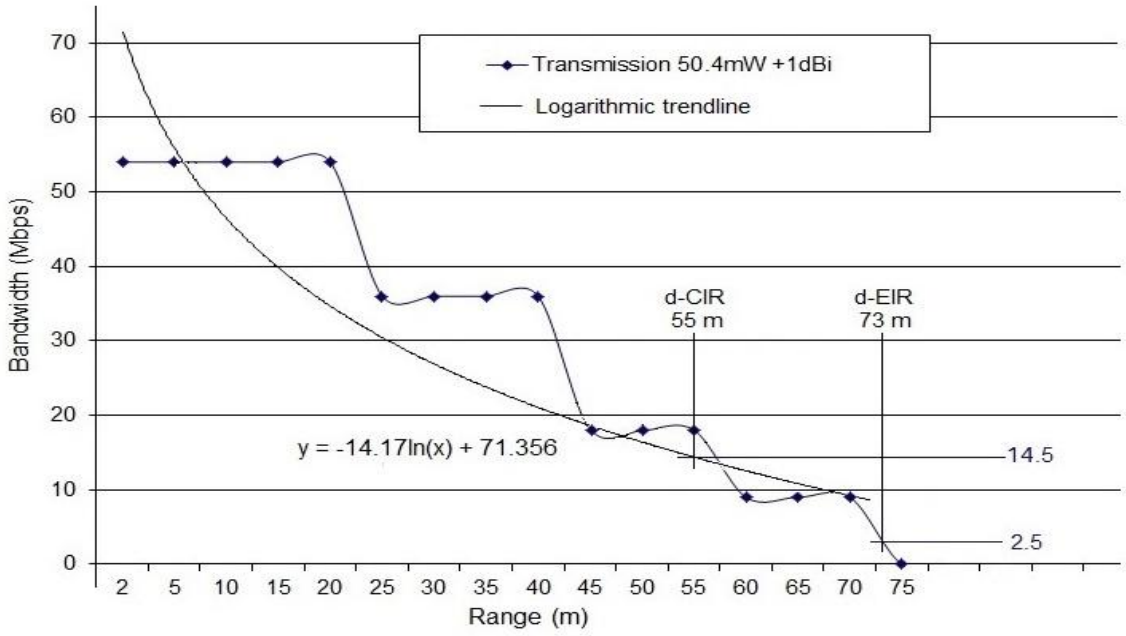

Figure 6.7: Single transceiver transmission characteristic with logarithmic trend graph

6.4.3 SFDR analysis results

Considering the resulting data obtained from the MIMO test network an interesting phenomenon observed was that the CIR (in the example's case 600 kbps max) requires between a minimum of approximately ten times the connected bandwidth-, to a maximum of approximately thirty times the connected bandwidth, to reconnect or reset [25]. This means the 600 kbps CIR fails at a connected bandwidth value below 6 Mbps, and reconnects or recovers from reset at approximately 18 Mbps connected bandwidth.

With specific reference to the observation above, attention is drawn now to the SINAD, which is a parameter for the quality of the output signal produced by a communications device, often defined as [49], [50]:

$$SINAD = \frac{P_{signal} + P_{noise} + P_{distortion}}{P_{noise} + P_{distortion}}$$

This suggests by comparison that the d-EIR is the transmission range at which the signal level of the CIR has deteriorated to the point that it is overcome by the noise and distortion level. Conversely, the d-CIR is the transmission range at which the CIR signal level is at a sufficiently higher ratio elevated above the noise and distortion level for acceptable video transmission.

This situation relatively represents what will henceforth be referred to as the *digital BW SINAD* ratio for OFDM WLAN based ISWNs [25], which can be calculated from the proposed equation:

$$BW\ SINAD\ (dBcir) = 10\ Log\ \frac{Effective\ bandwidth}{CIR} \quad \ldots\ldots\ldots (5)$$

For example, for the curve depicted in Figure 5, the *BW SINAD* can then be calculated as follows:

$$BW\ SINAD\ (dBcir) = 10\ Log \frac{BW_{dCIR} - BW_{dEIR}}{CIR} \quad \ldots\ldots\ldots\ldots (6)$$

$$\therefore BW\ SINAD\ = 10\ Log\ \frac{19 \times 10^6 - 5 \times 10^6}{600 \times 10^3}$$

$$\therefore BW\ SINAD\ = 13.35\ dBcir$$

The *sensitivity* specification of the first mobile node in Figure 6.6 as a radio receiver can also now be estimated as 19 Mbps for a 13.35 dB *SINAD* at throughput CIR of 600 kbps. (18 Mbps may be used being the closest standard *BW* value that the network can connect for an approximated value of 13 dB *SINAD*). For the second example, the BW SINAD can be calculated for the curve depicted in Figure 6.7 by the same method:

$$BW\ SINAD\ (dBcir) = 10\ Log\ \frac{BW_{dCIR} - BW_{dEIR}}{CIR} \ldots\ldots\ldots\ (6)$$

$$\therefore BW\ SINAD\ = 10\ Log\ \frac{14.5 \times 10^6 - 2.5 \times 10^6}{600 \times 10^3}$$

$$\therefore BW\ SINAD\ = 13.01\ dBcir$$

Again, the sensitivity specification of the second mobile node in Figure 6.7 as a radio receiver can now be estimated as 14.5 Mbps for a 13 dB SINAD at a throughput CIR of 600 kbps.

6.4.4 Estimation of test network SFDR parameters

With reference to Figure 6.2 and from data collected from Figure 6.6, the MIMO test minimum (*MIN*) spur free dynamic range performance can now be estimated:

$$SFDR_{MIN}\ (dBcir) = 10\ Log\ \frac{BW_{dCIR} - BW_{dEIR}}{CIR} \ldots\ldots\ldots\ (7)$$

$$\therefore\ SFDR_{MIN}\ = 10\ Log\ \frac{19 \times 10^6 - 5 \times 10^6}{600 \times 10^3}$$

$$\therefore SFDR_{MIN}\ = 13.35\ dBcir$$

Before the test network's full-scale (FS) dynamic range can be estimated, the ratio of connected bitrate versus real overall throughput bitrate for OFDM WLANs must be considered in order to define a correction factor that must be used in Eq. (7). Some industry publications suggest that the digital communications system will consume approximately one third (0.33) of the available bandwidth to establish and maintain the stability of the link, leaving two thirds (0.66) for throughput.

From recent results published by Microchip Technology, when testing their wireless microprocessors with Ethernet communications, a real throughput rate of between 31Mbps is suggested for a 802.11g connected link speed of 54 Mbps with more than one access node [54]. This 31 Mbps represents a factor of 0.57 of the total 54 Mbps. For a single connecting node a throughput of 34 Mbps is estimated, at a fraction of 0.629 of the connected 54 Mbps. To de-rate this factor slightly further, it was decided to use the golden number equivalent (GNE) as a correction factor which is approximately 0.618.

The MIMO test network full-scale (FS) dynamic range performance can now be estimated for the MIMO test network (where GNE=0.618):

$$SFDR_{FS}\ (dBfs) = 10\ Log\frac{(GNE)(BW_{FS} - BW_{dEIR})}{CIR} \ldots\ldots\ldots (8)$$

$$\therefore\ SFDR_{FS}\ = 10\ Log\ \frac{(0.618)(108 \times 10^6 -\ 5 \times 10^6)}{600 \times 10^3}$$

$$SFDR_{FS}\ = 22.34\ dBfs$$

Similarly, the single transceiver test network's *BW SINAD* (or SFDRmin) and SFDRfs can be calculated using the same equations:

$$BW\ SINAD\ (dBcir) = 10\ Log\frac{BW_{dCIR} - BW_{dEIR}}{CIR} \ldots\ldots\ldots (6)$$

$$\therefore BW\ SINAD\ = 10\ Log\ \frac{14.5 \times 10^6 -\ 2.5 \times 10^6}{600 \times 10^3}$$

$$\therefore BW\ SINAD\ = 13.01\ dBcir$$

Now:

$$SFDR_{FS}\,(dBfs) = 10\,Log\frac{(GNE)(BW_{FS} - BW_{dEIR})}{CIR} \quad \ldots(8)$$

$$\therefore\ SFDR_{FS} = 10\,Log\,\frac{(0.618)(54\times10^{6} - 2.5\times10^{6})}{600\times10^{3}}$$

$$SFDR_{FS} = 17.26\,dBfs$$

The results obtained by the study, for two dissimilar physical layers transporting the same class of service (CoS) traffic, can now be tabulated for comparison:

Table 1: Comparison of Experiment 1 and Experiment 2, physical layers

	MIMO Exp 1	Single transceiver Exp 2
SINAD	13.35 dB	13.01 dB
SFDRmin	13.35 dB	13.01 dB
SFDRfs	22.34 dB	17.26 dB
Sensitivity	19 Mbps for 13.36 dB SINAD at CIR=600 kbps	14.5 Mbps for 13.01 dB SINAD at CIR=600 kbps

From the table it is clear that SINAD and SFDRmin is exactly the same concept (since they are calculated with the same equation), although traditional types may prefer the legacy radio terminology of *SINAD* over *SFDRmin*.

It is no surprise that the MIMO option in Exp. 1 has a higher full scale dynamic range SFDRfs – this is mainly attributable to the higher connecting bitspeed at 108 Mbps.

It is noted with interest that the single transceiver has a much improved sensitivity rating. This was not clear from initial measurements, because the same d-CIR range was measured for both physical layers. However, with the use of the logarithmic trend graph it became possible to estimate the corresponding BW readings with closer accuracy and clearly reveal the difference in physical layer characteristic features.

6.5 CONCLUSION TO DYNAMIC PERFORMANCE

This chapter has considered the test network from two analogies. It has proposed the equations (5), (6), (7) and (8) to determine the dynamic performance descriptors namely SINAD parameters (in terms of radio receivers) and SFDR parameters (in terms of DACs).

The chapter has revealed a method to process data by the use of Excel logarithmic trend lines. This method was applied to extract meaningful input information to the proposed equations.

The equations and methods are necessary to grade the quality of similar or replicating test networks or physical layers for research purposes.

CHAPTER 7 DISCUSSION

7.1 THE HYPOTHESIS

This thesis formulates the hypothesis that connected bandwidth (BW) in Mbps is directly proportional to the power density, or alternatively the electric field strength, of the radio frequency (RF) wave at the receiving node. This implies that the connected BW will decrease at the same rate as the power density (or electric field strength) of the RF wave, until the decline in signal to noise (SN) ratio results in termination of wireless communication.

The hypothesis motivates the application of the inverse square law of irradiation (or radiated power) to estimate wireless network performance. This novel approach provides the simplified mathematical building blocks that are required to solve range, and capacity related issues of wireless systems.

7.2 TESTING THE HYPOTHESIS

To test the hypothesis, several experiments were conducted. The first experiment describes the method to evaluate any deployed network in order to define its service standards. The standards that are conformed to are leading IEEE.Y-1564 that defines the CIR and EIR capabilities of the network.

The second experiment demonstrates the improved capabilities when the RF wave is intensified at the receiving node in a passive manner by the application of higher gain antennas. The third experiment serves as a control for the second, where the original RF wave intensity is reduced in a passive manner and so demonstrates the reduced capabilities of the network.

The fourth and fifth experiments serve as a control set of experiments for the initial three experiments. During the fourth experiment a typical network is evaluated in terms of a

nominally high power setting, and during the fifth experiment, a typical network is evaluated in terms of a lower power setting, which is one quarter in magnitude of the high power setting in experiment four.

The hypothesis has been tested positively by the results obtained in the experiments described in this study, because they correlate with expected values. This also motivates the application of the inverse squared law of radiated power (or irradiation) as a mathematical tool to estimate information rate variations in ISM band OFDM WLANs, as applied in industrial wireless sensor networks.

7.3 ESTIMATION OF SERVICE REFERENCE CIR

By using a video bit stream of a pre-determined rate to specify the required committed throughput, the service level differential zone SLDZ can easily be measured and the CIR and EIR for each network option can be detected. Once the d-CIR and d-EIR transmission ranges for the network options are known, these values can be used in conjunction with a simple set of equations (3) and (4) to estimate range or bandwidth variations in network performance, in terms of dB. The observation of a video stream in order to evaluate network key performance indicators (KPIs) provides a fast, intuitive and easily interpreted method to confirm the CIR under actual operational conditions.

7.4 THE *DIGITAL BW SINAD*

An interesting phenomenon observed is that the CIR (in the example's case 600 kbps max) requires in all cases between a minimum of approximately ten times the connected bandwidth, to a maximum of approximately thirty times the connected bandwidth, to reconnect or reset.

This means the 600 kbps CIR fails at a connected bandwidth value below 6 Mbps, and reconnects or recovers from reset at approximately 18 Mbps connected bandwidth.

With specific reference to the observation above, the SINAD is considered here, which is an indication of a communication device's signal quality, often defined as [49], [50]:

$$SINAD = \frac{P_{signal} + P_{noise} + P_{distortion}}{P_{noise} + P_{distortion}}$$

By functional comparison, the d-EIR is the transmission range at which the signal level of the CIR has deteriorated to the point that it is overcome by the noise and distortion level. Conversely, the d-CIR is the transmission range at which the CIR signal level is at a sufficiently higher ratio elevated above the noise and distortion level for acceptable video transmission.

This situation relatively represents what will henceforth be referred to as the *digital BW SINAD* ratio which can be calculated from the proposed equation:

$$digital\ BW\ SINAD\ (dB_{CIR}) = 10\ Log\ \frac{Effective\ bandwidth}{CIR} \quad \ldots\ldots\ldots\ldots (5)$$

With reference to the results of the passive tests in Figure 4.1, the *BW SINAD* for each transmission characteristic may be calculated after applying the Excel logarithmic trend-lines. For example, for the curve *Tx +1dB*:

$$digital\ BW\ SINAD\ (dB_{CIR}) = 10\ Log \frac{BW_{d-CIR} - BW_{d-EIR}}{CIR} \quad \ldots\ldots\ldots\ldots (6)$$

$$\therefore digital\ BW\ SINAD\ = 10\ Log\ \frac{19 \times 10^6 - 5 \times 10^6}{600 \times 10^3}$$

$$\therefore digital\ BW\ SINAD\ = 13.35\ dB_{CIR}$$

For the curve *Tx +6dB*, using the same method, the *BW SINAD* is calculated at 13.18 dB_{CIR}, and for the curve *Tx –5dB* the *BW SINAD* is 15.44 dB_{CIR}. Acceptable results are noted since the SINAD required for microwave frequency is expected to be slightly higher than the 12 dB recommended for VHF.

Note the higher than expected value of 15.44 dB required for the *Tx –5dB* curve to produce acceptable results. The additional signal level that is required to produce acceptable results is probably required to overcome the additional return loss due to mismatch. The mismatch

probably occurs as a result of the additional connectors introduced to the system by the attenuator pads.

7.5 THE EFFECTS OF MIMO ON TRANSMISSION CHARACTERISTICS

Considering MIMO OFDM operation as the cutting edge technology of the day, we now consider the results presented in Table 5.4 and note the deviation of measured results from expected calculated results of the Wavion Technology, specifically within the near half-range region between 5 m and 140 m.

Analyzing the data samples with the use of Excel trend-lines software, which uses calculus based optimization to process information, reveals the mathematical equations that best describe the transmission characteristic curves as shown in Figure 7.1.

The effects of MIMO technology can be observed when considering the processed results of transmission testing. As shown in Figure 7.1, the slopes of the compared curves at close range, as well as the x-axis limitations, indicate the effects of MIMO technology.

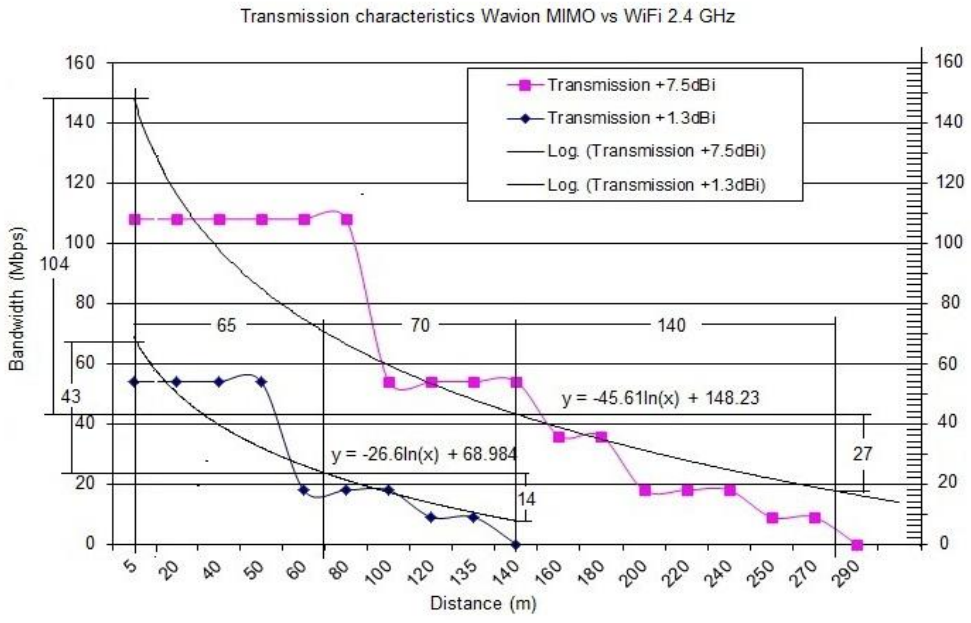

Figure 7.1. Processed transmission characteristics: Wavion MIMO vs. Wi-Fi

Figure 7.1 indicates mathematical trend-lines that are produced with the use of Excel software, that also reveals the fundamental line equation $y = -45.61\ ln(x) + 148.23$ for (Wavion) *Transmission +7.5 dBi* characteristics as well as $y = -26.6\ ln(x) + 68.98$ for (Wi-Fi) *Transmission +1.3 dBi* characteristics. Note that the processed trend lines indicated here are not corrected in terms of minimum point intersection as those depicted previously in Figure 5.4.

The gradients of the transmission curves can be calculated in terms of four half-range sections, and so evenly compared, namely (i) Wi-Fi half-to-max range (m_1), compared with (ii) Wavion half-to-max range (m_2), and (iii) Wi-Fi close-to-half range (m_3) compared with (iv) Wavion close-to-half range (m_4):

$$m_1 = \frac{\Delta y_1}{\Delta x_1} = \frac{14}{70} = 0.20$$

$$m_2 = \frac{\Delta y_2}{\Delta x_2} = \frac{27}{140} = 0.19$$

$$m_3 = \frac{\Delta y_3}{\Delta x_3} = \frac{43}{65} = 0.66$$

$$m_4 = \frac{\Delta y_4}{\Delta x_4} = \frac{14}{70} = 0.77$$

The distant half-range slopes m_1 and m_2 compare evenly at 0.20 and 0.19 respectively, with only a 0.01 difference in gradient. This confirms that they can be described by the same equation, if such an equation is based on the inverse square law of irradiance.

The near half-range slopes m_3 and m_4 with slopes respectively at 0.66 and 0.77 shows a 0.11 difference in gradient. This considerable difference can mathematically be attributed to the large difference in the *y*-intersect points of the curve equations. This is caused by the difference in system maximum capabilities, i.e. when comparing single transceiver technology with MIMO technology.

The above suggests that the application of multiple transceiver technology raises the *y*-intersect of the transmission curve, whereas increasing the range capabilities ultimately increases the *x*-intersect of the transmission curve.

7.6 DYNAMIC PERFORMANCE OF TEST NETWORK

To be able to evaluate the performance of any test network considered for experimentation, the proposed equation presented in chapter 6 was used to estimate the minimum SFDR of the network used in Experiment 1:

$$SFDR_{MIN}\ (dBcir) = 10\ Log\frac{BW_{dCIR} - BW_{dEIR}}{CIR} \quad \ldots\ldots\ldots\ldots (7)$$

The minimum $SFDR_{MIN}$ (or SINAD) was estimated at 13.35 dBcir for a throughput CIR of 600 kbps. The test network sensitivity was estimated at approximately 18 Mbps for a SINAD of 13 dB (CIR = 600 kbps).

To be able to estimate the useable dynamic range between minimum and full-scale operation, the equation (8) proposed in chapter 6 was used (where GNE=0.618):

$$SFDR_{FS}\ (dBfs) = 10\ Log\frac{(GNE)(BW_{FS} - BW_{dEIR})}{CIR} \quad \ldots\ldots\ldots (8)$$

$$\therefore\ SFDR_{FS}\ = 10\ Log\ \frac{(0.618)(108 \times 10^6 - \ 5 \times 10^6)}{600 \times 10^3}$$

$$SFDR_{FS}\ = 22.34\ dBfs$$

The phenomenon termed the *service level differential zone*, (SLDZ) [25] enables a method to set a reference in terms of committed throughput bandwidth between a client node and an access point at a specific range. The study of this phenomenon here provides a simplified method to determine the performance capabilities of a deployed IWSN in terms of the *digital BW SINAD* indicating *sensitivity*, the SFDRfs indicating *dynamic*

performance, or to determine the newly acquired capabilities of the network when higher gain antennas or amplification are used to improve performance.

7.7 COMPARATIVE ANALYSIS

The results obtained by the study, for two dissimilar physical layers transporting the same CoS traffic, can now be tabulated for comparison:

Table 7.1: Comparison of Exp 1 and Exp2 physical layers

	MIMO Exp 1	Single transceiver Exp 2
SINAD	13.35 dB	13.01 dB
SFDRmin	13.35 dB	13.01 dB
SFDRfs	22.34 dB	17.26 dB
Sensitivity	19 Mbps for 13.36 dB SINAD at CIR=600 kbps	14.5 Mbps for 13.01 dB SINAD at CIR=600 kbps

From the table it is clear that SINAD and SFDRmin is exactly the same concept (since they are calculated with the same equation), although traditional types may prefer the legacy radio terminology of *SINAD* over *SFDRmin*.

It is no surprise that the MIMO option in Exp. 1 has a higher full scale dynamic range SFDRfs – this is mainly attributable to the higher connecting bitspeed at 108 Mbps.

It is noted with interest that the single transceiver has a much improved sensitivity rating. This was not clear from initial measurements, because the same d-CIR range was measured for both physical layers. However, with the use of the logarithmic trend graph it became possible to estimate the corresponding BW readings with closer accuracy and clearly reveal the difference in physical layer characteristic features.

7.8 THE WAY FORWARD

The capability to define and predict a wireless network in mathematical terms provides the fundamental requirements to analyze the network with reasonable accuracy. With these in hand, future research should focus on multiple access optimization and energy saving.

The effects of enabling security protocol such as WPA2 (PSK) are well known to consume bandwidth and reduce the maximum range of WLANs as applied in the field of WSNs. However, to estimate these effects in terms of variables like committed throughput rate, remains a difficult task.

Future research should focus on estimating the effects of WPA2 (PSK) on the relative RF link budget of a WLAN based wireless sensor network.

CHAPTER 8 CONCLUSION

The study has introduced IWSNs to ISM-band OFDM WLANs, with specific reference to thermography and Android based computer technology. A novel method to estimate a specified committed information rate in terms of range and link budget was positively tested against expected values. These capabilities render OFDM WLANs operating within ISM bands an extremely useful communications transport medium for industrial wireless sensor networks, and specifically for cutting edge Android nodes with Linux based operating systems.

The study of a phenomenon, of which the significance has not previously been recognized and documented, here termed the *service level differential zone*, (SLDZ) enabled a method to set a reference in terms of committed throughput bandwidth between a client node and an access point at a specific range.

A hypothesis was proposed that connected bandwidth in OFDM WLANs is directly proportional to signal level in dBm. Following two analogies namely RF and DAC, the concept was mathematically proved by a heuristic statistical analysis approach, whereby data collected from transmission characteristics were compared with expected results, when the signals are intensified or attenuated to specifically known values. A method was revealed whereby collected data were processed in order to substantially improve the accuracy of the measurements.

Comparative studies by physical experimentation revealed that mobile nodes can be individually tested in terms of their respective SINAD parameters, as well as their SFDR parameters, without connecting external test equipment. With these parameters available, mobile Android/Linux computer nodes can in future be qualified for industrial use in terms of their throughput performance, which is a key requirement for the ITU-T Y.1564 and EtherSAM test methodologies.

The study has contributed sufficiently to present the following research outputs:

A full length research article [55] published by Elsevier's *Journal of Applied Research & Technology* (JART).

A paper published [25] by the South African Academy for Science and Arts' *South African Journal of Science and Technology* (SAJST).

A paper presented [56] at the S. A. Academy for Science and Arts' *Students' Symposium in Natural Sciences.*

A full length research article [57] to be published by Elsevier's *Journal of Applied Research & Technology* (JART).

REFERENCES

[1] L. Hou and N. W. Bergman, "System requirements for industrial wireless sensor networks," in *Proc. 15th IEEE EFTA*, 2010, Bilbao, Spain, pp. 1–8, 2010.

[2] V.C. Gungor and G.P. Hancke, "Industrial wireless sensor networks: Challenges, design principles, and technical approaches," *IEEE Trans. Ind. Electron.*, vol. 56, no. 10, pp. 4258–4264, Oct. 2009.

[3] M. Alan, C. David, P. Joseph, S. Robert, and A. John, "Wireless sensor networks for habitat monitoring," in *Proc. 1st ACM Int. Workshop Wireless Sensor Netw. Appl*., 2002, Atlanta, GA, USA.

[4] A. Carullo, S. Corbellini, M. Parvis, and A. Vallan, "A wireless sensor network for cold-chain monitoring," *IEEE Trans. Instrum. Meas*., vol. 58, no. 5, pp. 1405–1411, May 2009.

[5] A. Flammini, D. Marioli, E. Sisinni, and A. Taroni, "Design and implementation of a wireless fieldbus for plastic machineries," *IEEE Trans. Ind. Electron.*, vol. 56, no. 3, pp. 747–755, Mar. 2009.

[6] L. Bin and V. C. Gungor, "Online and remote motor energy monitoring and fault diagnosis using wireless sensor networks," *IEEE Trans. Ind. Electron.*, vol. 56, no. 11, pp. 4651–4659, Nov. 2009.

[7] Sun, Da-Wen. Computer vision technology for food quality evaluation. Academic Press, ISBN 978-0-12-373642-0, 2007.

[8] H. Korber, H. Wattar, and G. Scholl, "Modular wireless real-time sensor/actuator network for factory automation applications," *IEEE Trans. Ind. Informat.*, vol. 3, no. 2, pp. 111–119, May 2007.

[9] A. Willig, M. Kubisch, C. Hoene, and A. Wolisz, "Measurements of a wireless link in an industrial environment using an IEEE 802.11-compliant physical layer," *IEEE Trans. Ind. Electron.*, vol. 49, no. 6, pp. 1265–1282, Dec. 2002.

[10] Fluke Application Note 2788354, "Why thermography is good for your business." A-EN-N Rev B 12/2007 Publication ID:11226-eng.

[11] Fluke Application Note 2524871, "Inspecting furnaces and boilers." A-EN-N Rev B, 1/2008. Publication ID: 11062-eng.

[12] V. Sempere and J. Silvestre, "Multimedia applications in industrial networks: Integration of image processing in Profibus," *IEEE Trans. Ind. Electron.*, vol. 50, no. 3, pp. 440–448, Jun. 2003.

[13] B. Giguère, "RFC 2544: How it helps qualify a carrier Ethernet network," EXFO Appl. Note no. 183.1AN, 2008.

REFERENCES

[14] *ITU Ethernet Service Activation Test Methodology*, ITU-T Y.1564, 2016, http://www.itu.int/rec/T-REC-Y.1564/en

[15] *MEF Ethernet Services Attributes - Phase 2,* MEF Metro Ethernet Forum Technical Specification MEF 10.1, November 2006.

[16] A. J. Paulraj, R. U. Nabar, and D. A. Gore, Introduction to space-time wireless communication, Cambridge, UK: Cambridge University Press, 2003.

[17] H. Liu and G. Li, OFDM-based broadband wireless network – Design and optimalization, 1st Ed. ISBN 0-471-72346-0, 2005.

[18] M. Oltean, "An introduction to orthogonal frequency division multiplexing," Intel broadband wireless tutorial, 2004.

[19] J. Wolnicki. "The IEEE 802.16 WiMAX Broadband Wireless Access; Physical layer (PHY), Medium Access Control layer (MAC)", Radio Resource Management (RRM) Tech. Rep., 2005.

[20] H. Bolcskei and E. T. H. Zurich, "MIMO-OFDM Wireless Systems: Basics, Perspectives and Challenges," *IEEE Wireless Communications*, p. 31, August 2006.

[21] A. Dammann, R. Raulefs, and S. Kaiser, "Beamforming in combination with space-time diversity for broadband OFDM systems," in *Proc. IEEE conference on Communications*, vol. 4, pp 1147-1151, 2001.

[22] J. M. Ide, S. P. Kingsley, S. G. O'Keefe and S. A. Saario, "A novel wide band antenna for WLAN applications," in *Proc. IEEE Antennas and Propagation Society International Symposium*, 4Ano., pp. 243-246 vol. 4A, 2005.

[23] F. Karlsen, "Guidelines to low cost wireless system design," Wireless Communications, Nordic VLSI ASA, 2009.

[24] J. Akerberg, M. Gidlund, M. Bjorkman, "Future challenges in wireless sensor and actuator networks targeting industrial automation," *IEEE Trans. Ind. Electron*, 2011, pp. 410–415.

[25] P. van Rhyn and G. P. Hancke, "A method to estimate the performance optimisation of an industrial wireless Ethernet network by observation of the service level differential zone (SLDZ)." *South African Journal of Science and Technology*, vol. 28, no. 3, pp 259–260, September 2009.

[26] K. H. Carpenter, "A differential equation approach to minor loops in the Jiles-Atherton hysteresis model," *IEEE Transactions on Magnetics*, vol 27, no. 6, pp 4404-4406, Aug 2002.

[27] J. R. Naylor, "Testing Digital/Analog and Analog/Digital Converters," *IEEE Transactions on Circuits and Systems*, Vol. CAS-25, July 1978, pp. 526-538.

[28] *IEEE Standard for Terminology and Test Methods for Analog-to-Digital Converters*, IEEE Std. 1241-2000, ISBN 0-7381-2724-8, 2001.

[29] W. Kester, Analog-Digital Conversion, Analog Devices, 2004, ISBN 0-916550-27-3, Chapter 2 and 5. Also available as The Data Conversion Handbook, Elsevier/Newnes, 2005, ISBN 0-7506-7841-0, Chapter 2, 5.

[30] Wavion. "The ultimate solution for metro and rural Wi-Fi." Technical overview and description of multiple access base station for 2.4 GHz unlicensed band, April 2008.

[31] P. Pace, M. Belcastro, and E. Viterbo, "Fast and accurate PQoS estimation over 802.11g wireless network," in *Proc. IEEE Communications Society ICC*, 2008.

[32] Y. Ennaji, M. Boulmalf and C. Alaoui, "Experimental analysis of video performance over wireless local area networks," in *Proc. IEEE Communications Society ICC*, 2008.

[33] J. H. Lee, E. S. Lee, and D. S. Kim, "Association methods for industrial wireless sensor networks using dynamic hysteresis," *IEEE Trans. Ind. Electron*, 2011, pp.399–403.

[34] L. Wang, X. Fu, J. Fang, H. Wang, and M. Fei, "Optimal node placement in industrial wireless sensor networks using adaptive mutation probability binary particle swarm optimisation algorithm," IEEE 7th International Conference on Natural Computation, 2011.

[35] C. Y. Chang, J. P. Sheu, S. W. Chang, "An obstacle-free and power-efficient deployment algorithm for wireless sensor networks," *IEEE Trans. on Systems, Man and Cybernetics,–Part A: Systems and Humans*, vol. 39, pp. 795–806, 2009.

[36] J. Tang, B. Hao, and A. Sen, "Relay node placement in large scale wireless sensor networks," *Computer Communications*, vol. 29, pp. 490–501, 2006.

[37] W. C. Ke, B. H. Liu, and M. J. Tsai, "Constructing a wireless sensor network to fully cover critical grids by deploying minimum sensors on grid points is NP-Complete," *IEEE Trans. Computing*, 2007, vol. 56, pp. 710–715.

[38] E. J. Rivera-Lara, R. Herrerias-Hernandez, J. A. Perez-Diaz, and C. F. Garcia-Hernandez, "Analysis of the relationship between QoS and SNR for an 802.11g WLAN," in *Proc. IEEE Int. Conf. on Comms,. Theory and Quality of Service*, 2008, pp. 103–107.

[39] M. Boulmalf, H. El-Sayed, and A. Soufyane, "Measured throughput and SNR of IEEE 802.11g in a small enterprize environment," in *Proc. IEEE Vehicular Technology Conference*, 2005, vol. 2, pp. 1333–1337.

[40] S.-E Yoo, P. K. Chong, D. Kim, Y. Doh, M.-L. Pham, E. Choi, and J. Huh, "Guaranteeing real-time services for industrial wireless sensor networks with IEEE 802.15.4," *IEEE Trans. Ind. Electron*., vol. 57, no. 11, pp. 3868–3876, Nov. 2010.

[41] V. C. Gungor, D. Sahin, T. Kocak, S. Ergut, C. Bucella, C. Cecati, and G. P. Hancke, "Smart Grid Technologies: Communication technologies and standards," *IEEE Trans. Ind. Informat*., vol. 7, no. 4, pp. 529–539, Nov. 2011.

[42] V. C. Gungor, B. Lu, and G. P. Hancke, "Opportunities and challenges of wireless sensor networks in smart grid," *IEEE Trans. Ind. Electron*., vol. 57, no. 10, pp. 3557–3564, Oct 2010.

REFERENCES

[43] L. L. Bello, O. Mirabella, and A. Raucea, "Design and implementation of an educational testbed for experimenting with industrial communications networks," *IEEE Trans. Ind. Electron*., vol. 54, no. 6, pp. 3122–3133, Dec. 2007.

[44] J. Garcia, F. R. Paloma, A. Luque, C. Aracil, J. M. Quero, D. Carrion, F. Gamiz, P. Revilla, J. Perez-Tinao, M. Moreno, P. Robles, and L. G. Franquelo, "Reconfigurable distributed network control system for industrial plant automation," *IEEE Trans. Ind. Electron*., vol. 51, no. 6, pp. 1168–1180, Dec. 2004.

[45] Z. Sun, I. F. Akyildiz, and G. P. Hancke, "Capacity and outage analysis of mimo and cooperative communication systems in underground tunnels," *IEEE Trans Wireless Comms*., 2011.

[46] V. Hazen, "Pulling security out of thin air; A Wi-Fi security primer" Bicsi Application Note, 2006.

[47] Cisco Systems Inc., A comprehensive review of 802.11 wireless LAN security and the Cisco Wireless Security Suite, Cisco Press 2005.

[48] Wi-Fi Alliance. "Deploying Wi-Fi Protected Access (WPA™) and WPA2™ in the EnterprizeTM Wi-Fi Alliance Tech. Rep., 2008.

[49] T. Diallo, "EtherSAM: The new standard in Ethernet service testing," EXFO Application Note 230.2AN, 2011.

[50] A. Willig, "Recent and emerging topics in wireless industrial communications: A selection," *IEEE Trans. Ind. Informat.*, vol. 4, no. 2, pp. 102–124, May 2008.

[51] R.A. Wenner (Ed.), "A 2.4 GHz vertical collinear antenna for 802.11 applications," http://www.nodomainname.co.uk/Omnicolinear/2-4collinear.htm, last accessed Nov. 2016.

[52] R. Blake, Electronic Communication Systems, Cengage Learning, ISBN: 0766826848, 2001.

[53] J. C. Maxwell, "A Dynamical Theory of the Electromagnetic Field", The Scientific Papers of James Clerk Maxwell, pp. 579-584, ISBN 9781108012256, 2011.

[54] M. Wright and S. Thakur, "The Effect of adding radios on 802.11g network throughput," Application Note AN 1339, Microchip Technology Inc. 2010.

[55] P. van Rhyn and G. P. Hancke, "Simplified performance estimation of ISM-band, OFDM based WSNs according to the sensitivity/SINAD parameters," *Journal of Applied Research and Technology*, vol. 15, no.1, pp. 1–13, Feb. 2017. https://doi.org/10.1016/j.jart.2016.10.002

[56] P. van Rhyn," A method to determine the improvement in performance of wireless Ethernet by considering the service level differential zone (SLDZ)," in *Proc. of the S.A. Academy for Science and Art's Student Symposium in Natural Sciences*, Univ. of Johannesburg, 2008.

[57] P. van Rhyn and G. P. Hancke, "Simplified impact analysis of the effect of WPA2 (PSK) security protocol on the RF link budget of an ISM-band, OFDM based wireless thermography sensor network," *Journal of Applied Research and Technology*, Manuscript ID JART-D-16-00209, to be published.